EVALUATION OF CALL MOBILITY ON NETWORK PRODUCTIVITY IN LONG TERM EVOLUTION ADVANCED (LTE-A) FEMTOCELLS

Uttara Sawant, M.S.

Dissertation Prepared for the Degree of

DOCTOR OF PHILOSOPHY

UNIVERSITY OF NORTH TEXAS

December 2017

APPROVED:

Robert Akl, Major Professor
Ram Dantu, Committee Member
Song Fu, Committee Member
Xiaohui Yuan, Committee Member
Barrett Bryant, Chair of the Department of Computer Science and Engineering
Costas Tsatsoulis, Dean of the College of Engineering
Victor Prybutok, Dean of the Toulouse Graduate School

Sawant, Uttara. *Evaluation of Call Mobility on Network Productivity in Long Term Evolution Advanced (LTE-A) Femtocells*. Doctor of Philosophy (Computer Science and Engineering), December 2017, 112 pp., 33 tables, 33 illustrations, bibliography, 72 numbered references,

The demand for higher data rates for indoor and cell-edge users led to evolution of small cells. LTE femtocells, one of the small cell categories, are low-power low-cost mobile base stations, which are deployed within the coverage area of the traditional macro base station. The cross-tier and co-tier interferences occur only when the macrocell and femtocell share the same frequency channels. Open access (OSG), closed access (CSG), and hybrid access are the three existing access-control methods that decide users' connectivity to the femtocell access point (FAP). We define a network performance function, network productivity, to measure the traffic that is carried successfully.

In this dissertation, we evaluate call mobility in LTE integrated network and determine optimized network productivity with variable call arrival rate in given LTE deployment with femtocell access modes (OSG, CSG, HYBRID) for a given call blocking vector. The solution to the optimization is maximum network productivity and call arrival rates for all cells. In the second scenario, we evaluate call mobility in LTE integrated network with increasing femtocells and maximize network productivity with variable femtocells distribution per macrocell with constant call arrival rate in uniform LTE deployment with femtocell access modes (OSG, CSG, HYBRID) for a given call blocking vector. The solution to the optimization is maximum network productivity and call arrival rates for all cells for network deployment where peak productivity is identified. We analyze the effects of call mobility on network productivity by simulating low, high, and no

mobility scenarios and study the impact based on offered load, handover traffic and blocking probabilities. Finally, we evaluate and optimize performance of fractional frequency reuse (FFR) mechanism and study the impact of proposed metric weighted user satisfaction with sectorized FFR configuration.

ACKNOWLEDGEMENTS

I would like to thank my advisor Dr. Robert Akl for his constant support, guidance and encouragement. I appreciate his patience and advice in every step of the way, generously considering my full-time work schedule. He has been flexible with online meetings for research discussions, conference preparations, and research paper feedback, guiding me and believing in me irrespective of the roadblocks in the way.

I would like to thank the members of my committee Dr. Ram Dantu, Dr. Song Fu, and Dr. Xiaohui Yuan. Their support and feedback have made this research much better. The discussions during their advanced courses have helped me appreciate and develop new perspectives.

I thank and appreciate Sally Pettyjohn, Stephanie Deacon, and Matt Kernan for their support. Their help in securing department inventory, program timelines, and software support made it possible for me to work on my thesis effectively.

Thank you to my friends, Dr. Alan Livingston and Dr. Josephine Reyna, for being my unwavering support and willing to offer insight and perspective and reminding me to have fun in the process.

I thank my Toastmaster friends, Nancy Bateman and David Gray, for helping me deliver clear presentations and offering constructive feedback.

I thank all my friends and colleagues who provided positive and friendly environment with constructive feedback, tremendous support and guidance and helped me grow professionally.

This dissertation is a dedication to my parents, Mohan Sawant and Radha Sawant. I thank them for their support and keeping me grounded in the process. I thank my family for their unconditional love and support.

I acknowledge portions of chapters 3, 4, and 5 have been reproduced with permission from IEEE. Please see Appendix C for a detailed list of dissertation sections and published material.

TABLE OF CONTENTS

LIST OF TABLES

LIST OF FIGURES

CHAPTER 1

INTRODUCTION

1.1. LTE Overview

Mobile communications have become ubiquitous in today's world. The technology has evolved to go from short distance coverage to serving truly mobile users. This technology evolution is now managed by global standards-developing organizations such as the Third Generation Partnership Project (3GPP), involving several wireless companies and telecommunication professionals. The evolution process for mobile communication technologies started with 1G being the voice-driven analog mobile radio systems, 2G the first digital mobile systems, and 3G the first mobile systems supporting broadband data in the order of Mbit/s. The Long-Term Evolution (LTE) is often referred to as "4G" evolutionary step. The LTE Release 8 supported data rates slightly lower than the expected 4G target, leading to be referred to as "3.9". LTE-Advanced (LTE-A) which was introduced in Release 10, is known to be the true 4G since it met the data rate criteria. The tremendous increase in data rate consumption by mobile users, the continuous demand for new services, and the extremely high requirements for high mobility scenarios led to the evolution of 3G systems into 4G. Conversion into all-IP packet core, operator competition, spectrum limitations and efficiency measurement, have also contributed to the evolution process [21].

The idea of accessing the Internet from mobile devices is known as *mobile broadband*. The prime driver and one of the major challenges for the evolution of LTE is to support the Internet Protocol (IP)-based services in a mobile device that are currently hosted on a fixed broadband connection. 2G General Packet Radio Service (GPRS), 3G High Speed Packet Access (HSPA) and 4G LTE data services is the evolution taking place to support internet services on a mobile device. The IP supports a range of services with different requirements. The main service-related design parameters for a radio interface supporting a variety of IP-based services are:

- *Data rate.* Though low data rate services such as voice are important and fall into

majority of capacity-driven mobile networks, the higher data rate services drive the radio interface design. Web browsing, emails, audio and video streaming, are the types of services that users request the most, and push the peak data rates supported by the mobile systems. It is the primary design paramater driving the LTE development.

- *Delay.* The round-trip time taken by a packet from server to client and back is termed as latency. It is one of the important design parameters for LTE network, and hence of prime significance to network operators. This parameter becomes critical design factor for interactive services such as real-time gaming, but also web browsing and interactive file transfer, where low latency is more significant than other design requirements.
- *Capacity.* Every mobile operator wants to ensure the maximum spectrum utilization since it's expensive and limited resource. Therefore, operators not only look for peak data rates to the end-user, but also total system and system throughput per Hertz of licensed spectrum, known as spectral efficiency. It measures how effectively the operator bandwidth is utilized to satisfy maximum data rate requirements. It directly impacts the Quality-of-Service (QoS) for the individual end-users.

High spectrum flexibility coupled with high data rates and system capacity drive the needs for evolution of LTE mobile broadband technology. To meet the requirements of the LTE radio interface, the core network also needed to be evolved to support the high data rates and support IP-based services. This evolution process, known as System Architecture Evolution (SAE), has led to an Evolved Packet Core (EPC), developed to 3G and 4G core networks, focusing on the all-IP packet domain as shown in Fig. 1.1. The 3GPP standards group manages the mobile broadband evolution process. Fig. 1.2 shows the different phases of LTE introduced by 3GPP with inputs from several worldwide mobile operators, service providers and telecommunication professionals, and major features available in each release.

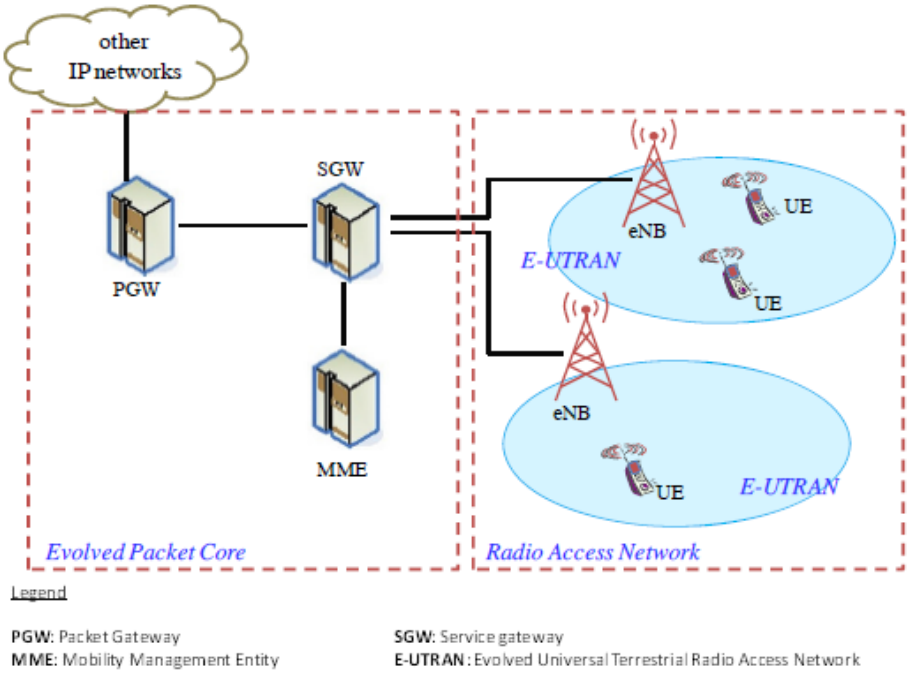

FIGURE 1.1. The Service Architecture Evolution in LTE network [16]

Rel-8	Rel-9	Rel-10	Rel-11	Rel-12	Rel-13	Rel-14
• Dec 2008 • First LTE release	• Dec 2009 • Femtocell • Beam forming • SON • eMBMS	• Mar 2011 • LTE Advanced • Carrier Aggregation • Enhanced ICIC • Relay Nodes	• Dec 2012 • Enhanced CA • CoMP • Enhanced PDCCH	• Jun 2014 • Machine Type Communication • WiFi Integration • LTE Unlicensed	• Dec 2015 • Enhanced CA • Enhanced MTC • Enhanced MIMO	• Current release • 5G standards

FIGURE 1.2. 3GPP LTE evolution phases

1.1.1. High Data Rate Requirements

In the previous section, we already established the high data rate and latency requirements for LTE. In this section, we review the limitations of a mobile communication channel, possible solutions, and techniques we can apply to meet the requirements despite the limitations. From Shannon—Hartley theorem expression in Eqn. 1.1, it is clear that the data rate is limited by the channel bandwidth, B and signal-to-noise ratio (SINR), where S is the average received signal power over the bandwidth and N is the average power of the

noise and interference over the bandwidth [66, 67].

$$C = B \cdot \log_2(1 + \frac{S}{N}) \tag{1.1}$$

Consider a communication channel where information is transmitted at a line rate R. This equation can be used to establish a bound on $\frac{E_b}{N_0}$ for any system that achieves reliable communication, by considering an average energy per bit of $E_b = \frac{S}{R}$, with noise spectral density of $N_0 = \frac{N}{B}$. Since the data rate cannot exceed the channel capacity, the above expression leads to following inequality given by Eqns. 1.2, and 1.3.

$$R \leq C = B \cdot \log_2(1 + \frac{S}{N}) = B \cdot log_2(1 + \frac{E_b \cdot R}{N_0 \cdot B}) \tag{1.2}$$

or,

$$\beta \leq log_2(1 + \beta \cdot \frac{E_b}{N_0}) \tag{1.3}$$

where, $\beta = \frac{R}{B}$ is the bandwidth utilization parameter. Rearranging the terms in the inequality Eqn. 1.3 gives us the lower bound on the required received energy per information bit, normalized to noise power density, for a given bandwidth utilization parameter β shown in Eqn. 1.3.

$$\frac{E_b}{N_0} \geq min(\frac{E_b}{N_0}) = \frac{2^\beta - 1}{\beta} \tag{1.4}$$

For high data rates in *noise-limited scenarios*, performance is always limited by the available received signal power or received signal-to-interference-noise ratio (SINR). For lower-bandwidth utilization or power-limited scenario, any increase in data rate requires similar increase in received signal power. For higher-bandwidth utilization or bandwidth-limited scenario, any increase in data rate requires much larger increase in received signal power unless bandwidth is increased in proportion to increased data rate. In conclusion, the above expressions and deductions indicate that the transmission bandwidth should be at least of the same order as the data rates required to efficiently utilize the available received signal power or SINR. Receive-antenna diversity concept in LTE enables to increase the overall received signal power for a given transmit power. Spatial multiplexing or Multiple Input

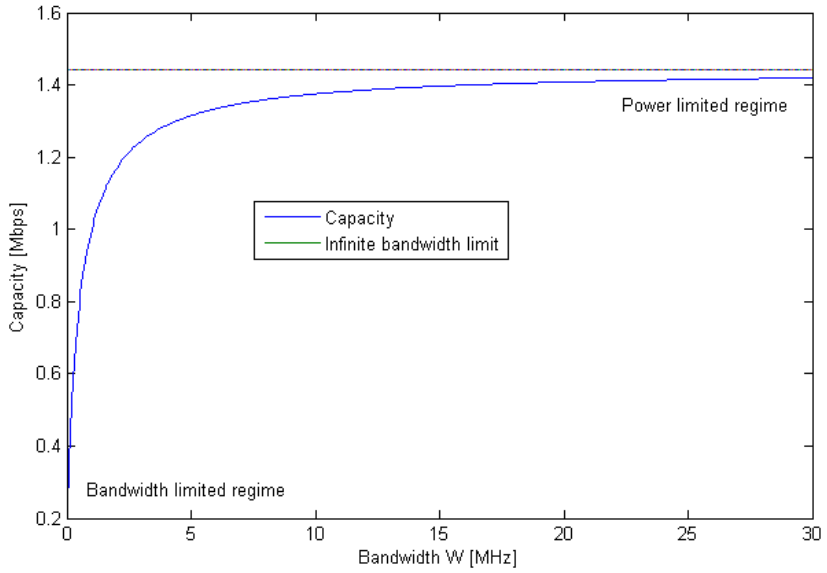

FIGURE 1.3. Channel capacity as a function of bandwidth [20]

Multiple Output (MIMO) can also be applied to achieve high data rates in LTE. By reducing the noise level, the received SINR can be improved at the terminal and high data rates can be achieved. In addition to noise, another factor that impacts the received SINR is inter-cell interference. Reducing cell size, beamforming, and antenna diversity can serve to address the *interference-limited scenarios* in high data rate requirement. Where noise factor can be unpredictable, interference can be calculated and controlled with several techniques [20, 21]. LTE small cells or specifically femtocells (to align with the topic of dissertation) experience interference-limited scenarios that impact network productivity.

1.1.2. OFDM Transmission and Number of Subcarriers

Before discussing the LTE femtocells, it is important to review the LTE OFDM or Orthogonal Frequency-Division Multiplexing, a transmission scheme used for 3GPP LTE and also for other technologies such as WiMAX. It can be seen as a type of multi-carrier multi-symbol transmission where there are several hundreds and thousands of narrow subcarriers separated by subcarrier spacing in the order of kHz. Once the subcarrier spacing has been selected, the number of subcarriers is derived based on the system bandwidth and this

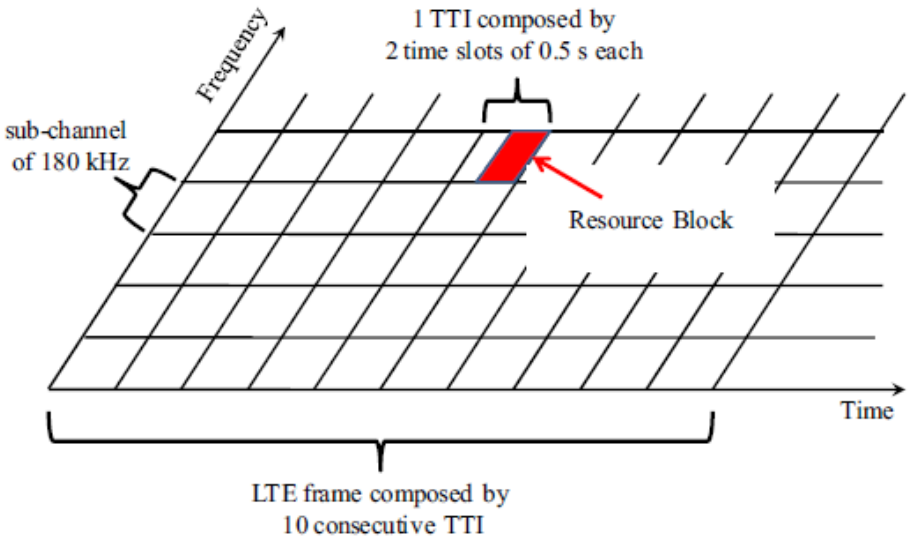

FIGURE 1.4. OFDM time-frequency grid [16]

controls the resource block allocation. The "physical resource" in case of OFDM transmission is represented as a time-frequency grid according to Fig. 1.4, where each "row" corresponds to one OFDM symbol on time axis and each "column" corresponds to one OFDM subcarrier on frequency axis. The multi-carrier multi-symbol nature of OFDM allows a multiple-access scheme, giving way to simultaneous frequency-separated transmission to/from multiple users as shown in Fig. 1.5. One step further, due to the use of OFDM in both downlink and uplink transmissions, the scheduler at the base station has access to resources along both time and frequency axes. It can, for each time slot and frequency subcarrier, make the granular decision to select the user with the best channel conditions. Fig. 1.6 shows the evolution of radio channel access technologies and how OFDMA is designed to meet requirements for LTE.

1.1.3. LTE Mobility

The theoretical target data rate for stationary users accessing LTE network is 1 Gbps, and for high mobility users, it is a maximum of 100 Mbps. In the process of meeting the goal, the network architecture required an update as well. A fully packet switched network supporting IP infrastructure and complete removal of circuit switching technology is the

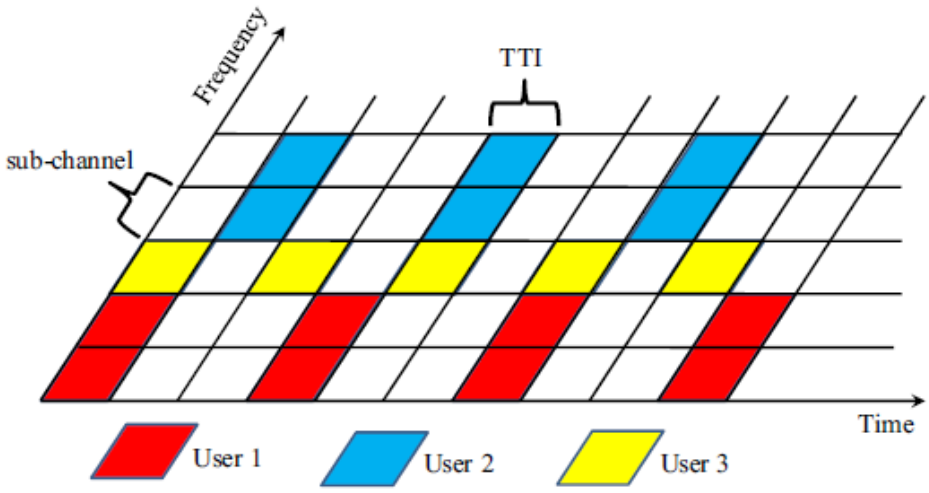

FIGURE 1.5. OFDM downlink and uplink resource grid user multiplexing [16]

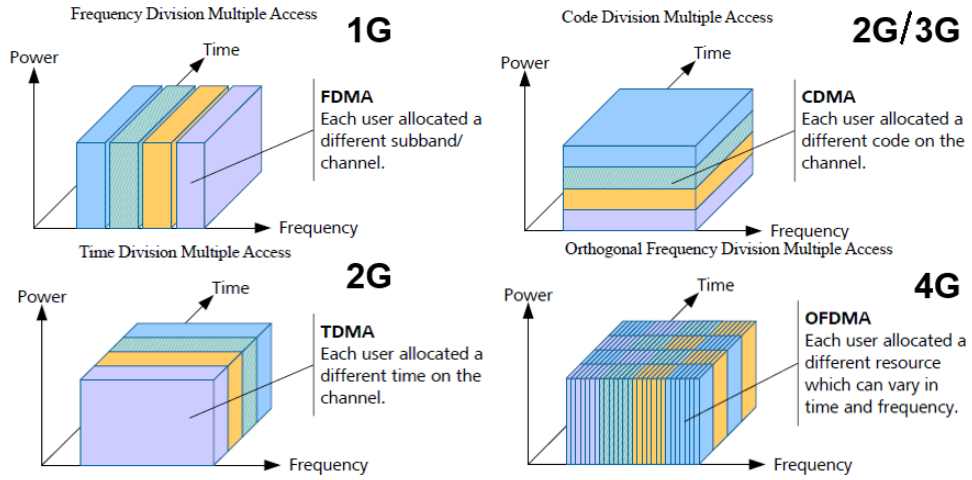

FIGURE 1.6. 1G to 4G: Radio channel access technology evolution [53]

roadmap to realize LTE network. As 3G evolved to 4G, the core network became packet-switched and evolved into the EPC. To support the high mobility requirement and latency goals, the Radio Network Controller (RNC) is removed and handover decision-making is moved to eNodeB. The eNodeB is also evolved and fully equipped with radio resource management, scheduling, re-transmission, coding, and multi-antenna techniques. By upgrading the eNodeB to handle handover events and communicate directly with the core, the latency goal is met and high mobility scenarios with high data rate requirements are possible.

1.2. LTE Femtocell Overlay and Access Modes

The increasing demand for high data rates by wireless subscribers especially the cell edge and indoor users has been a major driver for the concept of femtocells. Femtocells are low-powered low-cost mobile base stations which are deployed within the coverage area of the traditional macro base station. The growth in wireless capacity is exemplified by this observation from Martin Cooper of Arraycomm: The wireless capacity has doubled every 30 months over the last 104 years. This translates into an approximately millionfold capacity increase since 1957. Breaking down these gains shows a 25X improvement from wider spectrum, a 5X improvement by dividing the spectrum into smaller slices, a 5X improvement by designing better modulation schemes, and a whopping 1600X gain through reduced cell sizes and transmit distance. The enormous gains reaped from smaller cell sizes arise from efficient spatial reuse of spectrum or, alternatively, higher area spectral efficiency [5, 17].

One obvious solution to satisfy the growing demand in data rates would be to densify the existing mobile communications network by adding new macrocells. The direct advantage of such approach is better link-budget numbers and improvement in data rates. Some of the major drawbacks of relying on macrocells are the poor coverage for the cell edge users and lower data rates experienced by the indoor users. Another issue with this microization is the increasing cost of deploying the macrocells. An alternative or complement to a uniform densification of the macrocell layer is to deploy additional low-power femtocells within the coverage area of a macrocell. This femtocell base station is deployed by the end-user, typically within the home, connecting to the operator network using the end-users wireline broadband connection. The user installed home base station (HBS) communicates with the cellular network via a broadband connection such as digital subscriber line (DSL), cable modem or a separate radio frequency (RF) backhaul channel.

To improve the signal quality and boost the data rates, femtocells seem to be the obvious choice. With the femtocell solution, the subscriber is happy with high data rates and coverage, and the operators prefer to offload the traffic from the expensive macrocells and focus the radio resources on the truly mobile users. Frequency partitioning of the total

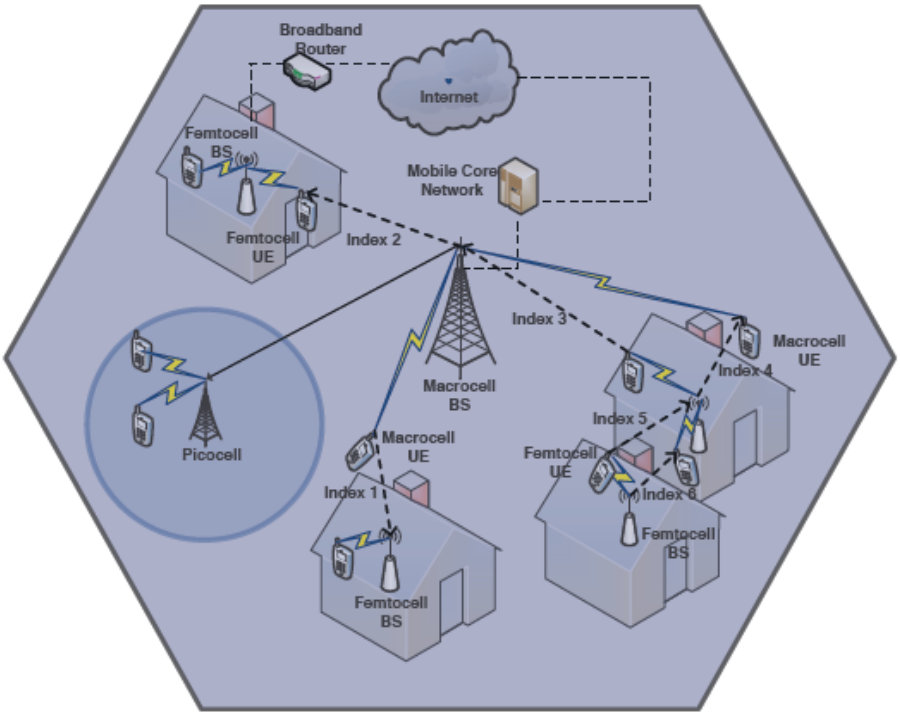

FIGURE 1.7. Small cell deployment in LTE network [49]

system bandwidth is done and different non-overlapping frequency bands are assigned to macrocells and femtocells to avoid strong interference between the respective layers. However, spectrum partitioning results in poor bandwidth utilization and low spectrum efficiency for the operators. Additionally, this process results in reduced throughput which is undesirable to users and operators. Therefore, the most preferred method of deploying femtocells is in the same spectrum used by the macrocells, and applying effective and smart ways to eliminate or minimize the interferences [21].

1.2.1. Femtocell Challenges

The several challenges facing femtocell deployment include resource allocation, timing or synchronization, backhaul quality, interference management, femtocell access modes, handoffs, mobility, emergency-911 servicing, and femtocell security. Co-tier and cross-tier interferences will minimize the benefits of the femtocells. *Co-tier interference* occurs between neighboring femtocells. For example, a femtocell UE (aggressor) causes uplink co-tier

interference to the neighboring femtocell base stations (victims) (e.g. index 5 in Fig. 1.7). On the other hand, a femtocell base station acts as a source of downlink co-tier interference to the neighboring femtocell UEs (e.g. index 6 in Fig. 1.7). *Cross-tier interference* occurs between femtocells and macrocells. For example, femtocell UEs (referred to as FUEs) and macrocell UEs (referred to as MUEs) act as sources of uplink cross-tier interference to the serving macrocell (e.g. index 3 in Fig. 1.7) and the nearby femtocells (e.g. index 1 in Fig. 1.7) respectively. On the other hand, the serving macrocell and femtocells cause downlink cross-tier interference to the FUEs (e.g., index 2 in Fig. 1.7) and nearby MUEs (e.g., index 4 in Fig. 1.7), respectively. The cross-tier and co-tier interferences occur only when the macrocell and femtocell share the same frequency channels. Due to the ad hoc nature of femtocell deployment, interference suppression techniques prove ineffective. In this process, interference cancellation will overshadow the benefits of the femtocells. Hence, interference avoidance techniques are explored and researched to greater extent as they will work better in geographically dependent femtocell networks. A typical femtocell deployment comprises of two tiers, the tier including the macrocell (tier-1) and the tier including the femtocells (tier-2) as shown in Fig. 1.7 [49].

1.2.2. Technical Aspects of Femtocells

The capacity potential of femtocells can be verified from Shannon's law, which relates the wireless link capacity (in bits per second) in a bandwidth to the SINR. The SINR is a function of the transmission power of the desired and interfering transmitters, path losses, and shadowing during terrestrial propagation. One way to increase the capacity is to reduce the distance between the transmitter and the receiver. In addition, more benefits can be obtained by exploiting interference cancellation and avoidance techniques [17]. The capacity benefits of the femtocells can be attributed to the following.

- Reduced distance between the femtocell and the user, which leads to higher received signal strength.
- Lowered transmit power, and mitigation of interference from neighboring macrocell and femtocell users due to outdoor propagation and penetration losses.

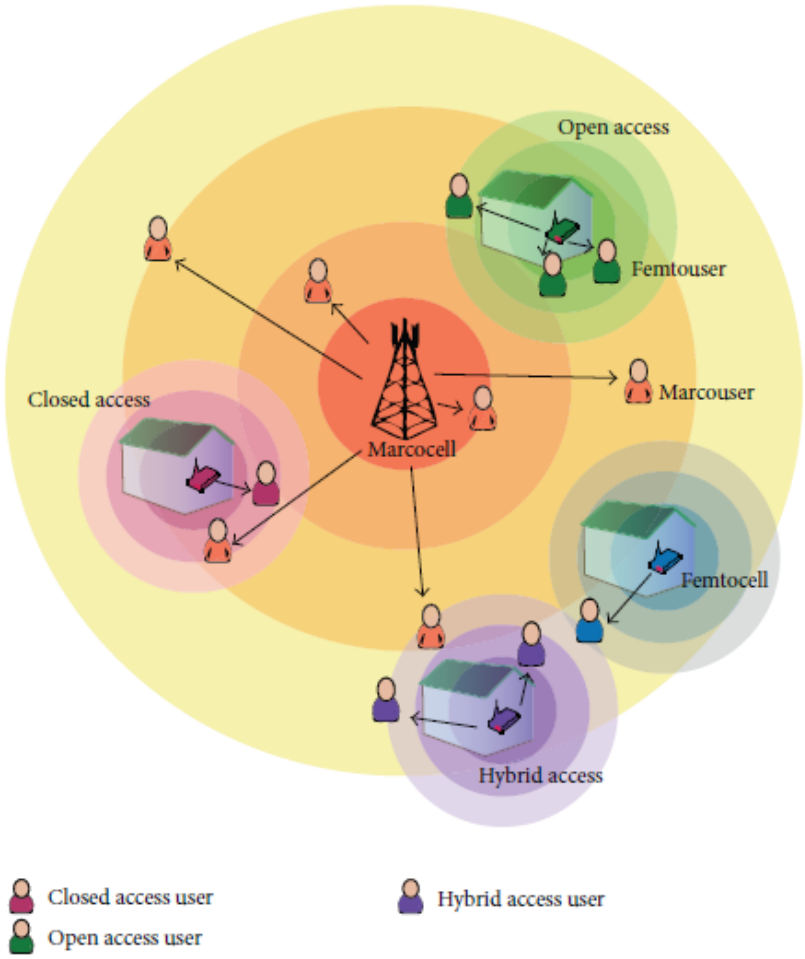

FIGURE 1.8. Femtocell access modes in LTE network [1]

- As femtocells serve only limited number of users, around one to four users, they can devote a larger portion of their resources (transmit power and bandwidth) to each subscriber. A macrocell, on the other hand, has a larger coverage area (500 m - 1 km radius) and a larger number of users; thus making it difficult to provide QoS for data users.

1.2.3. Business Aspects of Femtocells

Despite femtocells being the cost-effective solution, there is still a significant amount of investment. Operators will need to aggressively price femtocells, despite tight budgets and high manufacturing costs, to compete with ubiquitous Wireless Fidelity (WiFi). For example,

the North American operator Sprint charges a subsidized price of $99.99 per Airave femtocell for subscribing to a $20/month family plan. At the same time, the features femtocells have to provide are in many ways more sophisticated than what is in a consumer grade Wi-Fi access point [17].

1.2.4. Femtocell Access Modes

Open access (OSG), closed access (CSG), and hybrid access are the three existing access-control methods that decide users' connectivity to the Femtocell Access Point (FAP). In open access, whenever the users are within the range of a FAP, they get connected to the FAP easily. This includes a new set of signalling congestion in the network, as the number of handover attempts gets higher, compromising the level of sharing and security concerns for the regular user. In the case of closed access, only particular users get access to the FAP, thus avoiding unwanted traffic congestion and possible interferences. In this case, the QoS is guaranteed at the expense of decreasing spectral efficiency. Hybrid access transacts with both challenges by tuning the resource ratio according to the number of femtocell owners and subscribers. A limited amount of resources is available to the users who are within the coverage range and a "closed subscriber group" possesses the privilege to use the maximum service [1]. Fig. 1.8 shows different access control mechanism in the femtocell network.

1.3. Contributions

The dissertation describes three major scenarios and specifies contribution in each scenario. We define a network performance function, *network productivity*, for traffic that is carried successfully.

- *Scenario* Optimization of network productivity with variable call arrival rate in given LTE deployment with femtocell access modes (OSG, CSG, HYBRID) constrained by blocking threshold

  Purpose QoS guarantee, upper bound productivity, flexible mobility

  Contribution Maximum network productivity, call arrival rates for all cells

- *Scenario* Optimization of network productivity with variable femtocells distribution per macrocell with constant call arrival rate in uniform LTE deployment with femtocell access modes (OSG, CSG, HYBRID) constrained by blocking threshold

  Purpose QoS guarantee, upper bound productivity, flexible mobility, upper bound resource allocation

  Contribution Maximum network productivity, call arrival rates for all cells with femtocell number with peak productivity identified
- *Scenario* Fractional Frequency Reuse (FFR) mechanism performance

  Purpose QoS guarantee, upper bound productivity, upper bound resource allocation, upper bound network parameters, measurement of user throughput variance

  Contribution Study of proposed metric, weighted user satisfaction, with sectorized FFR to generate best possible performance

1.4. Organization

In Chapter 2, we review the existing literature and present references to previous research and papers that have studied LTE call mobility in similar scenarios and system models. We also review the existing metrics that evaluate FFR mechanism performance and how our proposed metric is similar and different in comparison.

Chapter 3 introduces *network productivity* used in our research to evaluate call mobility effects on LTE network performance. It specifies the system model and blocking probability model applied in our research. The optimization of network productivity for variable call arrival rate is introduced and how the femtocell access modes impact the performance is shown.

Chapter 4 studies a slightly different scenario for optimization of network productivity and its impact on femtocells serving in different access modes. Optimization is carried out on network deployment with variable femtocells per macrocell sector with constant call arrival rate.

Chapter 5 introduces new metric to evaluate LTE network performance and compares with existing metrics for networks that apply FFR mechanism. Results prove the proposed

metric performs better than existing metrics for given deployment.

Finally, in Chapter 6, we present our conclusions and summarize the contributions of this work.

CHAPTER 2

RELATED WORK

2.1. Network Productivity

In this section, we review the previous research related to network productivity. Extensive research on network productivity or network revenue is done for code-division multiple-access (CDMA) networks. In [62], the author applies shadow prices to measure the rate of change in design parameters such as channel allocation, channel reservation, network capacity, user demand, and routing proportions. The ability to evaluate such shadow prices enables configurations that can maximize network performance according to blocking criteria. The author presents models for the evaluation of shadow prices for different networks such as, single-rate circuit-switched networks, wireless networks, and multi-rate circuit-switched networks. There are three methods to handle handoff calls in the network. First method is to assign equal priority to handoff and new calls at the time of resource allocation. Second method is to assign higher priority to handoff calls over new calls and reserve and allocate resources to them. Third method is to place the handoff calls on a queue if no resource is available. Fixed Channel Assignment (FCA) sets aside fixed number of resources for handoff calls and applies second method to address handoff calls. The author uses FCA in their framework to handle handoff calls. Sum capacity is the largest sum of external call arrival rates that the network can handle to maintain the given call blocking threshold. The work also formulates the sum capacity that can be used to compare different adaptive routing schemes, determine the actual pricing of calls to reflect their effect on the entire network, trade off new call blocking with the forced call termination due to handoff failures in wireless networks, dimension networks to achieve a prescribed set of new call and handoff blocking probabilities, and determine the tradeoffs between calls of different rates in multi-rate networks. With this shadow pricing framework, a differential pricing methodology is developed to handle different network services. It proves that adjusting capacity distribution to traffic patterns in wireless networks carried out through optimization with

shadow prices results in significant improvement. Implied costs for multi-rate wireless networks are calculated and their use is demonstrated for quantifying mobility, traffic load, call pricing, network optimization and for evaluating trade-offs between calls of different rates [63]. User mobility is modeled by assigning call progression probabilities, call termination probabilities and call handoff probabilities. The author in [3] uses FCA in their framework to handle handoff calls. The performance metrics used are new call blocking and handoff drop probabilities. The implied cost is calculated for the network revenue, which considers the revenue generated by accepting a new call arrival into the network and penalty of forced termination due to handoff failure in any cell. The implied costs are used to study the effects of call arrival rates on the network performance metrics. Finally, a nonlinear constrained optimization problem is formulated to calculate the sum revenue for a given network by maximizing the net revenue using implied costs in a gradient descent algorithm. The implied cost analysis also shows that matching capacity distribution to external call arrival rates and mobility can significantly increase revenue. The effect of call arrival rate on the capacity of a CDMA cellular network is analyzed. First, the inter-cell and intra-cell interefferences of every cell on every other cell are calculated for a given network topology. Then, the capacity region for the number of simultaneous calls in every cell is defined for specified system parameters. This region is used to evaluate the new call blocking and handoff call blocking probabilities. In this region, the total number of simultaneous calls for all cells in the network is bound by the resources available in the network. The network throughput is calculated by considering the revenue generated by accepting a new call and the cost of a forced termination due to handoff failure. Implied costs are calculated for both high and low mobility of calls between cells, and the effect of mobility on pricing and network throughput is discussed. The implied costs are used to maximize the throughput with respect to the call arrival rates by applying a gradient descent algorithm. Call admission control (CAC) determines whether a new call should be admitted into the network. Designing a CAC algorithm that guarantees grade-of-service (GoS) and call blocking probabilities for arbitrary traffic distribution in CDMA networks is difficult. Previous research assumed an uniform

traffic distribution or discarded mobility to simplify the design complexity. The authors in [2] define a set of feasible call configurations that results in a CAC algorithm that captures the effect of having an arbitrary traffic distribution and whose complexity scales linearly with the number of cells. The incoming call to any cell is accepted if and only if the new state is a feasible state. To study the effect of mobility and to differentiate between the effects of blocking new calls and handoff calls, they define a net revenue function. The net revenue is the sum of the revenue generated by accepting a new call and the cost of a forced termination due to a handoff failure. The net revenue depends implicitly on the CAC algorithm. The authors calculate the implied costs which are the derivatives of the network throughput and capture the effect of increase in the number of calls admitted in one cell on the revenue of the entire network. Given a network topology with established traffic levels, the implied costs are used in the calculation of the CAC algorithm that enhances revenue and satisfies call blocking probabilities. Moreover, the new algorithm provides guaranteed GoS for all the cells in the network for an arbitrary traffic distribution. The work in [4] presents a novel approach for designing a CAC algorithm for CDMA networks with arbitrary call-arrival rates. The network is considered to be a set of feasible states based on the resource requirements. A new call is said to be successfully admitted to the network if the network state is one of the feasible states. The CAC algorithm uses global information; it incorporates the call-arrival rates and the user mobilities across the network and guarantees the users' QoS as well as prespecified blocking probabilities. On the other hand, its implementation in each cell uses local information; it only requires the number of calls currently active in that cell. The authors present several cases for a nontrivial network topology where the CAC algorithm guarantees GoS and blocking probabilities while achieving significantly higher throughput than that achieved by traditional techniques. They also calculate the network capacity i.e., the maximum throughput for the entire network, bound by prespecified blocking probabilities and QoS requirements. Traditional design rules for cellular networks are not directly applicable to CDMA networks where inter-cell interference is not mitigated by cell placement and careful frequency planning. Authors developed methodology to calculate sensitivities

of capacity to base station location, pilot-signal power and mobile transmission power and optimize network capacity. They also proposed CAC algorithm that can guarantee lower call blocking probabilities and achieve higher throughput than traditional CAC techniques.

A Heterogeneous Network (HetNet) comprises of multiple Radio Access Technologies (RATs) allowing an user to associate with a specific RAT and steer to other RATs in a seamless manner. To cope with the unprecedented growth of data traffic, mobile data can be offloaded to WiFi network in a Long Term Evolution (LTE) based HetNet. Two types of users or services are considered in this ecosystem; voice and data users. To maintain QoS for voice users, they are restricted to use LTE network. The mobile data users can be offloaded into WiFi network from LTE. The decision for RAT selection done by users themselves; user-initiated RAT selection, will result in non-optimal solution since users will always prefer the strongest network to satisfy their data requirement. Therefore, network-initiated RAT selection becomes significant, where the algorithm optimizes the different network parameters and maintains user data requirement. In [47, 48], an optimal RAT selection problem, Markov Decision Process (MDP), is considered to maximize the total system throughput in a LTE-WiFi system with offload capability. Another Constrained Markov Decision Process (CMDP) formulation is also developed, where maximizing the total system throughput is subject to a constraint on the voice user blocking probability. It is proved that the optimal policies for the association and offloading of voice and data users contain threshold structures. Based on the threshold structures, the authors propose algorithms for the association and offloading of users in LTE-WiFi HetNet. Simulation results are presented to demonstrate the voice user blocking probability and the total system throughput performance of the proposed algorithms in comparison to benchmark on-the-spot algorithm. LTE and WiFi networks operate at different frequencies. Therefore, they are orthogonal to each other. This means, the interference at each base station originates only from base stations of the same network. Average user rate and congestion probability are performance metrics considered in the work presented in [8]. In order to cope with increasing data demand on mobile wireless networks, operators are investigating the use of unlicensed spectrum in addition to their li-

censed spectrum. Today, it is possible to integrate WiFi networks into the wireless networks and perform offloading of traffic to a WiFi network. In future networks, we will see stronger association and aggregation of LTE and WiFi networks. The design and performance analysis of different offloading and aggregation strategies is a difficult task, due to the different RATs involved. One widely used tool for the analysis of such systems is stochastic geometry, but most existing works do not take the heterogeneity of the different RATs into account. This work models the LTE and WiFi networks as well as the users using a probabilistic approach based on stochastic geometry and uses the particular physical layer modeling process of the two RATs into account. Using these newly developed tools, the authors show that the max-throughput criterion, which takes the different physical layer characteristics of the two RATs into account, performs better than simple offloading and max-SINR association criteria. CDMA and LTE networks serve both streaming real-time traffic and elastic non real-time traffic. In order to evaluate the performance, the QoS is decided in terms of blocking probability of real-time calls and throughput for elastic calls. This evaluation is significant in network dimensioning that will determine the minimum number of base stations required to satisfy QoS of the users. Authors in [34] propose a rapid and accurate method for the evaluation of the QoS perceived by the users in the uplink of wireless cellular networks. In doing so, they consider variable call arrival rates into the network. Their analytical model determines the feasibility condition (FC) and sufficient feasibility condition (SFC) for the resource allocation. They use the SFC to approximate the QoS evaluation for the user demand. Simulation results show approximation to the FC and SFC condition results for CDMA and LTE networks. The manual and static inter-cell optimization in GSM and UMTS networks at the network planning stage does not adapt to the changing network conditions. Due to the ever-changing environmental conditions, the optimization becomes sub-optimal and results in load imbalance. For 3GPP LTE networks, self-optimization in self-organizing networks is an important design factor. Change in loads directed to certain cells in the networks causes load imbalance, which results in higher call blocking and lower utilization in neighboring cells with lower loads. In [65], the authors propose a load balancing framework, which fo-

cuses at balancing the load in the entire network, while keeping the network throughput with reasonable overhead, but still maintain within prescribed threshold. In this framework, the objective is formulated as a network-wide utility function balancing network throughput and load distribution, and then it is transformed to an integer optimization problem under resource allocation constraints using the Heaviest-First Load Balancing algorithm. In [36], the authors proposed new uplink CAC and resources allocation schemes for LTE. The proposed CAC scheme gives the priority to Handoff Calls (HC), without totally neglecting the requirements of New Calls (NC). The main objective of this approach is to provide QoS and to prevent network congestion. Two popular approaches are discussed in terms of how HC is treated with respect to call admission priority. The authors propose a CAC scheme for the LTE network, which prioritizes HC over NC, bound by call drop probability and maintain user fairness. System-level simulations for LTE-A systems focus on performance of base station and do not consider user-level performance. Previous research also considered simulation-focused performance analysis without a combination of analysis and simulation approach. None of the previous approaches have considered a combination of analytical and simulation-based approach to evaluate user performance. Authors in [41] propose a hybrid model consisting of both analysis and simulation. They study the probability of possible call distribution, first obtained by analysis, which is used as an input to the event-driven based simulator to calculate the throughput of a call state. Data throughput and spectral efficiency are important metrics used in the performance evaluation of the next generation cellular networks. To evaluate the performance of these networks, Monte Carlo simulation schemes are used. Such simulations do not provide the throughput of intermediate call state, instead they present the overall performance of the network. The benefit of the hybrid model is that the throughput of any possible call state in the system can be evaluated from the user perspective. The authors compare the throughput obtained from hybrid model with that obtained from event-driven based simulation. To simulate dynamic loads in the network, two approaches are implemented. First, keeping the mean hold time constant, the inter-arrival time is varied. Second, the inter-arrival time is kept constant, while the mean hold time is

varied. Numerical results are presented and they show the proposed hybrid model aligned with the results from simulation. The maximum difference of relative throughput between hybrid model and the simulation is found in the interval of (0.04%, 1.06%) over a range of call arrival rates, mean holding times and number of subcarriers in the system.

Authors in [35] propose to increase the performance of QoS parameters; call blocking probability, call dropping probability and system throughput by applying Soft frequency reuse (SFR) method and Call-Bounding scheme. The incoming calls are classified into traffic classes to determine the call priority. Video calls are the highest priority calls, followed by voice and data calls. The authors have combined the concept of SFR with call priorities assigned, translated into CAC-based approach to generate QoS parameters for throughput evaluation and comparison with traditional methods. Operators are deploying LTE networks to co-exist with current 2G and 3G networks. In some cases, LTE and WiFi are expected to function in sync, synthesizing a highly heterogeneous wireless network. Mobile devices choose the radio access technology based on a predefined handover policy. Here, the base stations manage their resources in a distributed manner without taking into consideration the network overlap. Therefore, the network utility for the operators and users is below optimal. In order to fully utilize the system resources and guarantee QoS, a joint centralized framework is needed. Authors in [60] propose a new utility function that can support multiple design requirements for mobile networks, including advanced traffic models, user classes, handover and session priorities. In the context of a heterogenous wireless network, transient parameters can have varying effects on each access network type. The work proposes a new utility function, joint utility-based resource and network assignment, that can support multiple design requirements for mobile networks including advanced traffic models, user classes, handover and session priorities. The authors integrate the new utility function with the Super Base Station framework with a global network-wide view and devise a novel trigger-based network and resource assignment framework that efficiently copes with the complexity of a heterogenous wireless network. The simulation results show that the proposed sub-optimal trigger-based framework performs equally well as the complex optimal scheme, with

acceptable user fairness, reduced handover rate and improved resource utilization. Similar parameters are studied in [56] where the author focuses on studying the interactions between three self optimization use cases aiming at improving the overall handover procedure in LTE femtocell networks. These self optimization use cases are handover, CAC and load balancing. The author has developed a comprehensive, unified LTE compliant environment to study the interaction between the three representative handover schemes to ensure that individual goals and combined goals are met when operating simultaneously. The result is a set of guidelines that can assist network operators and researchers in designing better handover coordination policies. In [22], revenue maximization in a static environment is examined in delay-tolerant networks as a solution to reduce the pressure on the cell traffic, where mobile users use available resources effectively and with a cheaper cost. Here, the authors have focused on optimal strategy for smartphones in hybrid wireless networks. This work deals with how to use the precious wireless resources that are usually wasted by under-utilization of networks. The authors are particularly interested in resources that can be used in an opportunistic manner with different technologies. They have designed new schemes for better and more efficient use of wireless systems by providing mathematical frameworks. In cognitive radio networks, the work focuses on how to optimally allocate resources to unlicensed or secondary users. Second contribution is in delay tolerant networks, where the authors devised an optimal strategy in the class of threshold strategies, wherein users activate their devices on meeting certain threshold. Finally, the authors investigate the interactions between physical, medium access and network layers and develop an analytical model that predicts the throughput of each connection at the network nodes. Work in [40] focuses on the user association optimization for different HetNets scenarios. The work proposes an optimal user association algorithm to improve downlink and uplink performance with opportunistic strategy to maintain QoS and user fairness for delay intolerant traffic and best effort traffic respectively. The algorithm is enhanced to support green HetNets by adapting the user association decision to the amount of renewable energy from base stations. Further adaptation is set to optimally design HetNets with hybrid energy sources.

The objective of a good handoff algorithm is to decide an optimal connection with respect to the user performance, with minimal handoff latency and number of handoffs. The handoff direction considered in this research is from a macrocell to a femtocell. This direction is difficult to manage since the algorithm has to decide from a list of candidate femtocells to handover the call to. The handoff criteria is RSS-based, and femtocell deployment does not create any changes to conventional macrocell-based mobility management procedures with LTE integrated macrocell-femtocell hierarchy. Handoffs examined in [45] show that there is a significant gain with respect to the probability that the user will be assigned to the femtocell while keeping the same number of handoffs. In [54], the authors propose a holistic optimization framework that jointly optimizes enhanced Inter-Cell Interference Coordination (eICIC) and the assignment of multiple component carriers in an LTE-A deployment for increasing spectrum utilization at the small cells with appropriate blanking support from the macrocells. LTE-A macrocells deployments are being enhanced with overlay of small cells, i.e. low-power base stations, to increase the network coverage and capacity. However, simultaneous co-channel transmission from macro and small cells cause increased inter-cell interference and under-utilization of the spectrum at the small cells. The following LTE-A design techniques are used to improve system performance in such deployments: 1) Carrier Aggregation (CA) to increase capacity by using additional carrier bandwidth; 2) eICIC, that includes a) Cell Selection Biasing (CSB) to increase small cell spectrum utilization via cell range expansion and b) blanking data transmission using Almost Blank Subframes (ABS) on the macrocells for an certain duration of time to increase cell-edge user throughput. The authors' objective is to maximize the CSB of the small cell, subject to user QoS constraints and ABS support from the macrocell that end up with analytical model, which accounts for the complex inter-dependencies between these techniques. Simulation results demonstrate that the new approach increases the small cell spectrum utilization and aggregate cell-edge throughput by as much as 200%.

2.2. FFR Metrics

In this section, we review the previous research related to FFR metrics. The basic mechanism of FFR is to partition the macrocell service area into spatial regions and each sub-region is assigned different frequency sub-bands for users. In [14], the authors propose a frequency reuse technique that generates maximum throughput while iterating through a combination of inner cell radius and frequency allocation to the macrocell. LTE standards support a new technology in order to enhance indoor coverage. Femtocells technology is achieved through access points installed by home users. However, interference problem between the co-channel femtocell and the macrocell decreases the system's capacity and as a result users' throughput. In this work, the authors study the interference mitigation techniques in integrated femtocell/macrocell networks and propose a frequency reuse mechanism that leads to increased overall system throughput. In particular, the mechanism aims to maximize throughput via a series of combinations between inner cell radius and frequency allocation to the macrocell. The authors propose a performance metric, user satisfaction, which generates higher throughput with lower variance with optimization. A similar performance study is done by authors in [11], where FFR partitions each cell into two regions; inner region and outer region and allocates different frequency band to each region. Since the users at the inner region are less exposed to inter-cell interference, the frequency resources in each inner region can be universally reused, that is, the frequency reuse factor is set to 1. The cell-edge regions are subject to increased interference, therefore, the frequency reuse factor is set to 3. Based on this frequency band allocation, FFR may reduce channel interference and offer increased system capacity. The work also implements adaptation algorithm that adjusts the performance metrics and optimizes the throughput with users' mobility. Work in [10] proposes a mechanism that selects the optimal FFR configuration based on throughput and user satisfaction. The mechanism selects the inner region radius and the frequency allocation that either maximizes the mean user throughput or the user satisfaction. The mechanism is evaluated through a set of frequency allocations to determine the optimal solution. Simulations results prove that throughput optimized by cell mean throughput shows

higher values, but higher variance for user throughput values. The throughput optimized by user satisfaction metric shows relatively low throughput value, but lower variance for user throughput values. In [39], the authors analyze the FFR scheme and apply the algorithm of user satisfaction defined in [14] over three types of networks, FFR with macrocells only, FFR with cell-centric macrocell and randomly located femtocells, and FFR with cell-centric macrocell and edge-centric femtocell. All configurations have uniformly distributed users in the network. The authors determine the best possible inner region radius and inner region frequency allocation to generate optimal network configuration with best possible user fairness and overall throughput. The authors conclude that the network configuration with edge-centric femtocells show better user fairness with respect to user satisfaction results and relatively higher overall throughput. In [12], the user satisfaction metric introduced by the authors is evaluated for users' mobility and the performance is compared with other reuse schemes. The presence of macrocell and femtocells deployed in co-channel deployment will result in increased level of inter-cell interference, that will affect the overall system throughput. FFR mechanism is proven to mitigate and manage interference in such integrated LTE deployment. The authors propose a dynamic mechanism that selects the optimal FFR scheme based on user satisfaction metric and guarantees user fairness. The proposed mechanism selects the optimal radius and the optimal frequency allocation between these regions with the goal to maximize the user satisfaction metric. The proposed mechanism is evaluated through several simulation scenarios including users' mobility and its selected FFR scheme is compared with other frequency reuse schemes in order to highlight its performance. The research is further extended in [70] where cell-edge reuse factor is set to 1.5 and results are generated to determine the optimal inner radius and inner region bandwidth.

In [57], authors present a fractional reuse optimization scheme based on capacity density, the concept of per-area capacity (bit/s/Unit of Surface), which show better performance compared to conventional Reuse-1 and Reuse-3 schemes. This work presents a fractional frequency reuse optimization scheme based on capacity density. It assigns a given user to the frequency sub-band with maximum achievable capacity density (bit/s/m^2). The

authors formulate the optimization problem to maximize per-user throughput subject to cell-edge performance and FFR constraints. A sectorized layout with three-dimensional antenna radiation patterns is analyzed, which includes the effect of antenna downtilting on the signal-to-interference-plus-noise ratio distribution. Results proved the optimization solution was improved with antenna electrical downtilt. Graph theory and similar optimization techniques are presented in [19]. FFR technique is the most effective ICI mitigation technique for OFDMA networks. The paper introduces modified Brélaz's algorithm based on graph coloring to wireless networks with particular number of users. Typically, a graph coloring problem involves coloring the graph nodes with orthogonal colors which are treated as base stations. However, in this algorithm, the graph nodes are treated as users and applied colors corresponding to resource bands. The paper also demonstrates graph construction on FFR configurations such as Reuse-3, FFR-A, and FFR-B and applies the modified algorithm on fixed and dynamic versions of FFR configurations. For symmetric load conditions, the Reuse-3 outperforms FFR-A and FFR-B. The dynamic version of FFR-A and FFR-B can achieve a 12% and 33% gain in cell throughput and service rate over conventional FFR, and render a 70% and 107% gain in cell throughput and service rate with respect to the Reuse-3 configuration. Future extensions include realizing the different variations of FFR by customizing the graph to each FFR principle. Work in [9] presents determining the optimal number of resource blocks in FFR mechanism as an optimization problem with user data rate and system bandwidth constraints. It formulates the optimization problem and reduces it to a linear and integer-based optimization from complex non-tractable problem. Through analytical and simulation processes, it proves the optimal solution is calculated when frequency reuse factor in cell-edge regions is 3 and radius of cell-center region is 2/3 of the overall cell radius. In [28], the authors formulate an optimization problem for resource allocation in FFR algorithm in OFDMA networks. FFR divides the cell area into inner and cell-edge regions, with universal frequency reuse in the area close to the base station and higher reuse factor in the cell-edge regions. In this optimization, the objective is to determine the optimal reuse factor in cell-edge region, frequency allocation, subcarrier allocation

to each user, and power allocation for each user subject to minimum data rate requirements for the user. The optimal solution is the one with minimum power utilization and optimal resource allocation.

Authors in [24] use two-stage heuristic approach to find optimal frequency partitioning. In proposed FFR, the system bandwidth is divided into three breakdowns, where different reuse factors are applied. The optimization problem is to maximize the normalized spectral efficiency (nSE) subject to user fairness and data rate requirements. With the optimal parameters, the results show that the gain of the nSE between proposed FFR and conventional schemes is more than 3%, with 16% improvement in cell-edge user throughput. The goal in [69] is to simulate, measure and determine the best possible resource allocation out of the two FFR schemes, soft frequency reuse and partial frequency reuse. The system-level simulation results confirm the reuse factor 1 deployment optimizes the overall network throughput, but lowers the cell-edge throughput. Each of the FFR schemes outperforms the other in cell throughput and residual error rate. The authors propose dynamic FFR scheme as future extension and conclude soft frequency reuse as the best possible FFR scheme. Authors in [55] propose a solution with wide area coverage and still maintain high spectral efficiency in OFDMA networks. The solution involves coordinated scheduling between sectors of the same site, and applying higher frequency reuse factor in cell-edge regions. The proposed algorithm is compared with equivalent WCDMA system. The resulting sector throughput increases with the number of active users. When terminals have one antenna and channels are Rayleigh fading, it results in a sector payload capacity between 1.2 (one user) and 2.1 bits/s/Hz/sector (for 30 users) in an interference-limited environment. In [25], the authors review some of the recent advances in ICIC research and discuss the assumptions, advantages, and limitations of the proposed mechanisms. They discuss the inter-relationship between ICIC, scheduling strategies, and power control schemes. The trade-offs for ICIC determination leads to discussion on increased backhaul signalling and communication for increased coordination between base stations, poor resource utilization due to inter-cell collision avoidance strategies and unfair resource allocation due to throughput maximization

techniques. They also discuss the ICIC strategies from the standards to alleviate the interference issues and address the trade-offs. They propose a scheduling algorithm to schedule users based on channel quality and QoS metrics. Authors in [38] investigate an OFDMA radio resource control (RRC) scheme, where RRC control is exercised at both RNC and base stations. The proposed protocol focuses on three types of diversity, mutual interference diversity, traffic diversity, and selective fading channel diversity. With two-level optimization at RNC and base station, the channel is always assigned to the user with the highest utility value, a function of channel and traffic conditions. The linear complexity of the proposed algorithm is another benefit and provides more insights into sector interference suppression and dynamic interference avoidance with the assumption of communication of perfect channel state information and fixed transmission power. In [27], the authors present an analytical solution based on fluid model in OFDMA networks. Three configurations are studied by applying the fluid model, Integer Frequency Reuse 1 (IFR), IFR-Reuse K, FFR, and Two Level Power Control (TLPC). The analytical and simulation results are closely matched and show better time management than traditional methods using Monte Carlo simulations. Work in [30] show comparative simulation results of scheduling algorithms in FFR configuration in OFDMA networks. A combined metric considering throughput and fairness is introduced by the authors, that aims at a more suitable metric than previous capacity-based ones. The results prove that if the user fairness is required to be maintained, FFR offers no gain if correct scheduling is applied. FFR scheme applied in OFDMA networks is studied in [23]. The authors compare the performance of Strict FFR, Soft FFR, and traditional reuse mechanism and show the performance trade-offs in terms of cell-edge throughput, bandwidth utilization, and cell-center throughput. The results prove that both FFR mechanisms present reduced performance for cell-center users and improvements in cell-edge region. The simulation also presents results with FFR employing different frequency reuse factors in the algorithm.

OFDMA systems exploit the channel state information at the transmitter (CSIT) for capacity improvement. Authors in [71] apply the CSIT in FFR systems in OFDMA networks. They also address the methods to enhance the spectrum efficiency and utilization of

cell-edge regions in time-varying channels. They propose four new FFR configurations with CSIT included resulting in Strict FFR for FDD and TDD, and Soft FFR for FDD and TDD schemes. The results show that the performance is improved for cell-edge regions in the new FFR configurations by taking advantage of CSIT in the calculation, maintaining the overall system performance. Authors in [52] propose a semi-centralized joint cell muting and user scheduling scheme for interference management in FFR configuration in OFDMA networks, satisfying two temporal fairness criteria, Inter-Section Proportional Temporal Fairness (IS-PTF) and Min-Max Temporal Fairness (MMTF). In addition, they have also proposed a novel cell muting pattern set construction method applied in the joint scheme. IS-PTF application indicates that the proposed algorithm performance is better than the conventional algorithm. MMTF allows dynamic load balancing with acceptable algorithm complexity. They look to apply the algorithm to complex LTE and HetNets configurations. In [18], the authors perform optimization on different FFR configurations in OFDMA networks. They derive approximate closed-form mathematical expressions for calculating the probability distributions of interference levels measured at the designated receivers. They study the system throughput in terms of overall throughput and cell-edge performance, considering both uplink and downlink transmissions, fairness, and FFR scheduling schemes. Using optimization process, they determine the best possible configuration in each simulation scenario, where they consider optimal bandwidth allocation, optimal user classification as cell-center or cell-edge user, and cross-check with analytical results. Discussion in [42] focuses on development of closed-form mathematical expressions for worst-case SIR for several sectorized FFR configurations. It involves optimization of several simulation parameters such as antenna height, path loss exponent, and distance to the serving base station. The simulation and analytical results show close agreement. In [44], the authors propose a novel distributed algorithm to provide secure traffic monitoring in wireless sensor networks. The proposed algorithm outperforms the conventional methods with almost negligible packet loss rate and significant throughput, taking into consideration high user mobility rates.

CHAPTER 3

NETWORK PRODUCTIVITY FIXED FEMTOCELL DEPLOYMENT

3.1. Introduction

In this chapter, we investigate the network performance for a given network topology and determine reward and penalty weights for each femtocell access mode. For any new call arrival, a reward weight is assigned. For any handoff call failure due to forced termination, a penalty weight is assigned. These weights influence the network performance. Once we determine the weights, we utilize the values for other scenarios in our research.

We study the network performance by determining the maximum productivity with variable call arrival for a given network topology and previously determined weights. We design a constrained optimization problem that maximizes network productivity subject to upper bounds on the blocking probabilities as well as subcarrier resources available per cell. The solution to the optimization problem yields maximum network productivity and call arrival rates per cell. With femtocells operating in three access modes, we present results for each access mode for the same network topology.

3.2. LTE System Model

The mechanism assumes a topology that consists of 1 macrocell with 3 sector sites such that each sector is served by a different directional antenna. The beam directions of different sector antennas are separated by 120°. A constant number of femtocells per macrocell sector and uniformly distributed multicast users are considered. We consider the downlink transmission scenario in a tier-based cellular OFDMA network as shown in Fig. 1.8. We consider universal frequency reuse, i.e. all cells use the same spectrum, which is shared between macrocell and femtocells. We consider the interference from the first tier of neighboring cells only. We also consider the effect of path loss and lognormal shadowing on the transmitted signal. In practice, the association of user with macrocell or femtocell is determined based on SIR. If the SIR experienced by user from macrocell is above threshold, then it will be associated with macrocell, otherwise, femtocell. In our research, however,

we consider a model where users present in macrocell region are associated with macrocell directly and those present in femtocell region are associated with the corresponding femtocell. Out of the total call arrivals to the cell, a fraction is assumed to occur in macrocell region, while the remaining are assumed to have occurred in femtocell region. In a network with universal frequency reuse, users will experience interference from femtocells and macrocells of neighboring cells. We consider the rate requirement to be same for all users. The blocking probability on link between cells and users is calculated, and then overall blocking probability for tier-based OFDMA network is determined. After reviewing several options for blocking probability model to fit our research [6, 7, 13, 29, 43, 46, 61], the blocking probability model used in the chapter is based on [43, 61].

3.2.1. Subcarrier Allocation

The objective of base station is to satisfy the rate requirement of each user by allocating the requested number of subcarriers, which depends upon its experienced SINR. There are K_{BS} orthogonal subcarriers available at the base station, each of bandwidth W Hz. The SINR for downlink transmission to macro user x on a subcarrier n can be expressed as [37],

$$SINR_{x,n} = \frac{P_{M,n}G_{x,M,n}}{N_0\Delta f + \sum_{M'} P_{M',n}G_{x,M',n} + \sum_{F} P_{F,n}G_{x,F,n}} \tag{3.1}$$

where, $P_{M,n}$ and $P_{M',n}$ is transmit power of serving macrocell M and neighboring macrocell M' on subcarrier n, respectively. $G_{i,M,n}$ is channel gain between macro user i and serving macrocell M on subcarrier n and $G_{i,M',n}$ corresponds to channel gain from neighboring macrocell M'. Transmit power of neighboring femtocell F on subcarrier n is denoted by $P_{F,n}$ and $G_{i,F,n}$ represents channel gain between macro user i and neighboring femtocell F on subcarrier n. Finally, N_0 is white noise power spectral density and Δf is subcarrier spacing.

In case of a femto user f, the received SINR on a subcarrier n can be given by [37],

$$SINR_{f,n} = \frac{P_{F,n}G_{f,F,n}}{N_0\Delta f + \sum_{M} P_{M,n}G_{f,M,n} + \sum_{F'} P_{F',n}G_{f,F',n}} \tag{3.2}$$

where, F' is the set of interfering femtocells. The channel gain G, given by the following equation [37] is dominantly affected by path loss, which is assumed to be modeled based on urban path-loss PL as defined in [59].

$$G = 10^{-PL/10} \tag{3.3}$$

Additionally, we calculate the data rate of a user i achieved using M number of subcarriers, which can be estimated via the SINR from the following equation [37],

$$R = W \cdot (\sum_{n=1}^{M} \log_2(1 + \alpha \cdot SINR_n)) \tag{3.4}$$

where, W denotes the available bandwidth for each subcarrier divided by the number of users that share the specific subcarrier and α is a constant for a target bit error rate (BER) defined by $\alpha = -1.5/ln(5 \cdot BER)$. Here, we set BER to 10^{-6}.

Since no frequency dependent fast fading is considered, SIR on each subcarrier is same, $SINR_1 = SINR_2 = SINR_M = SINR$, the number of subcarriers (M) required by any user based on data rate requirement can be expressed as,

$$M = \frac{R \cdot \log_{10} 2}{W \cdot \log_{10}(1 + \alpha \cdot SINR)} \tag{3.5}$$

3.2.2. Call Arrival

We assume that call arrivals in each cell are Poisson distributed with mean arrival rate λ. Let, a fraction of the total call arrivals, say f, be served directly by macrocell, then the arrival rate of macrocell calls is $\lambda_m = f\lambda$ and that of femtocell calls is $\lambda_f = (1 - f)\lambda$. Since the users associated with femtocells are categorized as guaranteed and non-guaranteed users, their call arrival rates are also defined.

3.3. LTE Blocking Probability Model

To quantify capacity improvement, blocking probability of voice traffic is typically calculated using Erlang B formula. This calculation is based on the assumption that all users require same amount of resources to satisfy their rate requirement. However, in an OFDMA system, each user requires different number of subcarriers to meet its rate requirement. This

resource requirement depends on the SIR experienced by a user. Therefore, the Erlang B formula cannot be employed to compute blocking probability in an OFDMA network. An analytical expression to compute the blocking probability of tier-based cellular OFDMA network is utilized. Then, we classify the users into various classes depending upon their subcarrier requirement. We consider the system to be a multi-dimensional system with different classes and evaluate the blocking probability of system using the multi-dimensional Erlang loss formula [43] [61]. LTE blocking probability for guaranteed and non-guaranteed users is not the same if the femtocell operates in hybrid mode. Blocking probability values are calculated using expressions from [61]. For our research, we consider all users belonging to one class with M subcarrier requirement. That means, we consider all users have the same data rate requirement.

3.3.1. LTE Blocking Model One User Class

Blocking model used for calculating blocking probability for LTE femtocell CSG and OSG modes is based on the model specified in [43]. Authors in [43] denote $\mathbb{P}_{BS-MS}(M^r)$ the probability that an incoming user belongs to class r and requires M^r number of subcarriers on the $BS-MS$ link to meet its rate requirement, where BS refers to the base station, and MS refers to mobile station. It is determined as,

$$\mathbb{P}_{BS-MS}(M^r) = (F_I)_{BS-MS}(I^{r+1}_{BS-MS}) - (F_I)_{BS-MS}(I^{r}_{BS-MS}) \tag{3.6}$$

where, $(F_I)_{BS-MS}(I^{r+1}_{BS-MS})$ is the CDF of interference to signal ratio on $BS-MS$ link.

Setting to one class, the equation becomes,

$$\mathbb{P}_{BS-MS}(M^1) = (F_I)_{BS-MS}(I^{1}_{BS-MS}) \tag{3.7}$$

When a user is in base region and experiences SIR γ_{BS-MS}, it requires M^n_D number of subcarriers with probability $\mathbb{P}_{BS-MS}(M^n_D)$. The availability of subcarriers is determined at BS. If they are available, then M^n_D subcarriers are allocated by the BS.

The state of the BS is defined as,

$$\Omega_{BS} = (M^1_D U^1_D, M^2_D U^2_D, ..., M^{N_D}_D U^{N_D}_D) \tag{3.8}$$

where, U_D^n is the number of users of n^{th} class and M_D^n is the subcarrier requirement of n^{th} class of user calls and N_D is the total number of classes. Thus, the state of BS can be modified as, $\Omega_{BS} = (M_{BS}^m U_{BS}^m)$, where $m = 1, 2, ..., N_D$, denoting the class of users arriving at the BS. M_{BS}^m denotes the subcarrier requirement of m^{th} class of user and U_{BS}^m denotes number of users of m^{th} class arriving at the BS.

Setting to one class by assigning $N_D = 1, m = 1$, the equation becomes,

$$\Omega_{BS} = (M_D^1 U_D^1) \tag{3.9}$$

The state space is finite and the constraints to be met are,

$$\sum_{m=1}^{N_D} M_{BS}^m U_{BS}^m \leq K_{BS}, U_{BS}^m \geq 0, 1 \leq m \leq N_D \tag{3.10}$$

where, K_{BS} is the total number of subcarriers present at the BS.

Rearranging the state space definition to one class, the constraints become,

$$M_{BS}^1 U_{BS}^1 \leq K_{BS}, U_{BS}^1 \geq 0 \tag{3.11}$$

From [43], the blocking probability for m^{th} class user arriving at the base station BS is given by,

$$\mathbb{P}_{B_{BS}}^m = \sum_{\Omega_m} \mathbb{P}_{\Omega_{BS}} = \sum_{\Omega_m} \frac{\prod_{m=1}^{N_D} \frac{(\rho_m)^{U_{BS}^m}}{U_{BS}^m!}}{\sum\limits_{\Omega_{BS}} \prod_{m=1}^{N_D} \frac{(\rho_m)^{U_{BS}^m}}{U_{BS}^m!}} \tag{3.12}$$

where, $\rho_m = \frac{\lambda_{BS}^m}{\mu}$ and λ_{BS}^m is the call arrival rate of m^{th} class user at the BS.

For single class user, the blocking probability becomes,

$$\mathbb{P}_{B_{BS}}^1 = \sum_{\Omega_m} \mathbb{P}_{\Omega_{BS}} = \sum_{\Omega_m} \frac{\prod_{m=1}^{1} \frac{(\rho_1)^{U_{BS}^1}}{U_{BS}^1!}}{\sum\limits_{\Omega_{BS}} \prod_{m=1}^{1} \frac{(\rho_1)^{U_{BS}^1}}{U_{BS}^1!}} \tag{3.13}$$

The average blocking probability on $BS - MS$ link $(\mathbb{P}_B)_D$ is given by,

$$(\mathbb{P}_B)_D = \sum_{m=1}^{N_D} \mathbb{P}_{B_{BS}}^m \mathbb{P}_{BS-MS}(M_D^m) \tag{3.14}$$

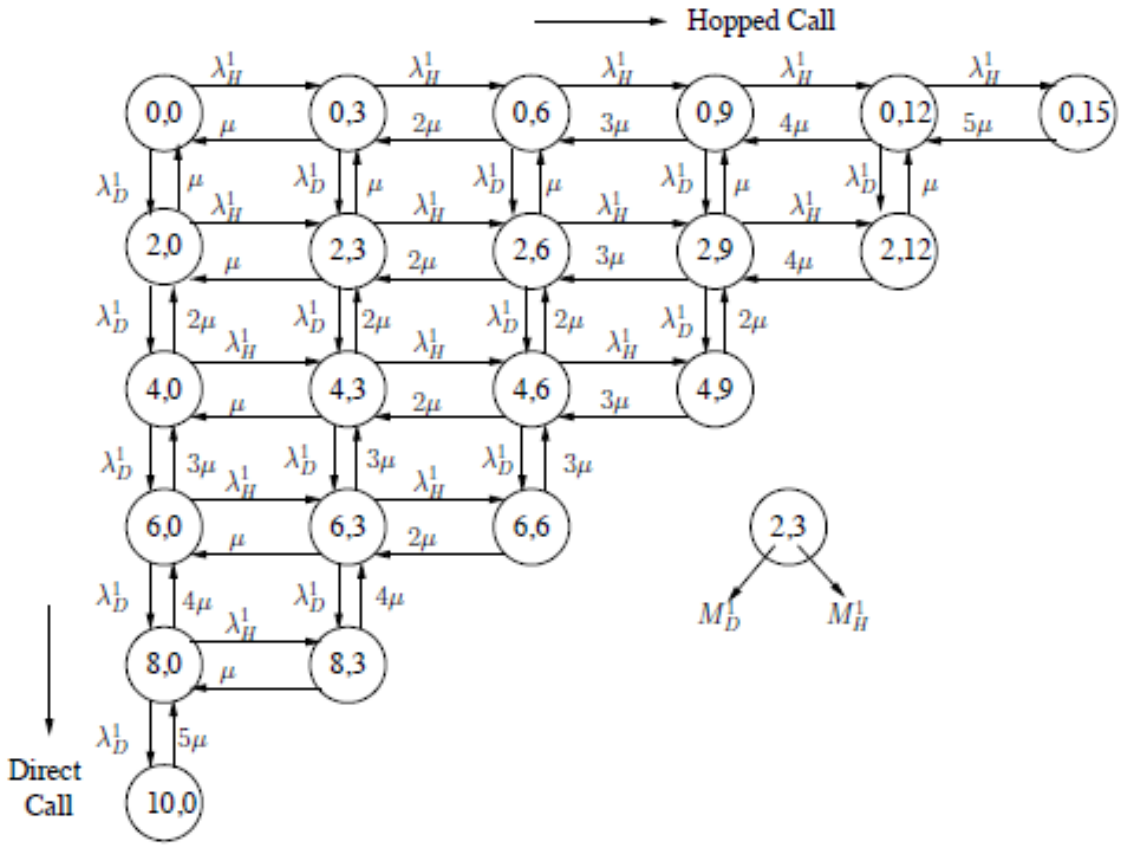

FIGURE 3.1. Markov state diagram showing direct and hopped calls [43]

The equation is reduced to the following if $N_D = 1$.

$$(\mathbb{P}_B)_D = \mathbb{P}^1_{B_{BS}} \mathbb{P}_{BS-MS}(M^1_D) \tag{3.15}$$

Since the authors in [43] assumed a relay-based system, the two-dimensional state diagram for a system with $K_{BS} = 10$, $K_{RS} = 6$, $M^1_D = 1$, and $M^1_H = 3$ is given by Fig. 3.1.

In our research, we only consider direct calls D and one user class, therefore, our state diagram becomes Fig. 3.2. In LTE, since we have multiple subcarriers per user, we assign multiple subcarriers per class and have users assigned to the class. Applying one set of class, we follow Markov chain in 1-dimension along Y-axis for direct calls. With this, we would still have a chain of states. In other words, $\Omega_{BS} = (M^1_D U^1_D)$ is not just 1 element, but represents a series of states. Work in [43] offers good application of Markov chain for LTE. On Y-axis, we hop each state for new call arrival. Each state is number of subcarriers assigned to user

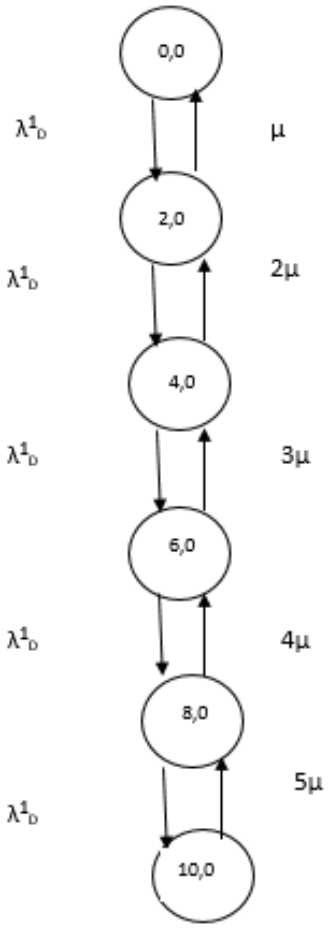

FIGURE 3.2. Markov state diagram showing direct calls for one user class

per class. Hence, we follow the Markov chain of states as shown in Fig. 3.2. To utilize this model, we keep bandwidth and number of channels constant and we calculate blocking probability for offered load. Applying the Eqn. 3.5, we calculate the number of subcarriers per user and number of simultaneous UEs or state diagram bubbles in our research as shown in Table 3.1.

3.3.2. Blocking Model for Hybrid Access Mode

Blocking model used for calculating blocking probability for LTE Hybrid mode is based on the model specified in [61]. In this model, channels are reserved for guaranteed users (SG) and cannot be accessed by the non-guaranteed users (NSG). If the reserved channels are occupied, the guaranteed users can use the remaining channels outside the

TABLE 3.1. Data Rate, Number of Subcarriers and Number of States

Data Rate (Kbps)	Number of Subcarriers per user	Number of States
2048	40	15
1024	20	30
512	10	60
256	5	120
64	1	600

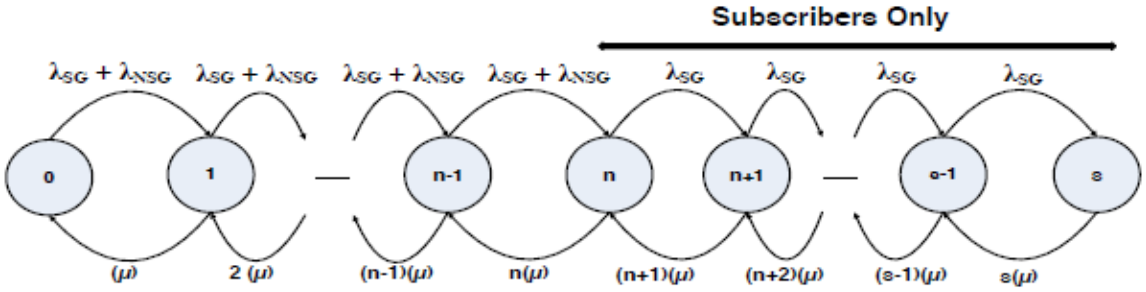

FIGURE 3.3. Markov state diagram showing direct calls for Hybrid access mode [61]

reserved range. Here, s represents the total number of channels, where, λ_{SG}, λ_{NSG}, μ_{SG}, and μ_{NSG} represent the call arrival rate and dwell time for guaranteed and non-guaranteed users respectively. From the Fig. 3.3, it is clear that the remaining states or channels n can be assigned to non-guaranteed users. In our research, we assign a fraction of total channels to the guaranteed users, and therefore, this model fits into Hybrid implementation for our research.

The authors calculate the blocking probabilities for SG and NSG users as follows,

$$P_j = [(\frac{\lambda_{SG} + \lambda_{NSG}}{\mu_{SG} + \mu_{NSG}})^j / j!]P_0, for\ 0 < j \leq n \tag{3.16}$$

$$P_j = [((\lambda_{SG})^{j-n}(\lambda_{SG} + \lambda_{NSG})^n)/(j!(\mu_{SG} + \mu_{NSG})^j)]P_0, for\ n < j \leq s \tag{3.17}$$

$$P_0 = 1/[\sum_{j=0}^{n}[(\frac{\lambda_{SG}+\lambda_{NSG}}{\mu_{SG}+\mu_{NSG}})^j/j!] + \sum_{j=n+1}^{s}\frac{(\lambda_{SG})^{j-n}(\lambda_{SG}+\lambda_{NSG})^n}{j!(\mu_{SG}+\mu_{NSG})^j}] \tag{3.18}$$

The blocking probability of the non-guaranteed users $P_{NSG,b}$ is dependent on number of unavailable channels, so

$$P_{NSG,b} = \sum_{j=n}^{s} P_j \tag{3.19}$$

where, P_j is given by Eqn. 3.17 and P_0 is given by Eqn. 3.18.

The blocking probability of the guaranteed users will be given by Eqns. 3.16, 3.17, and 3.18 and replacing j by s,

$$P_{SG,b} = ([(\frac{\lambda_{SG}+\lambda_{NSG}}{\mu_{SG}+\mu_{NSG}})^s/s!] + [[(\lambda_{SG})^{s-n}(\lambda_{SG}+\lambda_{NSG})^n]/[s!(\mu_{SG}+\mu_{NSG})^s]])P_0 \tag{3.20}$$

3.4. Traffic and Mobility Model

The call arrival process to cell i is assumed to be a Poisson process with rate λ_i independent of other call arrival processes. In the case of equal call arrival rates, $\lambda_i = \lambda$ for all i. The call dwell time is a random variable with exponential distribution having mean $\frac{1}{\mu}$ and is independent of earlier arrival times, call durations, and elapsed times of other users. At the end of a dwell time, a call may stay in the same cell, attempt a handoff to an adjacent cell, or leave the network. Define q_{ii} as the probability that a call in progress in cell i remains in cell i after completing its dwell time. In this case, a new dwell time that is independent of the previous dwell time begins immediately. Let q_{ij} be the probability that a call in progress in cell i after completing its dwell time goes to cell j. If cells i and j are not adjacent, then $q_{ij} = 0$. We denote by q_i the probability that a call in progress in cell i departs from the network. This mobility model is attractive because we can easily define different mobility scenarios by varying the values of these probability parameters [63]. For example, if q_i is constant for all i, then the average dwell time of a call in the network will be constant regardless of where the call originates and what the values of q_{ii} and q_{ij} are. Thus, in this case, by varying q_{ii}s and q_{ij}s, we can obtain low- and high-mobility scenarios and compare the effect of mobility on network throughput [4]. Let A_i be the set of cells

adjacent to cell i. Let ν_{ji} be the handoff rate out of cell j offered to cell i. ν_{ji} is the sum of the proportion of new calls accepted in cell j that go to cell i and the proportion of handoff calls accepted from cells adjacent to cell j that go to cell i. Thus,

$$\nu_{ji} = \lambda_j(1 - B_j)q_{ji} + (1 - B_j)q_{ji} \sum_{x \in A_j} \nu_{xj} \tag{3.21}$$

which can be rewritten as,

$$\nu_{ji} = (1 - B_j)q_{ji}\rho_j \tag{3.22}$$

where, ρ_i the total offered traffic to cell i, is given by

$$\rho_i(\overline{\lambda}, v) = \lambda_i + \sum_{j \in A_i} \nu_{ji}(\mathbf{B}, \overline{\rho}) \tag{3.23}$$

The total offered traffic can be obtained from a fixed point model [32], which describes the offered traffic as a function of the handoff and new call arrival rates, the handoff rates as a function of the blocking probabilities, and the offered traffic and the blocking probabilities as a function of the offered traffic.

3.5. Network Productivity Definition

Network productivity W is defined as the revenue generated by traffic with two components. First component is the revenue generated by accepting a new call and second component is the penalty incurred in forced termination due to handoff failure [3]. Hence, the final expression for network productivity applied to CSG and OSG femtocell deployments is,

$$W(B, \overline{\lambda}, \overline{\rho}) = \sum_{j=1}^{M} \{w_j\lambda_j(1 - B_j) - c_jB_j(\rho_j(\overline{\lambda}, v) - \lambda_j)\} \tag{3.24}$$

where, B_j is the blocking probability, ρ_j is the total offered load to cell j, λ_j is the call arrival rate, w_j is the revenue generated by accepting a call in cell j, and c_j is the cost of a forced termination of a call due to a handoff failure. When femtocells operate in hybrid access

mode, we need to consider reward and penalty terms associated with guaranteed and non-guaranteed users. Hence, the final expression for network productivity applied to Hybrid femtocell deployment becomes,

$$W(B,\overline{\lambda},\overline{\rho}) = \sum_{j=1}^{M}\{w_{g_j}\lambda_{g_j}(1-B_{g_j}) - c_{g_j}B_{g_j}(\rho_j(\overline{\lambda},v)-\lambda_{g_j}) + w_{ng_j}\lambda_{ng_j}(1-B_{ng_j}) - c_{ng_j}B_{ng_j}(\rho_j(\overline{\lambda},v)-\lambda_{ng_j})\} \tag{3.25}$$

where, B_{g_j} is the blocking probability for guaranteed users, ρ_j is the total offered load to cell j, λ_{g_j} is the call arrival rate for guaranteed users, w_{g_j} is the revenue generated by accepting a call from guaranteed user, and c_{g_j} is the cost of a forced termination of a call from guaranteed user due to handoff failure. Similar descriptions apply to the corresponding terms for non-guaranteed users.

3.6. Reward-Penalty Weights Assessment

3.6.1. Simulation Guidelines

Hybrid access reaches a compromise between the impact on the performance of guaranteed users and level of access granted to non-guaranteed users, allowing them to possess a limited amount of features [68, 72]. Reward weights are set to lower value than penalty weights since network performance is evaluated in worst possible conditions. Only high data rate, high mobility values are considered in weights assessment.

3.6.2. LTE Blocking Probability

Due to different resource allocation needs of guaranteed and non-guaranteed users, blocking probability will also differ. Typically, blocking probability for guaranteed users is less than non-guaranteed users. Since there is no user differentiation in macrocell coverage, same blocking probability is applied to each one of them. Guaranteed users experience less blocking compared to non-guaranteed since resources are reserved for them in the femtocell.

3.6.3. Network Productivity

We study the system behavior by calculating network productivity for different femtocell access modes. For low offered loads, the network productivity shows an increasing

trend and eventually drop as the network reaches saturation limit. Fig. 3.5 shows the comparative results of network productivity for each femtocell access modes with high data rate requirement and in high mobility scenario. We start the simulation with a specific setup for reward and penalty weights and determine the network productivity. Table 3.2 shows the initial setup for the LTE multi-tier network [62]. From Fig. 3.4, following conclusions can be made. Network with femtocells in CSG mode will show highest performance since only guaranteed users are allowed access to femtocell resource blocks. CSG and OSG femtocells show comparable results since guaranteed users in CSG are replaced by non-guaranteed users in OSG. Network with femtocells in Hybrid mode show lower performance due to penalty from handoff failure of guaranteed and non-guaranteed users combined. This is not desired network performance since Hybrid access mode is required to reach compromise between CSG and OSG. Hence, we tune the reward and penalty weights for the network. In the series of incremental changes, we update $c_j = 10$ for OSG macrousers since OSG mode is susceptible to higher number of handover attempts. This is still not desired network performance since the network does not fully capture difference in handover attempts between CSG and other modes. Therefore, we update $c_j = 1$ for CSG macrousers to simulate CSG femtocells experiencing fewer number of handover attempts. With this setup, the network does not fully capture difference in rewards for guaranteed users and non-guaranteed users. In the next step, we update $w_j = 2$ for CSG femtousers since guaranteed users in femtocell CSG mode experience less interference and handover attempts. This is still not desired network performance since the network does not fully capture difference in rewards for guaranteed users and non-guaranteed users for Hybrid mode. Now, we update to simulate the Hybrid feature of femtocells by tuning $w_j = 2$ for Hybrid femtousers since guaranteed users in femtocell Hybrid mode are prioritized in resource allocation and experience less interference and handover attempts. This is desired network performance since the network captures the properties of each femtocell access mode with guaranteed and non-guaranteed users. Hence, we utilize this network setup for upcoming results. Fig. 3.5 shows the network productivity for offered load with final reward and penalty weights. Table 3.3 shows the final setup

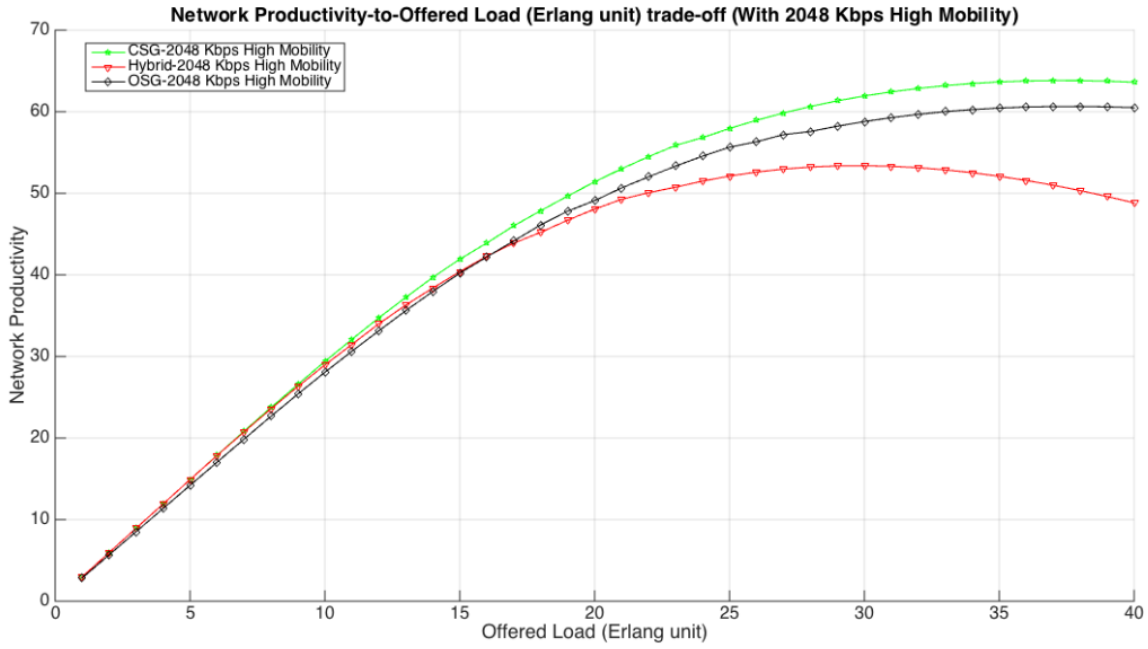

FIGURE 3.4. Initial setup showing network productivity for offered load

for the LTE network based on our research. Note that the network productivity metric is dimensionless unit and the results are interpreted as benchmark.

TABLE 3.2. Initial Set of Reward and Penalty Weights

Femtocell Access Mode	w_j	Femtocell Guaranteed Users c_j	w_j	Femtocell Non-Guaranteed Users c_j	w_j	Macrocell All Users c_j
Hybrid	1	5	1	5	1	5
CSG	1	5	NA	NA	1	5
OSG	NA	NA	1	5	1	5

3.7. Maximization of Network Productivity

We formulate a constrained nonlinear optimization problem with the objective function being the network productivity and constraints being the call blocking probabilities and

TABLE 3.3. Final Set of Reward and Penalty Weights

Femtocell Access Mode	w_j	Femtocell Guaranteed Users c_j	w_j	Femtocell Non-Guaranteed Users c_j	w_j	Macrocell All Users c_j
Hybrid	2	5	1	5	1	5
CSG	2	5	NA	NA	1	1
OSG	NA	NA	1	5	1	10

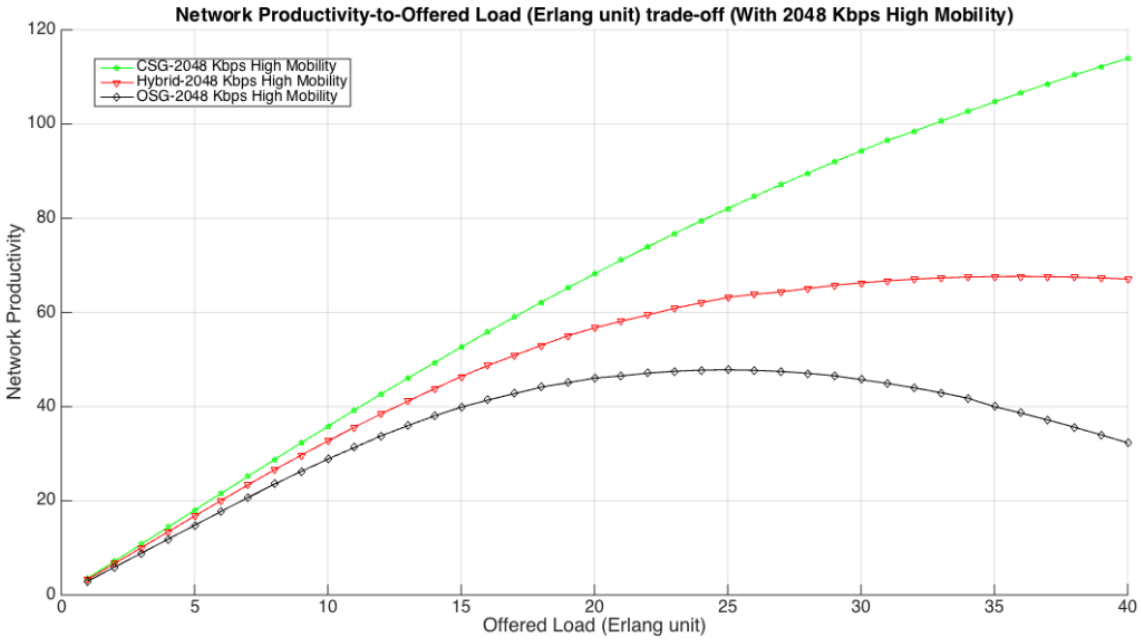

FIGURE 3.5. Final setup showing network productivity for offered load

subcarriers available at the base station [3]. The independent variables are the new call arrival rates per cell. Let $\overline{\eta}$ be the vector whose components represent the maximum call blocking probabilities for each cell and let $\overline{0}$ be the zero vector. Based on the user data rate requirement and the call arrival rate, the blocking probability is calculated such that the blocking threshold constraint is satisfied and maximum network throughput is determined.

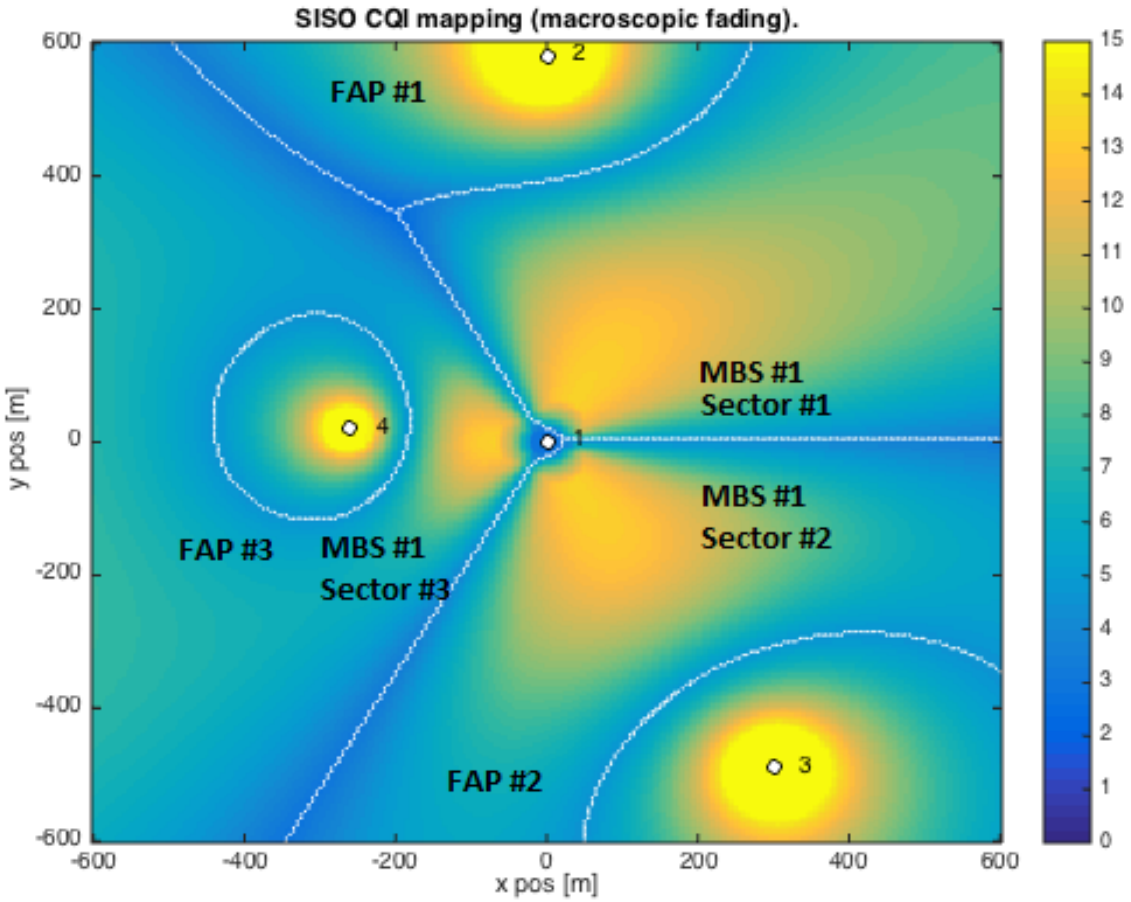

FIGURE 3.6. Network deployment showing 1 femtocell per macrocell sector

The optimization problem is,

$$\begin{aligned} \underset{\overline{\lambda}}{\text{maximize}} \quad & W(B, \overline{\lambda}, \overline{\rho}) \\ \text{subject to} \quad & B \leq \overline{\eta}, \\ & \overline{\lambda} \succeq \overline{0} \end{aligned}$$

3.8. Results

Table 3.4 shows the simulation parameters set for the research [31]. In femtocell, different blocking threshold values for guaranteed and non-guaranteed users are defined to indicate priority. Obviously, the blocking for guaranteed users is less than the non-guaranteed users, so as to allow femtocells to serve guaranteed users first. Non-guaranteed users blocking is much higher to be served after ensuring required subcarriers are allocated to guaranteed users. Table 3.5 shows the blocking probability threshold settings per cell. Table 3.6 shows

TABLE 3.4. Simulation Parameters for Optimized Productivity in Fixed Femtocell Setup

Parameter	Value
System Bandwidth	10 MHz
Subcarriers	50
Subcarrier Bandwidth	180 KHz
Cell Radius	250 m
Inter eNodeB distance	1000 m
Noise Power Spectral Density	-174 dBm/Hz
Subcarrier spacing	15 KHz
Channel Model	Typical Urban
Carrier Frequency	2000 MHz
Number of macrocells	1
Number of sectors per macrocell	3
Macrocell Transmit Power	40 W
Macrocell Antenna Gain	15dB
Macrocell Antenna Pattern	TS36.942 standard
Number of femtocells per macrocell sector	1
Femtocell Transmit Power	20 mW
Femtocell Antenna Gain	0 dB
Femtocell Antenna Pattern	Omni Directional
Femtocell Access Mode	OSG,CSG,Hybrid
Max Call Arrival Rate per macrocell sector	40
User Data Rate Requirement	2048 Mbps

the call arrival and subcarrier allocation parameters set for the research. Table 3.7 shows the call arrival and subcarrier allocation parameters applied only to femtocells. The numbers

TABLE 3.5. Blocking Probability Threshold Vector per cell

Femtocell Access	Femtocell Guaranteed Users	Femtocell Non-Guaranteed Users	Macrocell All Users
Hybrid	[0.005,0.0055,0.006,0.0065,0.07]	[0.1,0.2,0.3,0.4,0.5]	[0.01,0.015,0.02,0.025,0.03]
CSG	[0.005,0.0055,0.006,0.0065,0.07]	NA	[0.01,0.015,0.02,0.025,0.03]
OSG	NA	[0.1,0.2,0.3,0.4,0.5]	[0.01,0.015,0.02,0.025,0.03]

TABLE 3.6. Simulation Parameters for Macrocells and Femtocells

Parameter	Femtocells	Macrocells
Call Arrival Rate	0.5	0.5
Subcarrier Allocation	1.0	1.0

indicate the fraction of call arrival rates and subcarrier allocation reserved to guaranteed users in the femtocell. We assume low-mobility probability $q_{ij} = 0.012$ and high-mobility

TABLE 3.7. Simulation Parameters for Femtocells

Femtocell Acces Mode	Call Arrival Rate	Subcarrier Allocation
Hybrid	0.7	0.5
CSG	1.0	1.0
OSG	0.0	0.0

probability $q_{ij} = 0.06$ as shown in Table 3.8. From the table, it is clear that one set of network deployment is considered for consistency. The number of neighbors per cell is constant and set to 5. Network snapshot for this simulation is shown in the Fig. 3.6. Clearly, for low-mobility scenario, the probability that a call stays within the same cell q_{ii} is higher than high-mobility scenario. Inter-cell interference is set to specific values for each deployment

and varied by a uniform random distribution value between 0 and 1. Intra-cell mobility probability values are denoted by same subscript, q_{ii}. Inter-cell mobility probability values are denoted by different subscript, q_{ij}, indicating a probability value that a call accepted in cell i goes to cell j. The solution to the optimization problem gives the maximum productivity

TABLE 3.8. Simulation Parameters for Mobility Probabilities

Mobility	Neighbor Cells	q_{ij}	q_{ii}	q_i
No mobility	5	0.00	0.3	0.7
Low mobility	5	0.12	0.24	0.7
High mobility	5	0.06	0.00	0.7

that the network can generate for a given blocking probability vector. Using Matlab optimization module, we determine the optimal call arrival rate needed to design integrated LTE macrocell-femtocell network to meet given blocking probability threshold for the network. The result of the optimization process is call arrival rate per base station and the optimal network productivity. From Fig. 3.7, it is clear that productivity linearly increases as blocking threshold increases. Network productivity with Hybrid access femtocells is mid-way between CSG and OSG network deployment. The same network setup is used for all access plots to maintain consistency of results. Optimal network productivity for high, low and no mobility scenarios is shown in Figs. 3.7, 3.8 and 3.9. High mobility results show higher productivity than low and no mobility. The higher values of offered load and handover traffic for high mobility case explains the result trend. The maximum productivity is useful value as it provides the network administrator an upper bound to compare the actual productivity to, for an established traffic level. From the Tables 3.9, 3.10 and 3.11, we observe that during this time, the productivity is bound by blocking constraints with the solution being close to the initial values set for call arrival rates per cell. For both scenarios, the offered load to femtocells is higher than macrocells, which is desirable behavior since it supports macrocell offloading. Another simulation run to investigate the productivity trend for high molibity

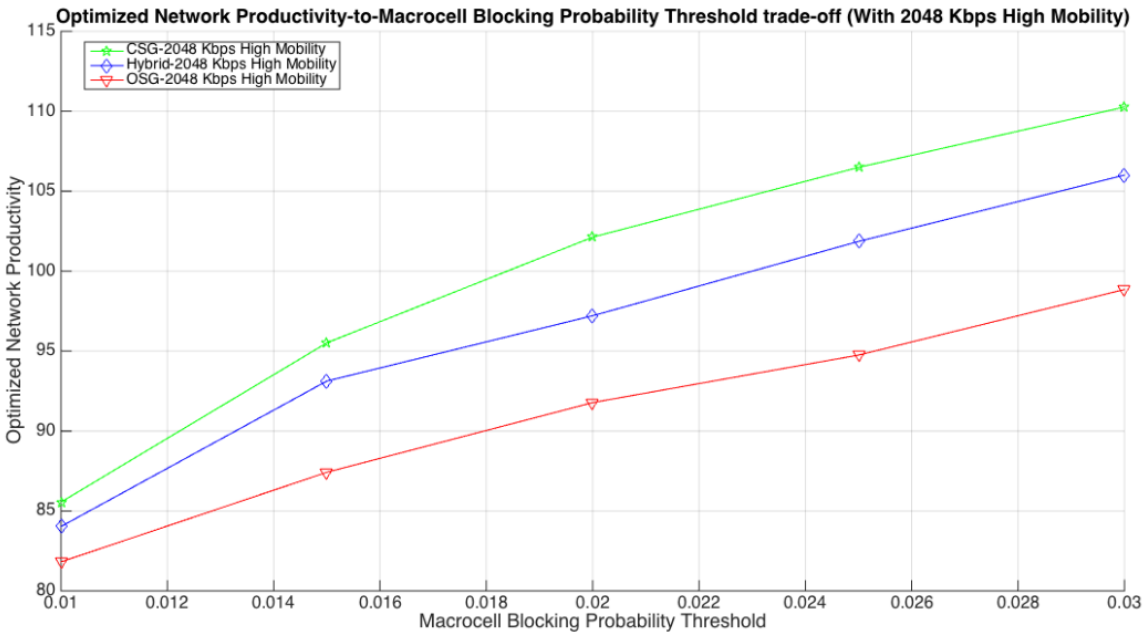

FIGURE 3.7. High mobility: Optimized network productivity for offered load

scenario by extending the blocking threshold shows similar increasing trend. Fig. 3.10 and Table 3.12 show the result with extended blocking threshold. However, the goal for any network operator is to maintain as low of blocking as possible and allow more calls in the network. Therefore, we focus on lower blocking thresholds for rest of the simulation.

3.9. Summary

The effect of call arrival rates and mobility on network performance of LTE heterogeneous system is analyzed. In this section, we propose a LTE heterogenous network setup which adheres to properties of three femtocell access modes. The basic principle of femtocell deployment is to provide high data rates to users with access and mitigate interference in tier-based network. Hybrid femtocell access is designed to mitigate such interference by prioritizing resources to guaranteed users to meet data rate requirement and allocating rest of the bandwidth to non-guaranteed users. Specific network events such as new call arrival and handoff termination are assigned reward and penalty weights which impact network performance. Starting with a proven set of reward-penalty weight pair, we fine-tune the weights to meet the LTE network properties for a given call blocking model. The final setup

TABLE 3.9. High Mobility Scenario: Call Arrival Rate and Optimized Network Productivity

Macrocell Blocking Probability	Femtocell Call Arrival	Call Arrival Rate Macrocell Call Arrival	Femtocell ρ_i	Offered Load Macrocell ρ_i	Optimized Productivity
Hybrid	Access				
0.01	11.3	8.6	14.97	12.45	84.03
0.015	12.3	9.9	16.39	14.15	93.13
0.02	12.5	10.9	16.87	15.36	97.21
0.025	12.9	11.75	17.52	16.46	101.86
0.03	13.2	12.57	18.00	17.38	106.01
CSG	Access				
0.01	9.9	8.6	13.42	12.21	85.57
0.015	10.9	9.9	14.89	13.96	95.52
0.02	11.5	10.9	15.79	15.25	102.13
0.025	11.8	11.75	16.30	16.30	106.49
0.03	12.3	12.0	16.59	16.60	110.0
OSG	Access				
0.01	18	8.6	22.19	13.24	81.82
0.015	18.5	9.9	23.02	14.81	87.42
0.02	18.9	10.9	23.67	16.01	91.78
0.025	19	11.75	23.96	16.99	94.75
0.03	19.5	12.57	24.68	17.99	98.85

of reward-penalty weights can be utilized as a stable starting point for further research with other channel models, frequency reuse scenarios and variable number of femtocells in dense deployments. For varying offered loads, optimized network productivity with hybrid access

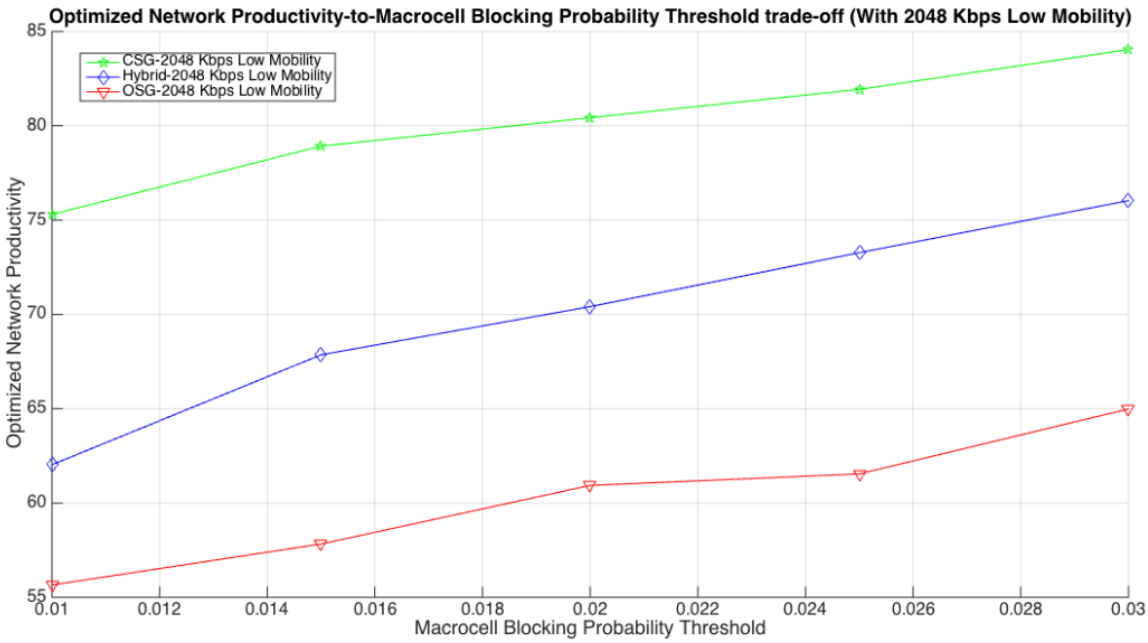

FIGURE 3.8. Low mobility: Optimized network productivity for offered load

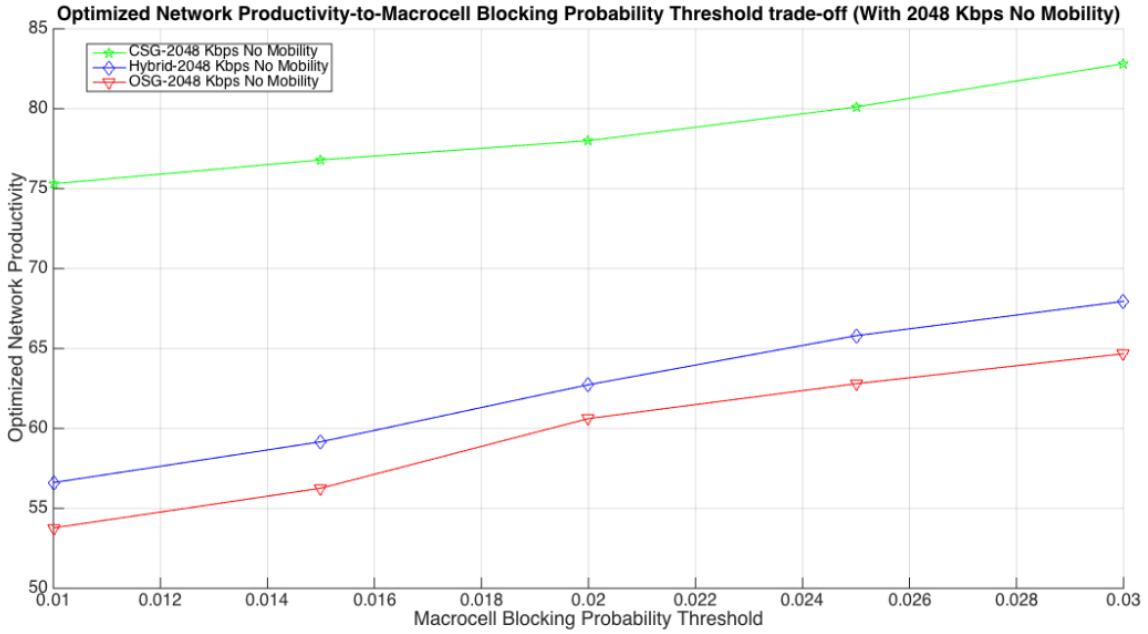

FIGURE 3.9. No mobility: Optimized network productivity for offered load

femtocells is mid-way between CSG and OSG network deployment. Results for low, high and no mobility scenarios are presented for comparison.

TABLE 3.10. Low Mobility Scenario: Call Arrival Rate and Optimized Network Productivity

Macrocell Blocking Probability	Femtocell Call Arrival	Call Arrival Rate Macrocell Call Arrival	Femtocell ρ_i	Offered Load Macrocell ρ_i	Optimized Productivity
Hybrid	Access				
0.01	8.2	6.6	8.65	7.07	62.03
0.015	8.8	7.5	9.30	8.02	67.86
0.02	9.0	8.0	9.52	8.53	70.41
0.025	9.2	8.6	9.75	9.16	73.27
0.03	9.5	9.0	10.07	9.58	76.03
CSG	Access				
0.01	8.5	8.0	9.02	8.53	75.30
0.015	8.8	8.6	9.35	9.15	78.92
0.02	9.0	8.7	9.56	9.26	80.43
0.025	9.1	9.0	9.67	9.57	81.93
0.03	9.3	9.3	9.89	9.89	84.04
OSG	Access				
0.01	11.5	6.6	12.02	7.16	55.65
0.015	11.8	7.0	12.33	7.58	57.83
0.02	12.2	7.6	12.76	8.21	60.93
0.025	12.4	7.6	12.97	8.22	61.55
0.03	12.5	8.6	13.11	9.24	64.99

TABLE 3.11. No Mobility Scenario: Call Arrival Rate and Optimized Network Productivity

Macrocell Blocking Probability	Femtocell Call Arrival	Call Arrival Rate Macrocell Call Arrival	Femtocell ρ_i	Offered Load Macrocell ρ_i	Optimized Productivity
Hybrid	Access				
0.01	7.6	6.05	7.6	6.05	56.61
0.015	7.7	6.9	7.7	6.9	59.16
0.02	7.9	7.6	7.9	7.6	62.73
0.025	8.15	8.3	8.15	8.3	65.81
0.03	8.3	8.8	8.3	8.8	67.95
CSG	Access				
0.01	8.5	8.0	8.5	8.0	75.30
0.015	8.5	8.5	8.5	8.5	76.80
0.02	8.7	8.5	8.7	8.5	78.00
0.025	8.8	9.0	8.8	9.0	80.11
0.03	9.1	9.3	9.1	9.3	82.81
OSG	Access				
0.01	11.5	6.0	11.5	6.0	53.77
0.015	11.8	6.5	11.8	6.5	56.26
0.02	12.2	7.5	12.2	7.5	60.62
0.025	12.4	8.0	12.4	8.0	62.17
0.03	12.5	8.5	12.5	8.5	64.67

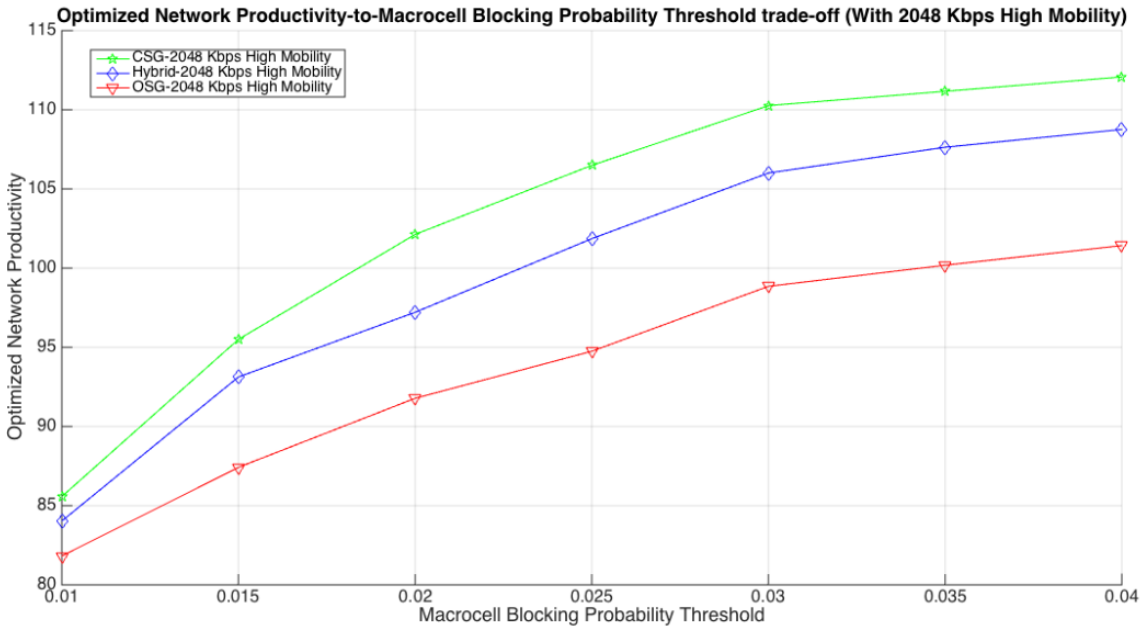

FIGURE 3.10. High mobility: Optimized network productivity for offered load with extended blocking threshold

TABLE 3.12. High Mobility Scenario: Call Arrival Rate and Optimized Network Productivity with Extended Blocking Threshold

Macrocell Blocking Probability	Femtocell Call Arrival	Call Arrival Rate Macrocell Call Arrival	Femtocell ρ_i	Offered Load Macrocell ρ_i	Optimized Productivity
Hybrid	Access				
0.01	11.3	8.6	14.97	12.45	84.03
0.015	12.3	9.9	16.39	14.15	93.13
0.02	12.5	10.9	16.87	15.36	97.21
0.025	12.9	11.75	17.52	16.46	101.86
0.03	13.2	12.57	18.00	17.38	106.01
0.035	13.4	12.8	18.32	17.75	107.63
0.04	13.5	13	18.41	17.96	108.76
CSG	Access				
0.01	9.9	8.6	13.42	12.21	85.57
0.015	10.9	9.9	14.89	13.96	95.52
0.02	11.5	10.9	15.79	15.25	102.13
0.025	11.8	11.75	16.30	16.30	106.49
0.03	12.3	12.0	16.59	16.60	110.26
0.035	12.4	12.1	17.12	16.84	111.17
0.04	12.5	12.2	17.20	16.92	112.07
OSG	Access				
0.01	18	8.6	22.19	13.24	81.82
0.015	18.5	9.9	23.02	14.81	87.42
0.02	18.9	10.9	23.67	16.01	91.78
0.025	19	11.75	23.96	16.99	94.75
0.03	19.5	12.57	24.68	17.99	98.85
0.035	19.7	12.8	24.96	18.28	100.19
0.04	19.9	13	25.21	18.54	101.42

CHAPTER 4

NETWORK PRODUCTIVITY VARIABLE FEMTOCELL DEPLOYMENT

4.1. Introduction

LTE femtocells are designed to increase capacity and coverage especially for the indoor and cell-edge mobile users. Typically, they are deployed to offload the macrocell users. However, due to co-location of femtocells in macrocell coverage, the co-tier and cross-tier interferences are high. The interference levels are different for each femtocell access mode. In this chapter, we conduct simulation and study the network performance of LTE network with increasing number of femtocells operating in three access modes.

We define network productivity which measures the network performance based on reward associated with new call arrivals and penalty accounted for forced termination due to handoff failure. Using specific parameter setup for reward and penalty weights for each network deployment from previous simulations, we present the effects of call mobility on network performance with increasing femtocell densification. Using Matlab optimization module, we also determine the best possible number of femtocells that yield maximum network throughput for a given blocking probability vector. We define a network performance function for traffic that is carried successfully. We take into account revenue generated by accepting a new call and the cost of forced termination due to handoff failure. The chapter concludes with a desired set of call arrival rate per cell to generate maximum productivity in the LTE network with increasing femtocells operating in three access modes.

4.2. LTE System Model

The mechanism assumes a topology that consists of a grid of 1 macrocell, each with 3 sector sites such that each sector is served by a different directional antenna. The beam directions of different sector antennas are separated by 120°. A constant number of femtocells per macrocell sector and uniformly distributed multicast users are considered. The femtocells per macrocell sectors is increased to simulate densification. We consider the downlink transmission scenario in a tier-based cellular OFDMA network as shown in Fig. 1.8. We con-

sider universal frequency reuse, i.e. all cells use the same spectrum, which is shared between macrocell and femtocells. We consider the interference from the first tier of neighboring cells only. We also consider the effect of path loss and lognormal shadowing on the transmitted signal. In practice, the association of user with macrocell or femtocell is determined based on SIR. If the SIR experienced by user from macrocell is above threshold, then it will be associated with macrocell, otherwise, femtocell. In this chapter, however, we consider a model where users present in macrocell region are associated with macrocell directly and those present in femtocell region are associated with the corresponding femtocell. Out of the total call arrivals to the cell, a fraction is assumed to occur in macrocell region, while the remaining are assumed to have occurred in femtocell region. In a network with universal frequency reuse, users will experience interference from femtocells and macrocells of neighboring cells. We consider the rate requirement to be same for all users. The blocking probability between cells and users is calculated, and then overall blocking probability for tier-based OFDMA network is determined. After reviewing several options for blocking probability model to fit our research [6, 7, 13, 29, 43, 46, 61], the blocking probability model used in the chapter is based on [43, 61].

4.2.1. Subcarrier Allocation

The objective of base station is to satisfy the rate requirement of each user, by allocating it the requested number of subcarriers which depends upon its experienced SINR. There are K_{BS} orthogonal subcarriers available at the base station, each of bandwidth W Hz. We calculate the data rate of a user i achieved using M number of subcarriers, which can be estimated via the SINR from the following equation [37],

$$R = W \cdot (\sum_{n=1}^{M} \log_2(1 + \alpha \cdot SINR_n)) \tag{4.1}$$

where W denotes the available bandwidth for each subcarrier divided by the number of users that share the specific subcarrier and α is a constant for a target bit error rate (BER) defined by $\alpha = -1.5/ln(5 \cdot BER)$. Here, we set BER to 10^{-6}. Since no frequency dependent fast fading is considered, SIR on each subcarrier is same, $SINR_1 = SINR_2 = SINR_M = SINR$,

the number of subcarriers (M) required by any users can be expressed as,

$$M = \frac{R \cdot \log_{10} 2}{W \cdot \log_{10}(1 + \alpha \cdot SINR)} \tag{4.2}$$

4.2.2. Call Arrival

We assume that call arrivals in each cell are Poisson distributed with mean arrival rate λ. Let, a fraction of the total call arrivals, say f be served directly by macrocell, then the arrival rate of macrocell calls is $\lambda_m = f\lambda$ and that of femtocell calls is $\lambda_f = (1 - f)\lambda$. Since the users associated with femtocells are categorized as guaranteed and non-guaranteed users, their call arrival rates are also defined.

4.3. LTE Blocking Probability Model

To quantify capacity improvement, blocking probability of voice traffic is typically calculated using Erlang B formula. This calculation is based on the assumption that all users require same amount of resources to satisfy their rate requirement. However, in an OFDMA system, each user requires different number of subcarriers to meet its rate requirement. This resource requirement depends on the SIR experienced by a user. Therefore, the Erlang B formula cannot be employed to compute blocking probability in an OFDMA network. An analytical expression to compute the blocking probability of tier-based cellular OFDMA network is utilized. Then, we classify the users into various classes depending upon their subcarrier requirement. We consider the system to be a multi-dimensional system with different classes and evaluate the blocking probability of system using the multi-dimensional Erlang loss formula [43] [61]. LTE blocking probability for guaranteed and non-guaranteed users is not the same if the femtocell operates in hybrid mode. Blocking probability values were calculated using expressions from [61].

4.4. Traffic and Mobility Model

The call arrival process to cell i is assumed to be a Poisson process with rate λ_i independent of other call arrival processes. In the case of equal call arrival rates, $\lambda_i = \lambda$ for all i. The call dwell time is a random variable with exponential distribution having mean

$\frac{1}{\mu}$ and is independent of earlier arrival times, call durations, and elapsed times of other users. At the end of a dwell time, a call may stay in the same cell, attempt a handoff to an adjacent cell, or leave the network. Define q_{ii} as the probability that a call in progress in cell i remains in cell i after completing its dwell time. In this case, a new dwell time that is independent of the previous dwell time begins immediately. Let q_{ij} be the probability that a call in progress in cell i after completing its dwell time goes to cell j. If cells i and j are not adjacent, then $q_{ij} = 0$. We denote by q_i the probability that a call in progress in cell i departs from the network. This mobility model is attractive because we can easily define different mobility scenarios by varying the values of these probability parameters [63]. For example, if q_i is constant for all i, then the average dwell time of a call in the network will be constant regardless of where the call originates and what the values of q_{ii} and q_{ij} are. Thus, in this case, by varying q_{ii}s and q_{ij}s, we can obtain low- and high-mobility scenarios and compare the effect of mobility on network throughput [4].

4.5. Maximization of Network Productivity

We formulate a constrained nonlinear optimization problem with the objective function being the network productivity and constraints being the call blocking probabilities [3]. The independent variables are the new call arrival rates λ and number of femtocells per macrocell sector F. Let $\overline{\eta}$ be the vector whose components represent the maximum call blocking probabilities for each cell and let $\overline{0}$ be the zero vector. Then, the optimization problem is,

$$\begin{aligned} \underset{\overline{\lambda},F}{\text{maximize}} \quad & W(B,\overline{\lambda},\overline{\rho}) \\ \text{subject to} \quad & B \preceq \overline{\eta}, \\ & \overline{\lambda} \succeq \overline{0}, \\ & F = 1,2,...,10 \end{aligned}$$

The solution to the optimization problem gives the maximum productivity that the network can generate for a given blocking probability vector. Using Matlab optimization module, we determine the optimal call arrival rate needed to design integrated LTE

macrocell-femtocell network to meet given blocking probability threshold for increasing femtocell deployment. The result of the optimization process is call arrival rate per base station and the optimal network productivity. We iterate the optimization for each network deployment with femtocell densification.

4.5.1. Extreme Densification

Network densification is a combination of spatial and spectral aggregation. Spatial densification is realized by increasing the number of antennas per node (user device and base station), and increasing the density of base stations deployed in the given geographic area, while ensuring nearly uniform distribution of users among all base stations. In our research, we focus on spatial densification by varying the density of femtocells per macrocell sector.

4.5.2. Simulation Guidelines

Hybrid access reaches a compromise between the impact on the performance of guaranteed users and level of access granted to non-guaranteed users, allowing them to possess a limited amount of features [68, 72]. Reward weights are set to lower value than penalty weights since network performance is evaluated in worst possible conditions. Only high data rate, high mobility values are considered for weights assessment.

4.6. Results

Network deployment with increasing number of femtocells show interesting trends in productivity, offered load, handover activity and cell blocking. The call arrival rates per cell interact with the parameters under review and generate results as explained in this section. Table 4.1 shows the simulation parameters set for the research [31]. Table 4.2 shows the call arrival and subcarrier allocation parameters set for the research. Table 4.3 shows the call arrival and subcarrier allocation parameters applied only to femtocells. The numbers indicate the fraction of call arrival rates and subcarrier allocation reserved to guaranteed users in the femtocell. For variable number of neighbors, the mobility probabilities are set as shown in Tables 4.4, 4.5 and 4.6. Inter-cell interference is set to specific values for each deployment and varied by a uniform random distribution value between 0 and 1.

TABLE 4.1. Simulation Parameters for Optimized Productivity in Variable Femtocell Setup

Parameter	Value
System Bandwidth	10 MHz
Subcarriers	50
Subcarrier Bandwidth	180 KHz
Cell Radius	250 m
Inter eNodeB distance	1000 m
Noise Power Spectral Density	-174 dBm/Hz
Subcarrier spacing	15 KHz
Channel Model	Typical Urban
Carrier Frequency	2000 MHz
Number of macrocells	1
Number of sectors per macrocell	3
Macrocell Transmit Power	40 W
Macrocell Antenna Gain	15dB
Macrocell Antenna Pattern	TS36.942 standard
Number of femtocells per macrocell sector	1-10
Femtocell Transmit Power	20 mW
Femtocell Antenna Gain	0 dB
Femtocell Antenna Pattern	Omni Directional
Femtocell Access Mode	OSG,CSG,Hybrid
Max Call Arrival Rate per macrocell sector	100
User Data Rate Requirement	2048 Mbps

TABLE 4.2. Simulation Parameters for Macrocells and Femtocells

Parameter	Femtocells	Macrocells
Call Arrival Rate	0.5	0.5
Subcarrier Allocation	1.0	1.0

TABLE 4.3. Simulation Parameters for Femtocells

Femtocell Acces Mode	Call Arrival Rate	Subcarrier Allocation
Hybrid	0.7	0.5
CSG	1.0	1.0
OSG	0.0	0.0

TABLE 4.4. High Mobility: Simulation Parameters for Mobility Probabilities with Variable Neighbors

Femtocells per Macrocell Sector	Neighbor Cells	Mobility q_{ij}	Probabilities q_{ii}	Values q_i
1	5	0.06	0.00	0.7
2	8	0.0375	0.00	0.7
3	11	0.027	0.00	0.7
4	14	0.021	0.00	0.7
5	17	0.0176	0.00	0.7
6	20	0.015	0.00	0.7
7	23	0.013	0.00	0.7
8	26	0.01153	0.00	0.7
9	29	0.0103	0.00	0.7
10	32	0.00094	0.00	0.7

TABLE 4.5. Low Mobility: Simulation Parameters for Mobility Probabilities with Variable Neighbors

Femtocells per Macrocell Sector	Neighbor Cells	Mobility q_{ij}	Probabilities q_{ii}	Values q_i
1	5	0.012	0.24	0.7
2	8	0.0075	0.24	0.7
3	11	0.00545	0.24	0.7
4	14	0.0043	0.24	0.7
5	17	0.0035	0.24	0.7
6	20	0.003	0.24	0.7
7	23	0.0026	0.24	0.7
8	26	0.0023	0.24	0.7
9	29	0.0021	0.24	0.7
10	32	0.0018	0.24	0.7

4.6.1. Blocking Probability Threshold

In femtocell, different blocking threshold values for guaranteed and non-guaranteed users are defined to indicate priority. Table 4.7 shows the blocking probability threshold settings per cell.

4.6.2. Reward-Penalty Weights Specification

We study the system behavior by calculating network productivity for different femtocell access modes. For low traffic, the network productivity shows an increasing trend and eventually drops as the network reaches saturation limit. Fig. 3.5 shows the comparative values for reward and penalty weights for each femtocell access modes with high data rate requirement and in high mobility scenario. Table 4.8 shows the weights assigned for the LTE network based on our previous research [51]. From Fig. 4.3, it is clear that productivity linearly increases with femtocells as resources are added to the network for all access

TABLE 4.6. No Mobility: Simulation Parameters for Mobility Probabilities with Variable Neighbors

Femtocells per Macrocell Sector	Neighbor Cells	Mobility q_{ij}	Probabilities q_{ii}	Values q_i
1	5	0	0.3	0.7
2	8	0	0.3	0.7
3	11	0	0.3	0.7
4	14	0	0.3	0.7
5	17	0	0.3	0.7
6	20	0	0.3	0.7
7	23	0	0.3	0.7
8	26	0	0.3	0.7
9	29	0	0.3	0.7
10	32	0	0.3	0.7

TABLE 4.7. Blocking Probability Threshold per cell

Femtocell Access	Femtocell Guaranteed Users	Femtocell Non-Guaranteed Users	Macrocell All Users
Hybrid	0.005	0.1	0.01
CSG	0.01	NA	0.01
OSG	NA	0.1	0.01

modes. Network productivity with hybrid access femtocells is mid-way between CSG and OSG network deployment. The same network setup is used for all access plots to maintain consistency of results. Uniform deployment is ensured by associating equal number of femtocells per macrocell sector. For example, if femtocells per macrocell sector is 3, simulation

ensures 3 femtocells are deployed and are associated with each macrocell sector. Simulation is designed to not assign 2 femtocells and 4 femtocells to macrocell sector and disrupt the uniformity. Fig. 4.1 shows a network snapshot for 6 femtocells distribution per macrocell sector.

TABLE 4.8. Reward-Penalty Weights Specification

Femtocell Access Mode	Femtocell Guaranteed Users w_j,c_j	Femtocell Non-Guaranteed Users w_j,c_j	Macrocell All Users w_j,c_j
Hybrid	2,5	1,5	1,5
CSG	2,5	NA,NA	1,1
OSG	NA,NA	1,5	1,10

4.6.3. Network Productivity Regions

The optimization problem provides optimal call arrival rate for macrocell and femtocell that maximizes the productivity and satisfies the blocking constraints. The call arrival rate to macrocell remains constant with the varying femtocells in the network. As the femtocells are added, the call arrival rate to each femtocell is updated to divide the rate proportionately in the network. We observe 3 regions in the Fig. 4.2 based on the productivity trend. Region 1 is network deployment where femtocells is less than 6 per macrocell sector. Region 2 is network deployment when femtocells is equal to 6 per macrocell sector. Region 3 is network deployment when femtocells is greater than 6 per macrocell sector. For the given effective call arrival rate of 100, the region division occurs at 6 femtocells. This point varies when effective call arrival rate is changed. We observe that the productivity linearly increases until the network has 6 femtocells per macrocell sector. In region 1, the upper bound is set to the incoming call arrival rate per cell. The lower bound call arrival rate is set to pre-determined value that satisfies the blocking constraints per cell.

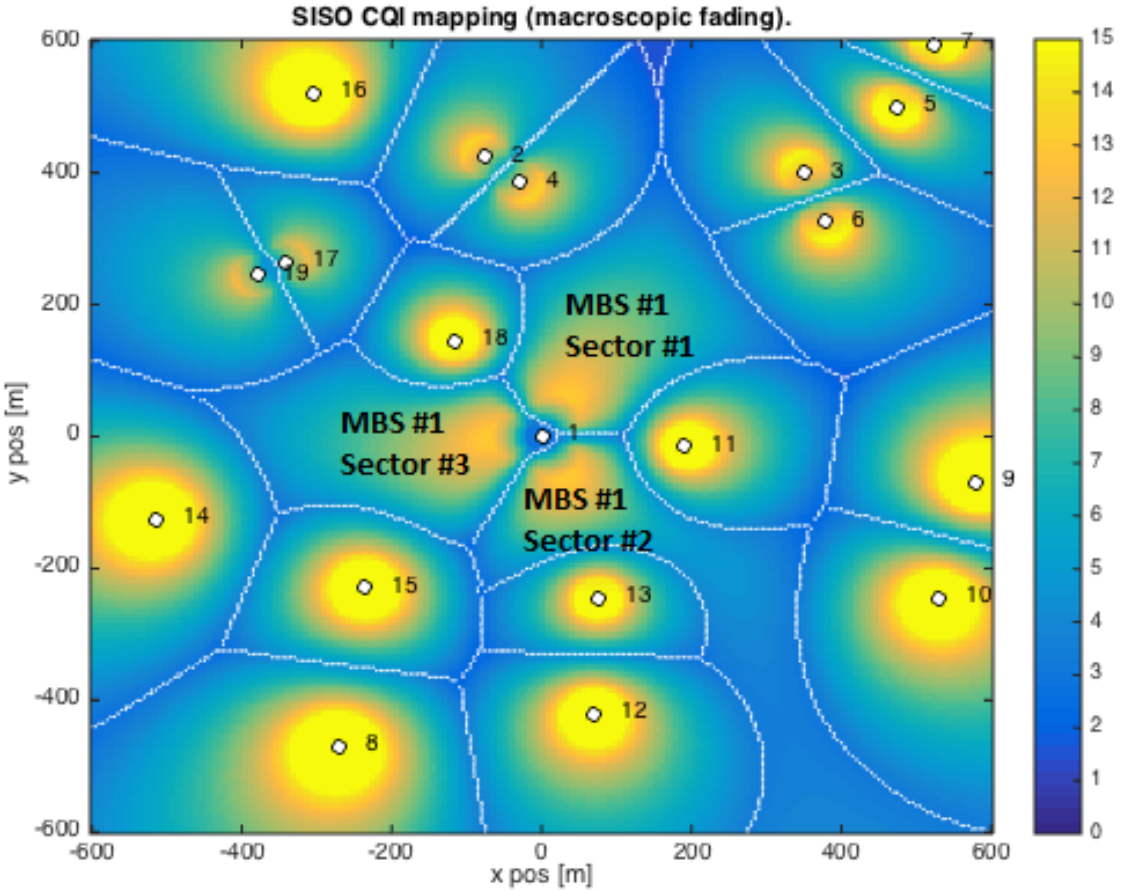

FIGURE 4.1. Network deployment showing 6 femtocells per macrocell sector

From the Tables 4.9, 4.12, we observe that during this time, the productivity is bound by blocking constraints more than call arrival as the lower bound is significantly less than the upper bound arrival rate. When number of femtocells per macrocell sector is 6 at the peak point in region 2, the productivity is bound by blocking threshold and upper bound arrival rate. After the network crosses 6 femtocells (region 3) and as the call arrival rate (upper bound) is proportionately set, it becomes less than the pre-determined lower bound, resulting in constraint violation which the simulation identifies. The simulation adjusts the lower bound arrival rate, preserves the optimization constraint and compensates with decline in productivity. Therefore, during this simulation time, the productivity is bound by call arrival rate more than the blocking constraints as the lower bound is close to the upper bound call arrival rate. Fig. 4.5 shows the three regions for high mobility scenario.

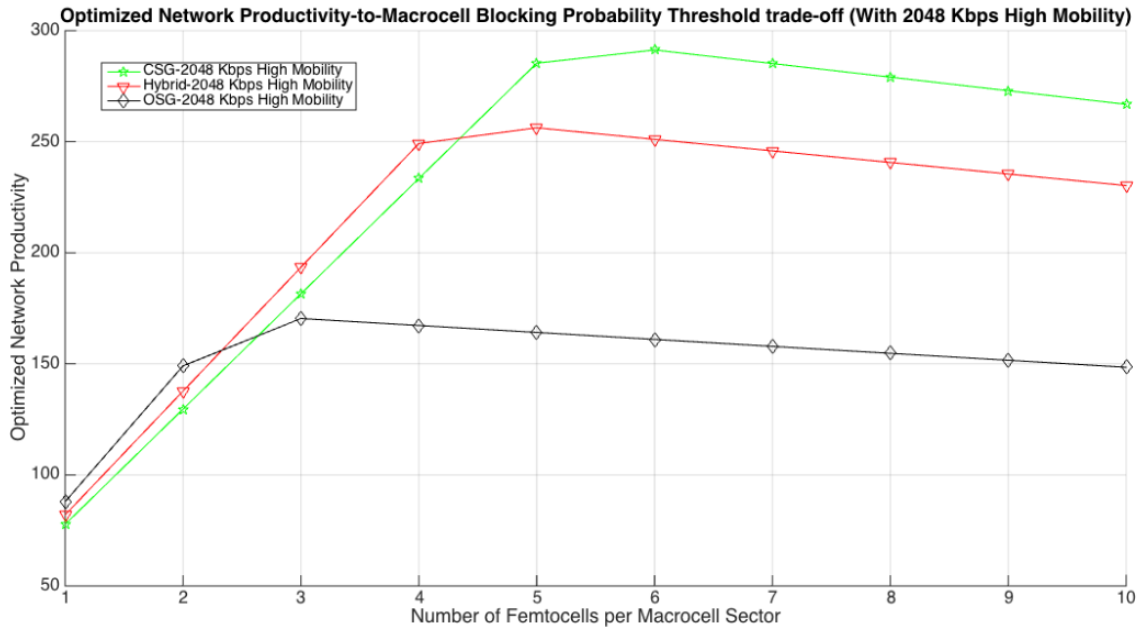

FIGURE 4.2. High Mobility: Optimized network productivity for variable femtocells

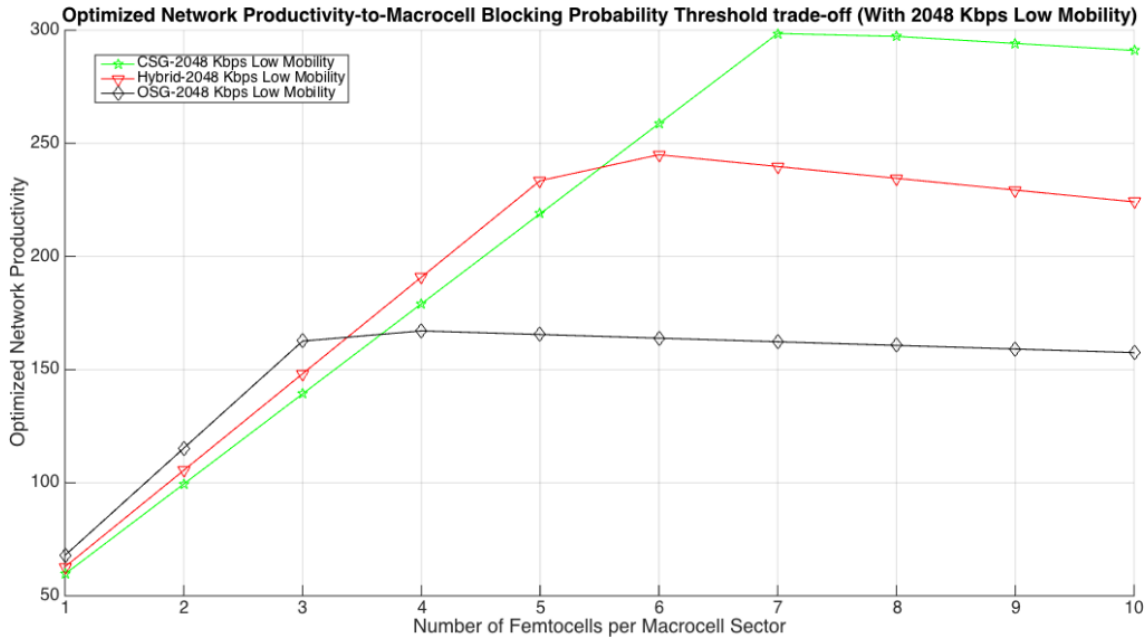

FIGURE 4.3. Low Mobility: Optimized network productivity for variable femtocells

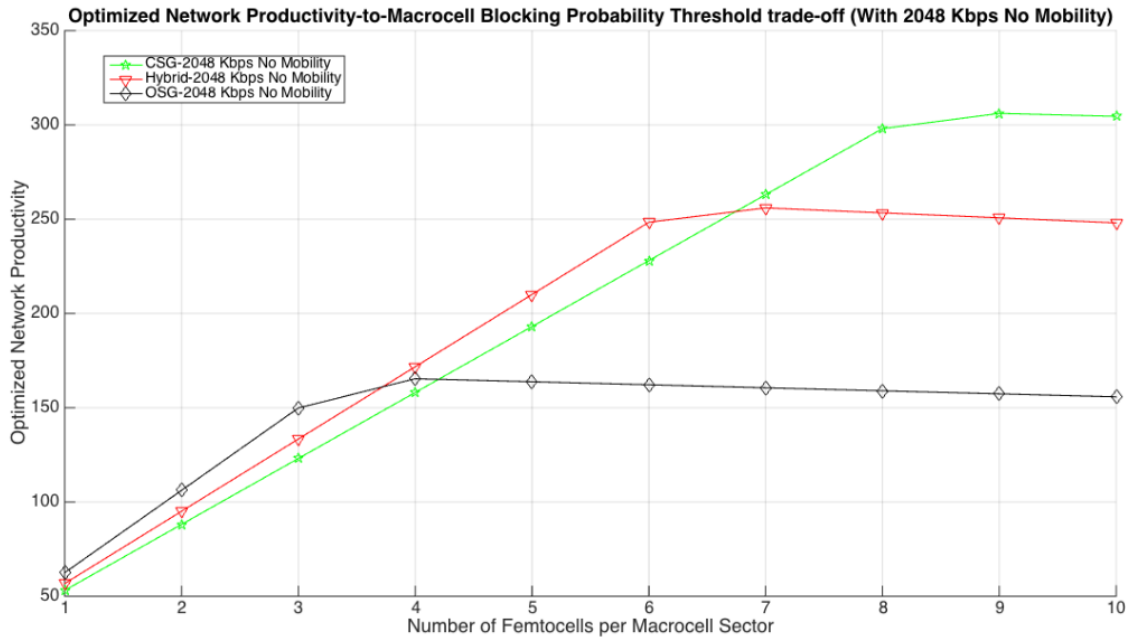

FIGURE 4.4. No Mobility: Optimized network productivity for variable femtocells

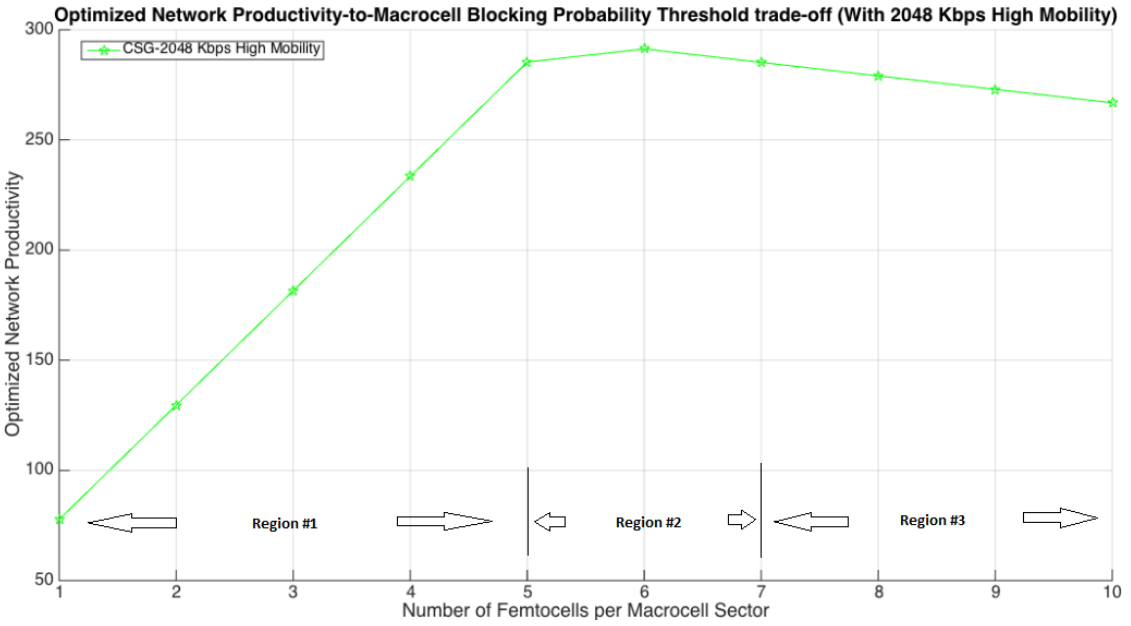

FIGURE 4.5. High Mobility: Three productivity regions for variable femtocells

4.6.4. Network Productivity Peak Point

From the results, this observation gives us the point in network deployment when the maximum productivity is reached. The peak point is influenced by the call arrival rate

proportion generated due to network densification. Network productivity is controlled by different factors (first, blocking probability threshold and second, call arrival rate) at different points in the simulation, which are created again by the network deployment.

The peak point for femtocells in different access modes, indicated by * in the tables in this chapter, is shifted due to the arrival rate directed to the femtocells. From Table 4.9, it is clear that even though the peak point is different, the trend still satisfies the underlying rate proportion and pivots when productivity goes from being controlled by blocking probability to being controlled by the arrival rate.

The offered load to femtocells decreases as densification increases. From Table 4.10, the trend indicates femtocell load is higher than macrocell load until the peak point is reached. After crossing the peak point, reverse trend is observed where macrocell offered load is higher than femtocell load. This trend can be explained by the inherent rate proportion created due to the network deployment. Also, note that offered load impacts positively to the network productivity (reward) as indicated in Section 3.5. Therefore, a decrease in productivity after peak point can also be explained by offered load trend.

4.6.5. Handover Observation

Table 4.11 shows the effective handover traffic directed to each cell for the simulation. While the peak point pulls down the offered load to femtocells, it shows reverse effect on handover traffic. It is clear from the results that handover traffic to femtocells shifts from being lower than handover traffic to macrocells at the peak point. After crossing the peak point, femtocell handover traffic is higher than macrocell handover traffic. This trend indicates femtocell handover traffic shows effective increase compared to macrocell handover traffic. This desirable trend indicating higher femtocell handover may be utilized to drive macrocell offload and impact productivity. However, by definition of productivity in Section 3.5, it is also clear that handover negatively impacts productivity (penalty) and hence its unique trend cannot be applied to the advantage of productivity. Future research can identify fraction of handover traffic that positively and negatively impacts productivity and utilize each to drive network productivity beyond current peak point, maintaining the QoS

for guaranteed users and GoS for the network. The handover trend is also relevant and consistent for low mobility scenario as indicated in Table 4.15. This is one of the major highlights of our research. As expected for no mobility scenario, since the call arrives and completes in the same cell, there is no occurrence of handover event. Therefore, handover metrics are set to 0 as per calculations and shown in Table 4.19. For obvious reasons, handover metrics for high mobility are higher than low mobility scenario and this observation aligns with the expectation.

4.6.6. Low Mobility Call Arrival Rate

Network productivity trend described for high-mobility scenario in 4.6.3 and 4.6.4 also apply to low-mobility scenario. One point to highlight the difference is the call arrival rate lower bound for CSG and OSG access modes as shown in Table 4.13 and 4.9. For femtocell count of 8 per macrocell sector, the call arrival rate is set to 5.75 in low mobility scenario and to 5.25 in high mobility scenario. A value of 5.25 would have also worked in low mobility scenario, however, it would have resulted in sharp decline in network productivity instead of gradual drop as shown in Fig. 4.3. Any one of the values for lower bound still maintains the same peak point in network productivity. Call arrival rates and network productivity trend for no mobility scenario show similar results as shown in Table 4.17.

4.7. Summary

The effect of call arrival rates and mobility on network performance of LTE heterogeneous system is analyzed. In this chapter, we propose a LTE heterogenous network model for three femtocell access modes that is subject to increasing femtocell densification. By executing optimization process on the model, we identify the call arrival rates per cell that will result in maximum productivity satisfying the given blocking threshold per cell. We also determine the number of femtocells at which the maximum productivity starts to peak satisfying blocking threshold and aligning proportionately with call arrival rates. These values will provide upper bounds on the productivity for given blocking thresholds. With the help of corresponding offered load, handover traffic and blocking probabilities, we explain

the optimized network productivity trend in the results and verify that the offered load positively impacts productivity while the handover traffic negatively impacts productivity by definition. Results for low, high and no mobility scenarios are presented for comparison.

TABLE 4.9. High Mobility: Call Arrival Rate and Optimized Network Productivity

Femtocell per Macrocell Sector	Femtocell Call Arrival lb,ub	Macrocell Call Arrival lb,ub	Optimized Productivity
Hybrid	Access		
1	10.9,50	8.6,50	81.98
2	10.9,25	8.6,50	137.71
3	10.9,16.67	8.6,50	193.45
4	10.9,12.5	8.6,50	249.19*
5	9,10	8.6,50	256.28*
6	7.3,8.3	8.6,50	251.08*
7	6.14,7.14	8.6,50	245.87
8	5.25,6.25	8.6,50	240.67
9	4.56,5.56	8.6,50	235.47
10	4,5	8.6,50	230.26
CSG	Access		
1	8.6,50	8.6,50	77.71
2	8.6,25	8.6,50	129.61
3	8.6,16.67	8.6,50	181.52
4	8.6,12.5	8.6,50	233.43
5	8.6,10	8.6,50	285.35*
6	7.3,8.3	8.6,50	291.32*
7	6.14,7.14	8.6,50	285.20*
8	5.25,6.25	8.6,50	279.08
9	4.56,5.56	8.6,50	272.96
10	4,5	8.6,50	266.84
OSG	Access		
1	20,50	8.6,50	87.94
2	20,25	8.6,50	149.06*
3	15.67,16.67	8.6,50	170.41*
4	11.5,12.5	8.6,50	167.27*
5	9,10	8.6,50	164.14
6	7.3,8.3	8.6,50	161.00
7	6.14,7.14	8.6,50	157.87
8	5.25,6.25	8.6,50	154.73
9	4.56,5.56	8.6,50	151.60
10	4,5	8.6,50	148.46

TABLE 4.10. High Mobility: Offered Load and Optimized Network Productivity

Femtocell per Macrocell Sector	Femtocell Load ρ_i	Macrocell Load ρ_i	Optimized Productivity
Hybrid	Access		
1	14.53	12.38	81.98
2	14.65	12.44	137.71
3	14.69	12.46	193.45
4	14.69	12.45	249.19*
5	12.38	11.98	256.28*
6	10.23	11.47	251.08*
7	8.64	11.06	245.87
8	7.45	10.75	240.67
9	6.50	10.49	235.47
10	5.75	10.30	230.26
CSG	Access		
1	11.95	11.95	77.71
2	11.94	11.94	129.61
3	11.87	11.87	181.52
4	11.83	11.83	233.43
5	11.90	11.90	285.35*
6	10.25	11.50	291.32*
7	8.66	11.08	285.20*
8	7.46	10.77	279.08
9	6.51	10.50	272.96
10	10.31	266.84	
OSG	Access		
1	24.37	13.52	87.94
2	25.19	14.17	149.06*
3	20.41	13.53	170.41*
4	15.37	12.53	167.27*
5	12.31	11.91	164.14
6	10.16	11.4	161.00
7	8.57	10.99	157.87
8	7.39	10.68	154.73
9	6.44	10.43	151.60
10	5.69	10.24	148.46

TABLE 4.11. High Mobility: Handover Traffic and Optimized Network Productivity

Femtocell per Macrocell Sector	Femtocell Handover ν_{ji}	Macrocell Handover ν_{ji}	Optimized Productivity
Hybrid	Access		
1	3.62	3.78	81.98
2	3.75	3.84	137.71
3	3.79	3.86	193.45
4	3.79	3.85	249.19*
5	3.38	3.38	256.28*
6	2.89	2.87	251.08*
7	2.50	2.46	245.87
8	2.20	2.15	240.67
9	1.94	1.89	235.47
10	1.75	1.70	230.26
CSG	Access		
1	3.35	3.35	77.71
2	3.34	3.34	129.61
3	3.28	3.27	181.52
4	3.23	3.23	233.43
5	3.30	3.30	285.35*
6	2.92	2.90	291.32*
7	2.52	2.48	285.20*
8	2.21	2.17	279.08
9	1.95	1.90	272.96
10	1.76	1.71	266.84
OSG	Access		
1	4.37	4.92	87.94
2	5.19	5.57	149.06*
3	4.74	4.93	170.41*
4	3.87	3.93	167.27*
5	3.31	3.31	164.14
6	2.89	2.80	161.00
7	2.43	2.39	157.87
8	2.14	2.08	154.73
9	1.88	1.83	151.60
10	1.69	1.64	148.46

TABLE 4.12. High Mobility: Blocking Probability calculated for all cells

Femtocell per Macrocell Sector	Femtocell Blocking Guaranteed Users	Femtocell Blocking Non-Guaranteed Users	Macrocell Blocking All Users
Hybrid	Access		
1	0.0036	0.00017	0.0097
2	0.0032	0.0987	0.0097
3	0.0032	0.0987	0.0097
4	0.0032	0.0987	0.0097
5	0.0016	0.0721	0.0097
6	0.0008	0.0509	0.0097
7	0.0004	0.0374	0.0097
8	0.0002	0.0282	0.0097
9	0.0001	0.0218	0.0097
10	0.0001	0.0172	0.0097
CSG	Access		
1	0.00029	NA	0.00023
2	0.0002	NA	0.0017
3	0.0097	NA	0.0097
4	0.0097	NA	0.0097
5	0.0097	NA	0.0097
6	0.0058	NA	0.0097
7	0.0032	NA	0.0097
8	0.0019	NA	0.0097
9	0.0011	NA	0.0097
10	0.0007	NA	0.0097
OSG	Access		
1	NA	0.0952	0.0097
2	NA	0.0952	0.0097
3	NA	0.0536	0.0097
4	NA	0.0232	0.0097
5	NA	0.0111	0.0097
6	NA	0.0058	0.0097
7	NA	0.0032	0.0097
8	NA	0.0019	0.0097
9	NA	0.0011	0.0097
10	NA	0.00071	0.0097

TABLE 4.13. Low Mobility: Call Arrival Rate and Optimized Network Productivity

Femtocell per Macrocell Sector	Femtocell Call Arrival lb,ub	Macrocell Call Arrival lb,ub	Optimized Productivity
Hybrid	Access		
1	8.35,50	6.6,50	62.80
2	8.35,25	6.6,50	105.48
3	8.35,16.67	6.6,50	148.16
4	8.35,12.5	6.6,50	190.83
5	8.35,10	6.6,50	233.52*
6	7.3,8.3	6.6,50	244.96*
7	6.14,7.14	6.6,50	239.75*
8	5.25,6.25	6.6,50	234.55
9	4.56,5.56	6.6,50	229.35
10	4,5	6.6,50	224.14
CSG	Access		
1	6.6,50	6.6,50	59.62
2	6.6,25	6.6,50	99.43
3	6.6,16.67	6.6,50	139.25
4	6.6,12.5	6.6,50	179.07
5	6.6,10	6.6,50	218.90
6	6.6,8.3	6.6,50	258.72*
7	6.6,7.14	6.6,50	298.54*
8	5.75,6.25	6.6,50	297.26*
9	5.05,5.56	6.6,50	294.16
10	4.5,5	6.6,50	291.06
OSG	Access		
1	15.5,50	6.6,50	67.90
2	15.5,25	6.6,50	115.25
3	15.5,16.67	6.6,50	162.61*
4	12,12.5	6.6,50	167.12*
5	9.5,10	6.6,50	165.52*
6	7.83,8.3	6.6,50	163.91
7	6.64,7.14	6.6,50	162.31
8	5.75,6.25	6.6,50	160.70
9	5.05,5.56	6.6,50	159.09
10	4.5,5	6.6,50	157.49

TABLE 4.14. Low Mobility: Offered Load and Optimized Network Productivity

Femtocell per Macrocell Sector	Femtocell Load ρ_i	Macrocell Load ρ_i	Optimized Productivity
Hybrid	Access		
1	8.80	7.08	62.80
2	8.83	7.09	105.48
3	8.83	7.09	148.16
4	8.84	7.10	190.83
5	8.84	7.09	233.52*
6	7.78	7.05	244.96*
7	6.52	6.98	239.75*
8	5.58	6.93	234.55
9	4.86	6.90	229.35
10	4.25	6.85	224.14
CSG	Access		
1	7.01	7.02	59.62
2	7.01	7.02	99.43
3	7.01	7.01	139.25
4	7.01	7.01	179.07
5	7.01	7.01	218.90
6	7.01	7.01	258.72*
7	7.01	7.01	298.54*
8	6.11	6.96	297.26*
9	5.39	6.93	294.16
10	4.78	6.88	291.06
OSG	Access		
1	16.09	7.28	67.90
2	16.19	7.35	115.25
3	16.24	7.39	162.61*
4	12.65	7.27	167.12*
5	10.04	7.15	165.52*
6	8.31	7.07	163.91
7	7.05	7.01	162.31
8	6.11	6.96	160.70
9	5.38	6.93	159.09
10	4.78	6.87	157.49

TABLE 4.15. Low Mobility: Handover Traffic and Optimized Network Productivity

Femtocell per Macrocell Sector	Femtocell Handover ν_{ji}	Macrocell Handover ν_{ji}	Optimized Productivity
Hybrid	Access		
1	0.4629	0.4836	62.80
2	0.4850	0.4966	105.48
3	0.4862	0.4948	148.16
4	0.4940	0.5008	190.83
5	0.4916	0.4872	233.52*
6	0.4485	0.4503	244.96*
7	0.3865	0.3851	239.75*
8	0.3385	0.3352	234.55
9	0.3054	0.3009	229.35
10	0.2570	0.2521	224.14
CSG	Access		
1	0.4226	0.4217	59.62
2	0.4207	0.4204	99.43
3	0.4195	0.4189	139.25
4	0.4182	0.4181	179.07
5	0.4126	0.4127	218.90
6	0.4157	0.4156	258.72*
7	0.4140	0.4140	298.54*
8	0.3683	0.3663	297.26*
9	0.3358	0.3324	294.16
10	0.2856	0.2817	291.06
OSG	Access		
1	0.5924	0.6809	67.90
2	0.6990	0.7557	115.25
3	0.7485	0.7901	162.61*
4	0.6311	0.6506	167.12*
5	0.5236	0.5316	165.52*
6	0.4500	0.4520	163.91
7	0.4137	0.4137	162.31
8	0.3660	0.3639	160.70
9	0.3336	0.3302	159.09
10	0.2838	0.2799	157.49

TABLE 4.16. Low Mobility: Blocking Probability calculated for all cells

Femtocell per Macrocell Sector	Femtocell Blocking Guaranteed Users	Femtocell Blocking Non-Guaranteed Users	Macrocell Blocking All Users
Hybrid	Access		
1	0.0044	0.00022	0.01
2	0.0037	0.0175	0.01
3	0.0033	0.1	0.01
4	0.0033	0.1	0.01
5	0.0033	0.1	0.01
6	0.0021	0.081	0.01
7	0.0011	0.0602	0.01
8	0.0006	0.0459	0.01
9	0.0004	0.0358	0.01
10	0.0002	0.0283	0.01
CSG	Access		
1	0.00029	NA	0.00033
2	0.0002	NA	0.0017
3	0.0017	NA	0.01
4	0.0017	NA	0.01
5	0.01	NA	0.01
6	0.01	NA	0.01
7	0.01	NA	0.01
8	0.0064	NA	0.01
9	0.0042	NA	0.01
10	0.0028	NA	0.01
OSG	Access		
1	NA	0.0994	0.01
2	NA	0.0994	0.01
3	NA	0.0994	0.01
4	NA	0.0546	0.01
5	NA	0.0294	0.01
6	NA	0.0168	0.01
7	NA	0.0102	0.01
8	NA	0.0064	0.01
9	NA	0.0042	0.01
10	NA	0.00028	0.01

TABLE 4.17. No Mobility: Call Arrival Rate and Optimized Network Productivity

Femtocell per Macrocell Sector	Femtocell Call Arrival lb,ub	Macrocell Call Arrival lb,ub	Optimized Productivity
Hybrid	Access		
1	7.5,50	6.05,50	56.76
2	7.5,25	6.05,50	95.09
3	7.5,16.67	6.05,50	133.41
4	7.5,12.5	6.05,50	171.74
5	7.5,10	6.05,50	210.06
6	7.5,8.3	6.05,50	248.39*
7	6.6429,7.14	6.05,50	255.99*
8	5.75,6.25	6.05,50	253.35*
9	5.0556,5.56	6.05,50	250.71
10	4.5,5	6.05,50	248.06
CSG	Access		
1	5.8,50	6.05,50	53.13
2	5.8,25	6.05,50	88.12
3	5.8,16.67	6.05,50	123.11
4	5.8,12.5	6.05,50	158.07
5	5.8,10	6.05,50	193.06
6	5.8,8.3	6.05,50	228.05
7	5.8,7.14	6.05,50	263.03
8	5.8,6.25	6.05,50	298.02*
9	5.3056,5.56	6.05,50	306.11*
10	4.75,5	6.05,50	304.52*
OSG	Access		
1	14.3,50	6.05,50	62.49
2	14.3,25	6.05,50	106.18
3	14.3,16.67	6.05,50	149.86*
4	12,12.5	6.05,50	165.39*
5	9.5,10	6.05,50	163.79*
6	7.83,8.3	6.05,50	162.18
7	6.6429,7.14	6.05,50	160.58
8	5.75,6.25	6.05,50	158.97
9	5.0556,5.56	6.05,50	157.37
10	4.5,5	6.05,50	155.76

TABLE 4.18. No Mobility: Offered Load and Optimized Network Productivity

Femtocell per Macrocell Sector	Femtocell Load ρ_i	Macrocell Load ρ_i	Optimized Productivity
Hybrid	Access		
1	7.5	6.05	56.76
2	7.5	6.05	95.09
3	7.5	6.05	133.41
4	7.5	6.05	171.74
5	7.5	6.05	210.06
6	7.5	6.05	248.39
7	6.6429	6.05	255.99
8	5.75	6.05	253.35
9	5.0556	6.05	250.71
10	4.5	6.05	248.06
CSG	Access		
1	5.8	6.05	53.13
2	5.8	6.05	88.12
3	5.8	6.05	123.11
4	5.8	6.05	158.07
5	5.8	6.05	193.06
6	5.8	6.05	228.05
7	5.8	6.05	263.03
8	5.8	6.05	298.02
9	5.3056	6.05	306.11
10	4.75	6.05	304.52
OSG	Access		
1	14.3	6.05	62.49
2	14.3	6.05	106.18
3	14.3	6.05	149.86
4	12.0	6.05	165.39
5	9.5	6.05	163.79
6	7.83	6.05	162.18
7	6.6429	6.05	160.58
8	5.75	6.05	158.97
9	5.0556	6.05	157.37
10	4.5	6.05	155.76

TABLE 4.19. No Mobility: Handover Traffic and Optimized Network Productivity

Femtocell per Macrocell Sector	Femtocell Handover ν_{ji}	Macrocell Handover ν_{ji}	Optimized Productivity
Hybrid	Access		
1	0	0	56.76
2	0	0	95.09
3	0	0	133.41
4	0	0	171.74
5	0	0	210.06
6	0	0	248.39
7	0	0	255.99
8	0	0	253.35
9	0	0	250.71
10	0	0	248.06
CSG	Access		
1	0	0	53.13
2	0	0	88.12
3	0	0	123.11
4	0	0	158.07
5	0	0	193.06
6	0	0	228.05
7	0	0	263.03
8	0	0	298.02
9	0	0	306.11
10	0	0	304.52
OSG	Access		
1	0	0	62.49
2	0	0	106.18
3	0	0	149.86
4	0	0	165.39
5	0	0	163.79
6	0	0	162.18
7	0	0	160.58
8	0	0	158.97
9	0	0	157.37
10	0	0	155.76

TABLE 4.20. No Mobility: Blocking Probability calculated for all cells

Femtocell per Macrocell Sector	Femtocell Blocking Guaranteed Users	Femtocell Blocking Non-Guaranteed Users	Macrocell Blocking All Users
Hybrid	Access		
1	0.0049	0.00021	0.0098
2	0.0034	0.0164	0.0098
3	0.0030	0.096	0.0098
4	0.0030	0.096	0.0098
5	0.0030	0.096	0.0098
6	0.0030	0.096	0.0098
7	0.0020	0.0788	0.0098
8	0.0012	0.0619	0.0098
9	0.0007	0.0496	0.0098
10	0.0005	0.0405	0.0098
CSG	Access		
1	0.0000024	NA	0.000000027
2	0.0014	NA	0.000000017
3	0.0014	NA	0.0002
4	0.0086	NA	0.0098
5	0.0086	NA	0.0098
6	0.0086	NA	0.0098
7	0.0086	NA	0.0098
8	0.0086	NA	0.0098
9	0.0065	NA	0.0098
10	0.0045	NA	0.0098
OSG	Access		
1	NA	0.0997	0.0098
2	NA	0.0997	0.0098
3	NA	0.0997	0.0098
4	NA	0.0668	0.0098
5	NA	0.0368	0.0098
6	NA	0.0215	0.0098
7	NA	0.0131	0.0098
8	NA	0.0084	0.0098
9	NA	0.0055	0.0098
10	NA	0.0037	0.0098

CHAPTER 5

FRACTIONAL FREQUENCY REUSE MECHANISM METRICS

5.1. Introduction

In this chapter, we review the proposed metric for Fractional Frequency Reuse (FFR), weighted user satisfaction. The fundamental goal of introducing LTE femtocells is to increase capacity and coverage especially for the indoor and cell-edge mobile users. However, co-tier and cross-tier interferences are high due to co-location of femtocells in macrocell coverage. FFR mechanism is one of the most effective femtocell interference avoidance techniques. We propose a new metric to determine inner region radius and frequency allocation which optimizes the total cell throughput and serves as many number of users in the network. We already know that FFR technique is designed to serve cell edge users. With introduction of new metric, we extend that idea to serve as many users in the network. The new metric is applied to sectorized FFR configurations and their performance is evaluated under different network conditions.

Different techniques such as cooperation among macrocell base stations and femtocells and clustering, can be considered to reduce inter-tier and intra-tier interferences. FFR is one of the interference management techniques which require minimal or no coordination among the femtocells and macrocell. We evaluate the performance of the sectorized FFR mechanism with five metrics; four existing and one proposed metric and determine the values for inner region radius and frequency allocation for optimal results. The new metric is evaluated for average user equipment (UE) throughput, variance in UE throughput, total cell throughput, femtocell density, different channel models and inter-eNodeB distance.

5.2. FFR Mechanism

In FFR, the whole frequency band is divided into several sub-bands, and each one is exclusively assigned to inner and outer region of the cell. In order to ensure that the mutual interference between users and base station remains below a harmful level, adjacent cells use different frequencies. The interference scenarios that appear in such integrated femtocell-

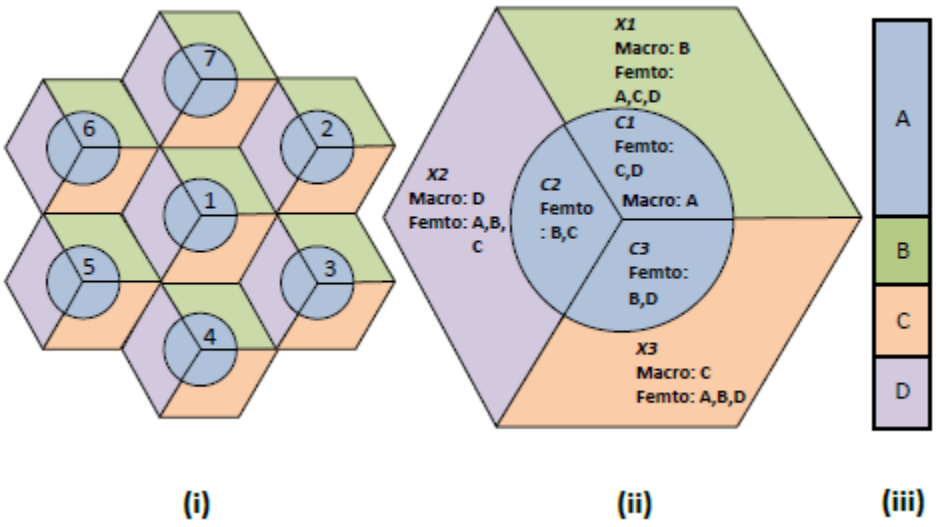

FIGURE 5.1. FFR-3 deployment with LTE femtocells [49]

macrocell environments during the downlink transmission are considered in our research. In particular, the interference caused to a FUE by a macrocell, the interference caused to a MUE by a femtocell and the interference caused to a FUE by a neighboring femtocell are point of interest.

The macrocell coverage area is partitioned into center-zone and edge-zone including three sectors per macrocell. The entire frequency band is divided into two parts; one part is solely assigned to the center-zone (e.g., sub-band A in Fig. 5.1) and the other part is partitioned into three sub-bands (e.g., sub-bands B, C, and D) and assigned to the three edge-zones [49]. Sectoring reduces interference between co-channel cells as shown in Fig. 5.2. For the case of cluster size of $N = 4$, only 2 of the 6 co-channel cells cause interference to the middle cell for the sector labeled *S2* in the case of 120° cell sectoring (the cells with radiation sectors colored red and green). The other 4 cells, although they are radiating at the same frequencies, cause no interference because the middle cell is not in their radiation angles.

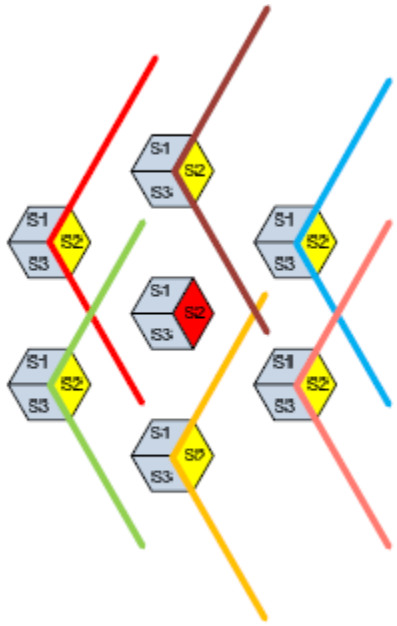

FIGURE 5.2. 120° sectoring in FFR-3 [64]

5.3. LTE System Model

The mechanism assumes a topology that consists of a grid of 7 macrocells, each with 3 or 6 sector sites such that each sector is served by a different directional antenna. The beam directions of different sector antennas are separated by 120° and 60° from each other for FFR-3 and FFR-6 methods respectively. A constant number of femtocells per sector site and uniformly distributed multicast users are considered. In order to find the optimal inner region radius and frequency allocation in the FFR deployment, the mechanism divides each cell into two regions and calculates the total throughput for 40 Frequency Allocations (FA), assuming Frequency Reuse 1 and Frequency Reuse x for inner and the outer regions respectively [49], where x is the frequency reuse factor of 3 for FFR-3 and 6 for FFR-6 respectively. Each FA corresponds to paired value of fraction of inner region resource blocks and inner region radius. The simulation is carried out in Vienna LTE System Simulator modified to support FFR-3 mechanism [31]. Following is the update made to the Simulator to support FFR-3 mechanism.

- Simulator is updated to support 3-sector macrocell with femtocell configuration with

FFR sub-bands assigned to femtocells.

- Antenna azimuth offset is updated from 30 (hexagonal sectors) to 0 (hexagonal cells) resulting in sectorized cell.
- Special settings are made for FUEs located in inner region, but using outer region sub-bands and FUEs located in outer region, but using inner region sub-band.

Following is a set of steps carried out to set up the system model.

- FA1: All 25 resource blocks are allocated in inner region. No resource blocks are allocated to the outer region.
- FA2: 24 resource blocks are allocated in inner region. $1/x$ resource block allocated to the outer region. ⋮
- FA39: 1 resource block allocated in inner region. $24/x$ resource blocks allocated to the outer region.
- FA40: No resource blocks are allocated in inner region. $25/x$ resource blocks allocated to the outer region.

For each FA, the mechanism calculates the total throughput, user satisfaction, fairness index, and weighted throughput values based on new metrics [33]. This procedure is repeated for successive inner cell radius (0 to R, where R is the cell radius). From the above calculations, the mechanism selects the optimal FFR scheme that maximizes the cell total throughput. The system model described above can be used for LTE bandwidths ranging from 1.4 MHz to 20 MHz. Using the system model, the simulation will calculate performance metrics for each value of inner region radius and frequency allocation.

5.4. Existing Metrics Definition

We use a metric defined by authors in [11], user satisfaction (US). It is calculated as the sum of the users' throughput divided by the product of the maximum user throughput and the number of users (X). US ranges between 0 and 1. When US approaches 1, all the users in the corresponding cell experience similar throughput. However, when US approaches 0, there are huge differences in throughput values across the users in the cell. This metric

will be utilized in scenarios where fairness to the users is significant such as cell throughput and Jain fairness index.

$$US = \frac{\sum_{x=1}^{X} T_x}{max\_user\_throughput \cdot X} \tag{5.1}$$

To obtain a metric of fairness for performance evaluation, we use the Jain fairness metric introduced in [33]. Assuming the allocated throughput for user i is x_i, Jain fairness index is defined as,

$$JI_x = \frac{(\sum_{i=1}^{X} x_i)^2}{X \cdot \sum_{i=1}^{X} x_i^2} \tag{5.2}$$

This metric is interesting due to its unique properties. It is scale-independent, applicable for different number of users and it is bound between [0, 1], where 0 means "total unfairness" and 1 means "total fairness" in terms of throughput division among the users [15].

With metric WT_x defined by the authors in [15], the aim is to not only lower variance of the per-user throughput values but also generate higher values of the cell total throughput. In this chapter, we refer to it as weighted fairness.

$$WT_x = JI_x \cdot T_x \tag{5.3}$$

where, x is the corresponding user (either femto user or macro user).

5.5. Proposed Metric Definition

We introduce a new metric, weighted throughput based on user satisfaction, WT_{US}, to add user satisfaction-based weights to the cell throughput value T corresponding to specific inner radius and inner bandwidth such that the resultant throughput is higher than the corresponding throughput optimized for user satisfaction US alone and all the users in the corresponding cell experience similar throughput.

$$WT_{US} = US \cdot T \tag{5.4}$$

TABLE 5.1. Simulation Parameters for FFR Metric

Parameter	Value
System Bandwidth	5 MHz
Subcarriers	25
Subcarrier Bandwidth	180 KHz
Cell Radius	250 m
Inter eNodeB distance	1000 m
Noise Power Spectral Density	-174 dBm/Hz
Subcarrier spacing	15 KHz
Channel Model	Typical Urban
Carrier Frequency	2000 MHz
Number of macrocells	7
Number of sectors per macrocell	3 (FFR-3)
Macrocell Transmit Power	40 W
Macrocell Antenna Gain	15dB
Macrocell Antenna Pattern	TS36.942 standard
Number of femtocells per macrocell sector	1-9
Femtocell Transmit Power	20 mW
Femtocell Antenna Gain	0 dB
Femtocell Antenna Pattern	Omni Directional
Femtocell Access Mode	Open
Number of total users	500 (FFR-3)

5.6. Results

Table 5.1 are the simulation parameters set for the research [50]. With the defined system model and simulation parameters, the simulation calculates several metrics for each value of inner region radius and inner region subcarriers. A sample uniform deployment

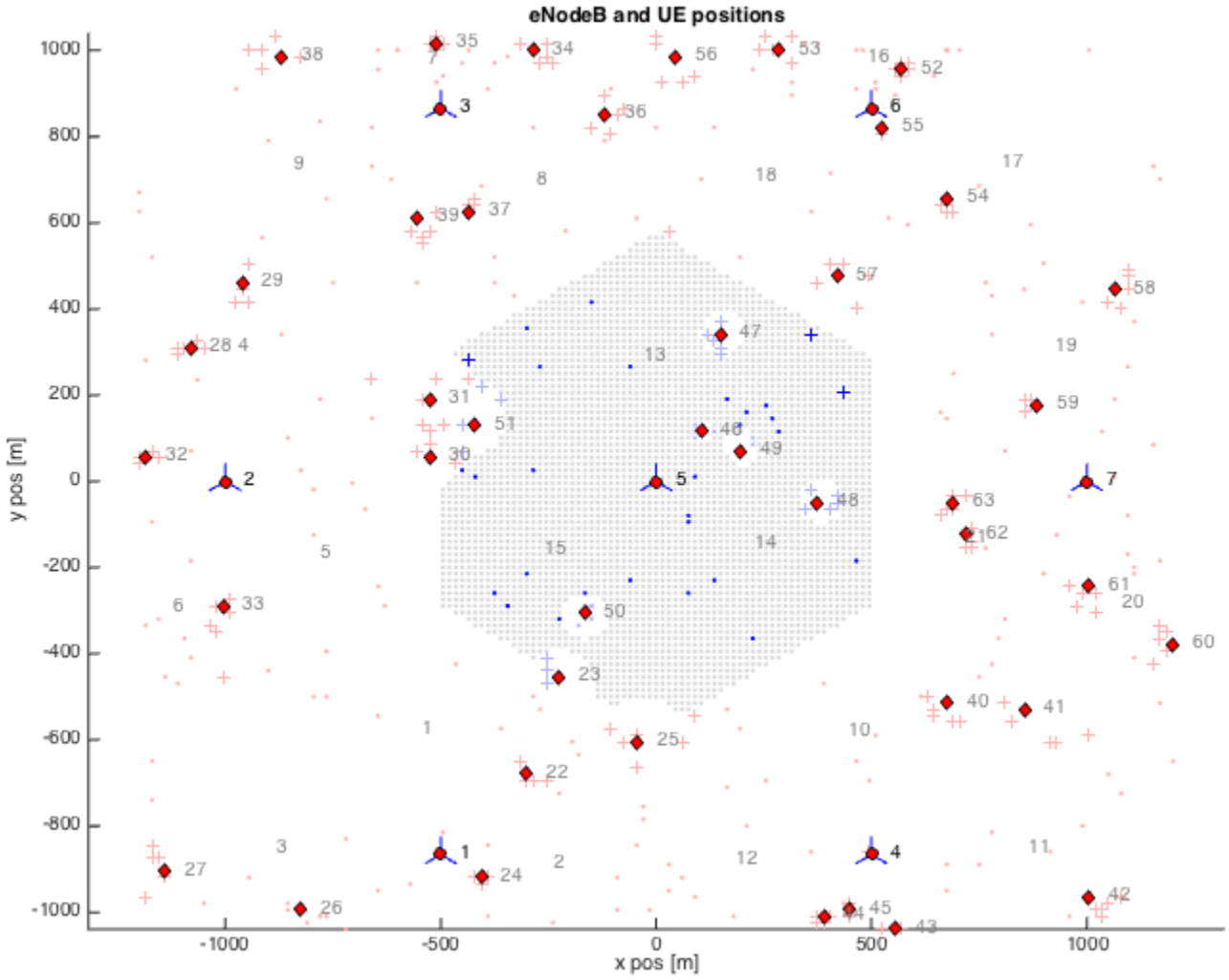

FIGURE 5.3. FFR-3 uniform deployment for FFR metric simulation

considered in simulation with corresponding SINR maps is shown in Figs. 5.3 and 5.4. Macrocells are located at cell centers. Femtocells are located at uniform distance from the macrocells shown with red filled diamond markers. Active users are shown with blue dots and deactivated users are marked red. In case of FFR-3, the 3 center macrocells with directional antenna configuration, femtocells and associated users are considered for results.

5.6.1. Simulation Assumptions

Note that we assume the simulation is run considering stable downlink data traffic. Handover is a typical and frequently occurring event in integrated macrocell-femtocell environment. For simulation purposes, a network snapshot where user association to macro-

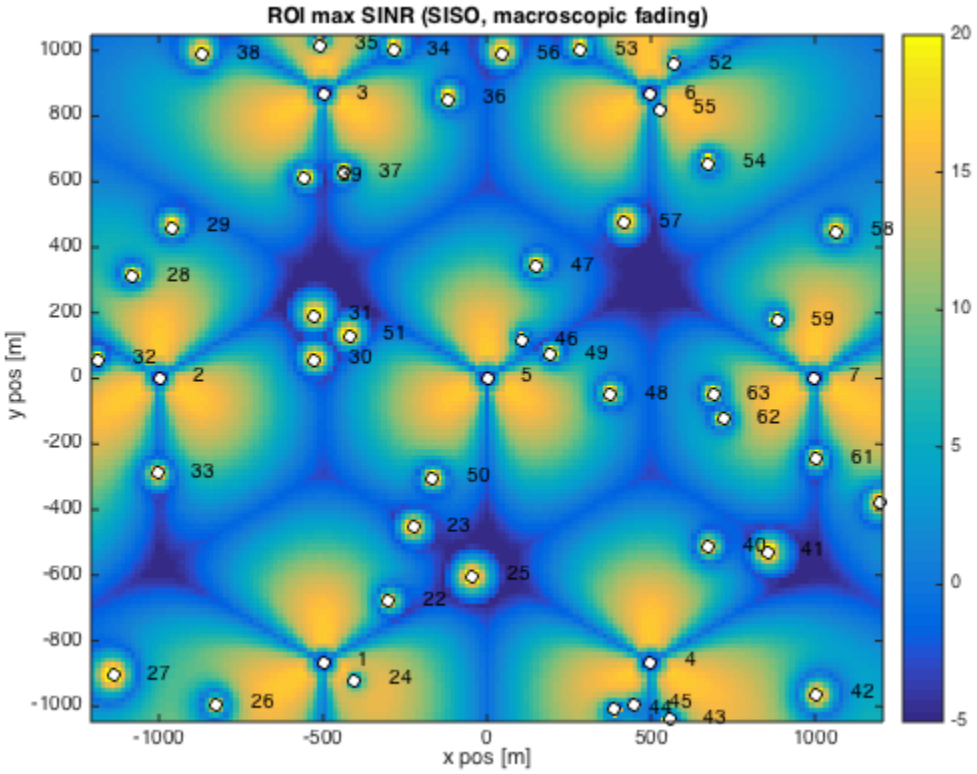

FIGURE 5.4. FFR-3 SINR maps for FFR metric simulation

cell or femtocell remains stable for the duration of the simulation run is considered. With sectorized macrocell, the actual number of femtocells in a macrocell will be 6 when we set femtocells per macrocell sector to 2 in case of FFR-3. The performance of proposed metric is highlighted with downward direction arrow in all the results.

5.6.2. Average Throughput and Variance

We introduce the new metric due to the following reasons, better performance in terms of average user throughput and effective user fairness in terms of variance in user throughput. The results shown in Figs. 5.5, 5.6 and 5.7 prove the user throughput optimized with new metric shows better performance and low variance. The new metric maintains relatively high total cell throughput, keeping high average user throughput and serving majority of the users in the cell.

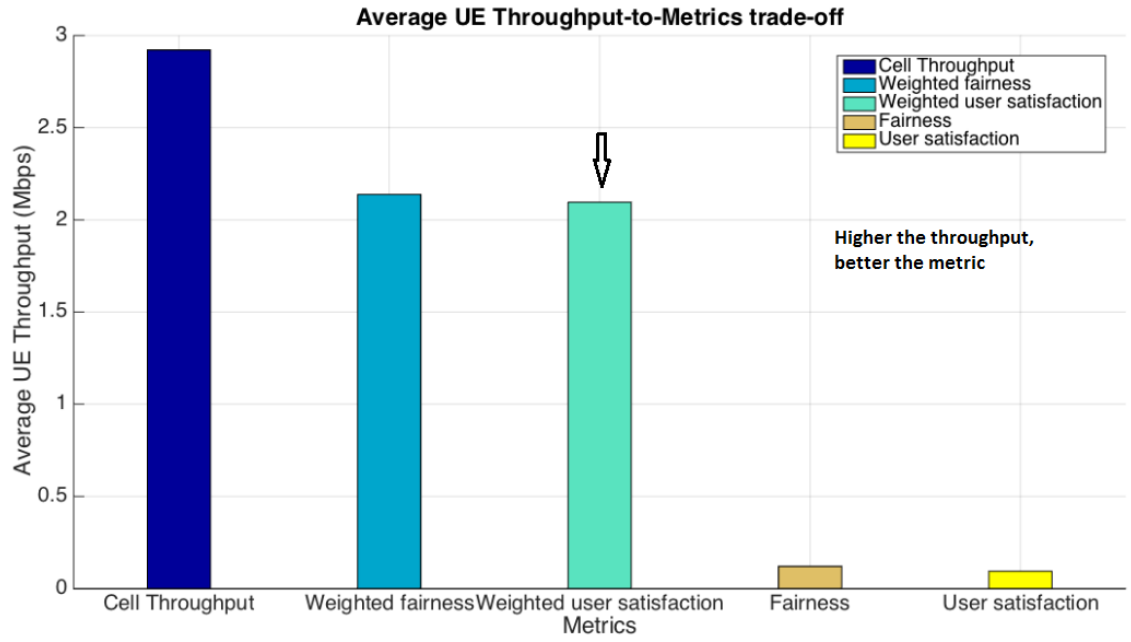

FIGURE 5.5. Comparison of average user throughput

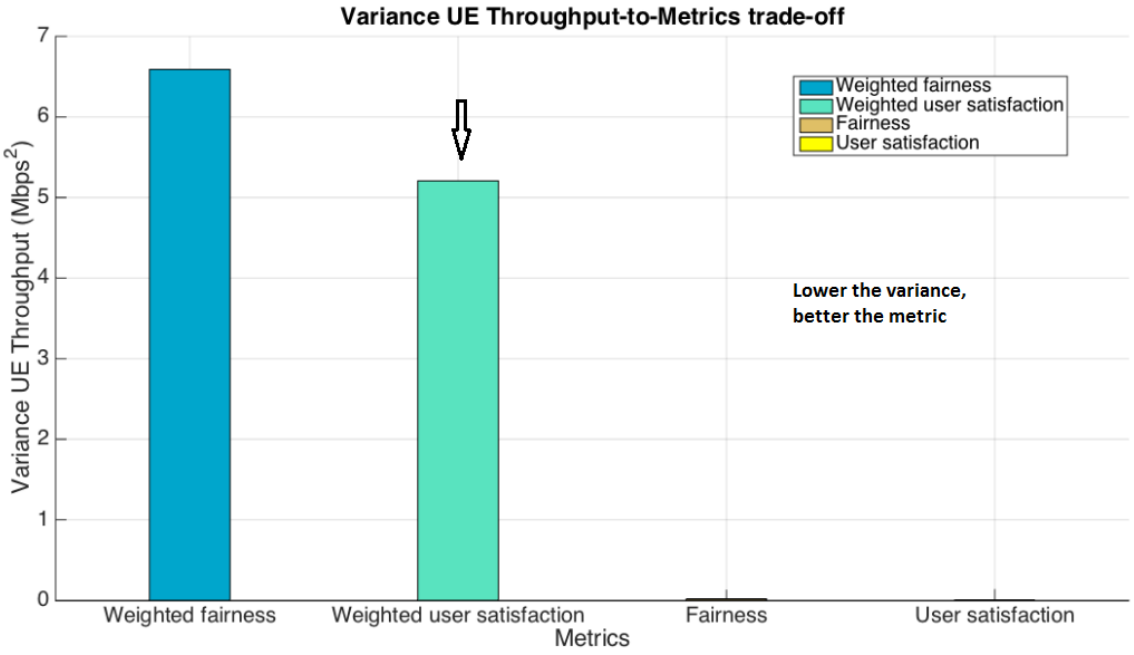

FIGURE 5.6. Comparison of variance in user throughput

5.6.3. Variable Inter-Site Distance

We study the behavior of the system by simulating deployment over variable inter-site distance. As inter-eNodeB distance increases, it is clear that the new metric performs slightly

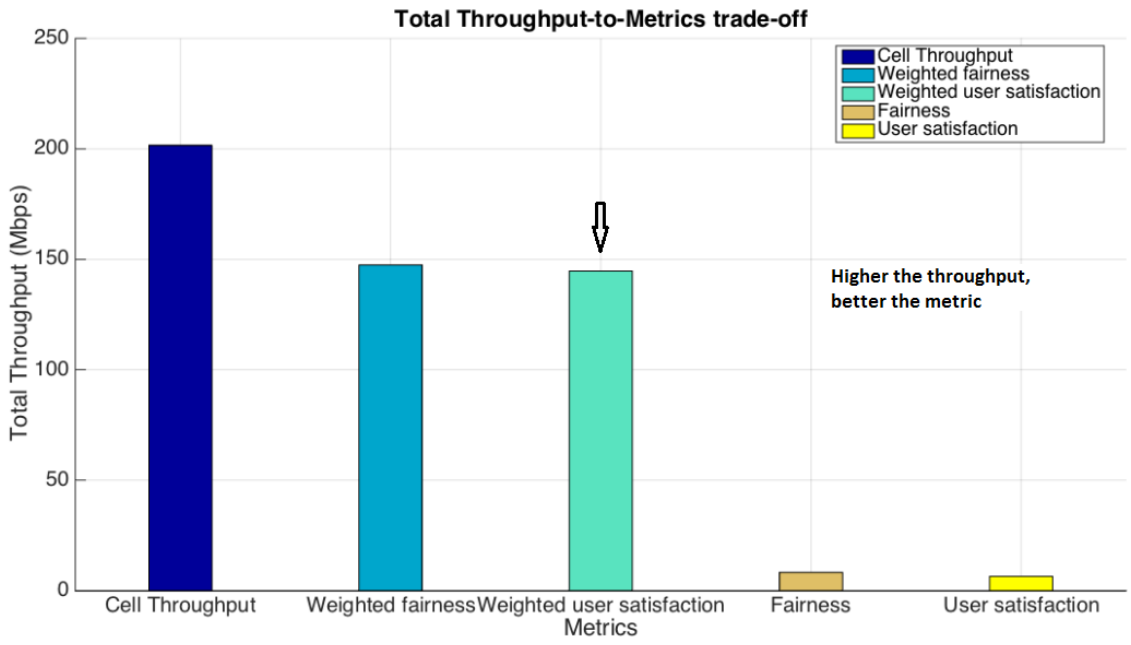

FIGURE 5.7. Comparison of total cell throughput

better than the weighted fairness metric. The network performance optimized with cell total throughput is the best of all metrics since the goal is to only maximize the throughput at the expense of significant throughput differences across individual users. The advantage of the new metric is that it performs relatively better by ensuring all users experience similar throughput. Fig. 5.8 shows the comparative results of average UE throughput optimized for cell total throughput, weighted fairness and weighted user satisfaction.

5.6.4. Variable Femtocells

The performance of the new metric is analyzed for various deployment scenarios with increasing number of femtocells, keeping the total number of users constant. Clearly, as the number of femtocells increases in the network, the throughput also increases as shown in the Fig. 5.9. Note that the simulation increases femtocells per macrocell sector to accomplish the result. In this result, the new metric performs close to the other metrics as the number of femtocell density increases. Simulation analysis found minor difference in the average UE throughput values though they appear similar. This result proves that the new metric will be useful in extreme network densification scenarios.

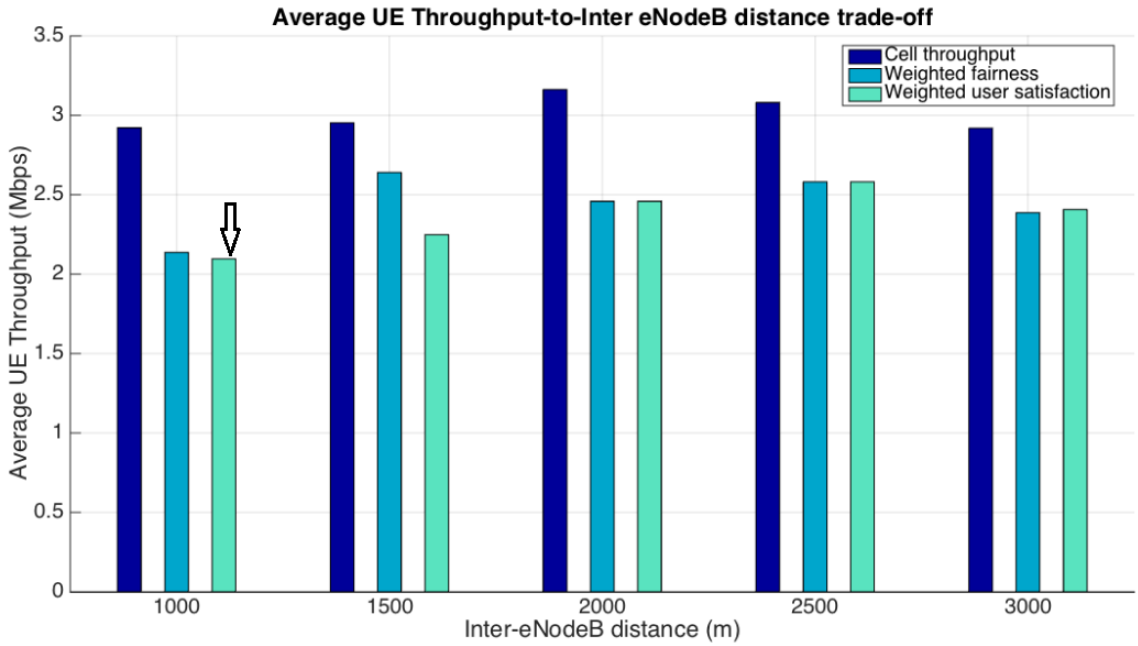

FIGURE 5.8. Comparison of average UE throughtput for variable inter-eNodeB distance

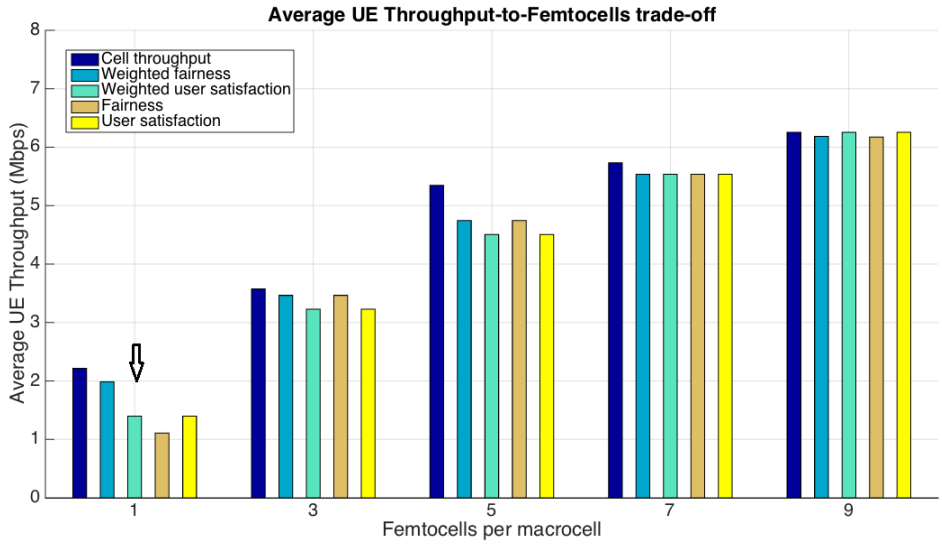

FIGURE 5.9. Comparison of average UE throughput for variable number of femtocells

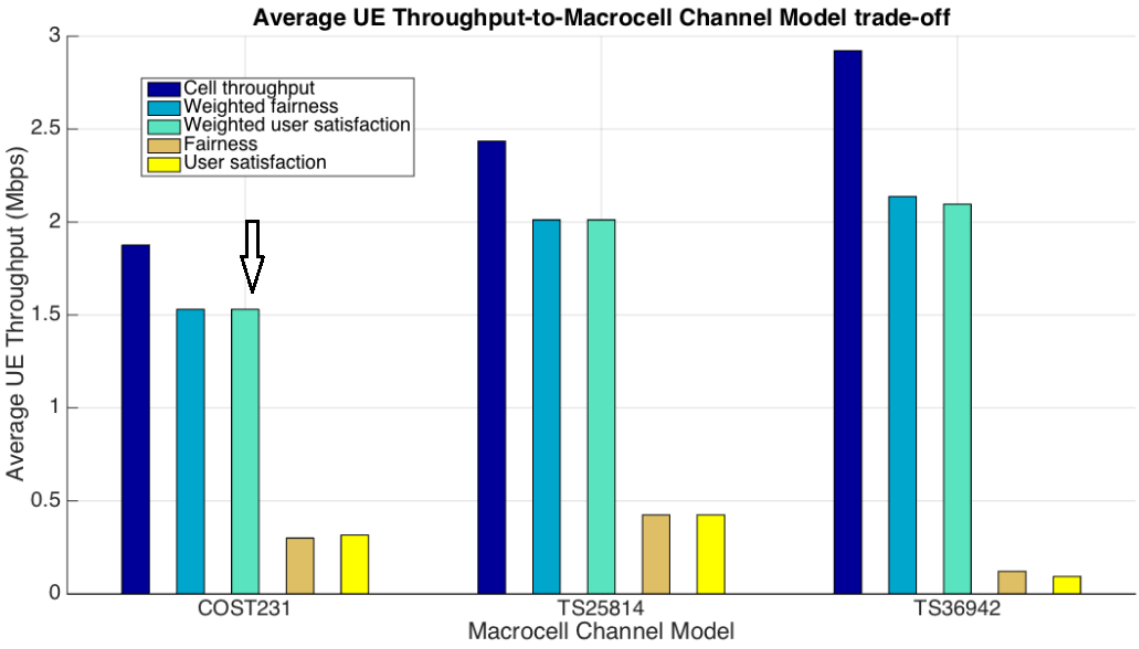

FIGURE 5.10. Comparison of average UE throughput for different macrocell channel models

5.6.5. Channel Models

We analyze the new metric performance with 3 different types of channel models associated with the macrocells. The femtocells are set to dual slope channel model throughout the simulation. The macrocell channel model is changed to COST231 [26], TS25.814 [58] and TS36.942 [59] standards. The new metric performance is similar to weighted fairness for COST231 and TS25.814, slightly lower than weighted fairness for TS36.942 channel model. This result proves our new metric can serve as a best fit replacement for weighted fairness for different macrocell channel models.

5.7. Summary

In this chapter, we propose a new metric that calculates the optimal inner region radius and frequency allocation for FFR mechanism. The application of the FFR method based on weighted throughput user satisfaction makes a trade-off between the existing approaches, as it increases the cell total throughput and keeps the variance of per-user throughput values to the minimum. With the simulation results, we prove the new metric is best fit replacement

for weighted user fairness with better results in average user throughput, variance in user throughput and total cell throughput. For inter-eNodeB distance, femtocell densification and macrocell channel model, our metric shows comparable performance with weighted user fairness. The effectiveness of the new metric can be further explored by applying it to different static FFR mechanisms such as Partial Frequency Reuse and Soft Fractional Frequency Reuse. Another future step for this work is to integrate several realistic network parameters in the proposed method and evaluate it in real conditions such as user mobility. Future work can also address applying the new metric to configurations with variable number of macrocells. With extreme densification and mobility, a possible research extension would be to review the impact of call mobility with the proposed metric.

CHAPTER 6

CONCLUSIONS

6.1. Summary

LTE femtocells experience interference-limited scenarios that impact network productivity. The issue is evident when these femtocells operate in open access mode or when they share the same frequency spectrum with the overlay macrocells. In addition to technical limitations, they are few business and civic limitations to femtocell deployment. Sharing the spectrum with macrocells is bandwidth efficient to the operators. If operating the femtocell in open access is not acceptable, we can operate the femtocell in other access modes; closed and hybrid. Hybrid access mode shows mid-way performance and is the preferred access mode by most operators, where bandwidth efficiency is addressed and subscribers are given preference. One aspect that may disturb this advantage is call mobility. We performed simulations in Matlab to determine the effect of call mobility on network productivity for each femtocell access mode for variable call arrival rate. In the process, we also determined the maximum number of femtocells and call arrival rate that can generate maximum productivity and address interference for each access mode. This provided an upper bound on infrastructure costs to the operator and satisfied customers' demand effectively. Due to the non-uniform deployment of femtocells and users, there is a possibility that some users will experience high throughput if closer to the cell, and some users will experience low throughput. We introduced weighted user satisfaction, a throughput balancing metric for LTE FFR mechanism that can be applied with and without user mobility. With this metric, we proved that user throughput values showed lower variance with minor compensation on average cell throughput. Chapter 1 provided an overview of LTE ecosystem and highlighted the scenarios and contributions.

Chapter 2 reviewed the previous research related to network productivity and FFR metrics. While some work focuses on similar targets such as productivity, their constraints for evaluation were different. Extensive work has been done on FFR metrics in previous

research. As shown in our simulation, the application of the FFR method based on weighted throughput user satisfaction makes a trade-off between the existing approaches, as it increased the cell total throughput and lowered the variance of per-user throughput values. In some scenarios, we proved the new metric is best fit replacement for weighted user fairness with better results in average user throughput, variance in user throughput and total cell throughput.

In Chapter 3, we defined network productivity as the revenue generated by accepting a new call and penalty incurred by handoff failure due to forced termination. For multi-tier LTE network deployment, we set up the reward and penalty weights for each access mode. We defined the fraction of calls arriving at macrocell and proportionately assign call arrival rate for underlying femtocells. LTE blocking probability was calculated based on cell type and user type. Guaranteed users experienced less blocking compared to the non-guaranteed users when the femtocell operates in Hybrid and CSG modes. Blocking threshold was also set differently based on cell type. Similar to call arrival rate, a fraction of subcarriers was assigned to guaranteed users in the simulation. By setting inter-cell and intra-cell interference values, we derived the best possible values for reward and penalty weights in the productivity expression for each femtocell access mode. By formulating optimization problem, we proved that as the offered load increases, the network productivity also increases for a given blocking threshold vector.

Chapter 4 studied a slightly different scenario where number of femtocells per macrocell sector is varied. We applied constrained optimization process and determined the maximum number of femtocells per macrocell sector that will generate maximum productivity for a given blocking threshold. This provided an upper bound to the network operators for the number of femtocells to be deployed in the network and meet blocking constraints. We correlated the offered load, handover traffic, blocking probabilities to explain the network productivity trend for low, high and no mobility scenarios. We derived interesting observations from handover event in the optimization process when the network throughput made a transition at peak productivity. This is one of the major highlights of our research.

Previous FFR metrics that guarantee similar throughput for all users were examined in Chapter 5. This chapter reviewed the metrics and applied an iterative algorithm to select a FFR scheme that maximized throughput and returned a specific inner region radius and frequency allocation. We proposed a new metric, weighted throughput user satisfaction, that performs better than previous metrics, by maintaining higher throughput and lowering variance among users. We also proved that there are few scenarios where our metric performs similar to other metric and identified that as best fit replacement scenario.

6.2. Future Research

We conclude by outlining possible directions for future research:

- We presented a methodology for LTE integrated macrocell-femtocell network with call mobility with all users requesting same data rate. With users requesting different data rates (based on applications they support), the methodology can be extended to support varying data rate requirements and apply throughput optimization based on new inputs. Another future extension to our work would be to enable the network self-organize if call mobility varies between low-mobility and high-mobility. We utilized handover traffic results to explain network productivity trend. By extending that observation, we can regulate the subcarrier allocation to femtocells to handle additional traffic due to increased femtocell handover, maintaining guaranteed user demand and interference below pre-determined threshold. Splitting the handover traffic into guaranteed and non-guaranteed user traffic at the femtocells may provide more insight into productivity improvement. Future research can identify fraction of handover traffic that positively and negatively impacts productivity and utilize each to drive network productivity beyond current peak point, maintaining the QoS for guaranteed users and blocking thresholds. For LTE blocking model, multiple user classes can be considered and network productivity impact can be analyzed. As noted in [2], implied cost calculation of the network revenue with respect to the maximum number of calls allowed to be admitted are used in the determination of a CAC algorithm that enhances revenue and guarantees maximum

call blocking probabilities. Current research can be extended to determine implied costs to study its impact on network productivity.

- FFR metric applied to mobility scenario can be improved to consider mobility probabilities similar to [51]. Users with variable data rate requirements will impact the results with the proposed metric. This aspect needs further investigation to verify if proposed metric generates similar or better performance with varying data rates. Further, the metric results can be normalized for better comparison. The mobility results can be extended to macrocell-femtocell integrated network deployment.

APPENDIX A

LIST OF ACRONYMS

3GPP	Third Generation Partnership Project
CA	Carrier Aggregation
CAC	Call Admission Control
CDMA	Code Division Multiple Access
CSG	Closed Subscriber Group
eICIC	Enhanced Inter-Cell Interference Coordination
EPC	Evolved Packet Core
FAP	Femtocell Access Point
FCA	Fixed Channel Assignment
FFR	Fractional Frequency Reuse
FRF	Frequency Reuse Factor
GoS	Grade of Service
HBS	Home Base Station
LTE	Long Term Evolution
MIMO	Multiple Input Multiple Output
OFDMA	Orthogonal Frequency Division Multiple Access
OSG	Open Subscriber Group
QoS	Quality of Service
RAT	Radio Access Technology
RNC	Radio Network Controller
SAE	System Architecture Evolution
SIR	Signal-to-Interference Ratio
SINR	Signal-to-Interference Noise Ratio

APPENDIX B

LIST OF PUBLICATIONS

- U. Sawant and R. Akl, *Subcarrier Allocation in LTE Network Deployment with Mobility*, IEEE UEMCON 2017, The 8th IEEE Annual Ubiquitous Computing, Electronics & Mobile Communication Conference, New York, USA, October 2017, 8 pgs.
- U. Sawant and R. Akl, *Evaluation of Adaptive and Non Adaptive LTE Fractional Frequency Reuse Mechanisms*, IEEE WOCC 2017, The 26th Annual Wireless and Optical Communications Conference, New Jersey, USA, April 2017, 6 pgs.
- U. Sawant and R. Akl, *A Novel Metric to Study the Performance of Sectorized Fractional Frequency Reuse Techniques in LTE*, IEEE WTS 2017, The 16th Annual Wireless Telecommunications Symposium, Chicago, USA, April 2017, 7 pgs.
- U. Sawant and R. Akl, *Performance Evaluation of Network Productivity for LTE Heterogeneous Networks with Reward-Penalty Weights Assessment*, IEEE CCWC 2017, The 7th Annual Computing and Communication Workshop Conference, Las Vegas, USA, January 2017, 6 pgs.
- R. Akl and U. Sawant, *Grid-based Coordinated Routing in Wireless Sensor Networks*, Proceedings of IEEE CCNC 2007: Consumer Communications and Networking Conference, Las Vegas, USA, January 2007, pp. 860-864.

APPENDIX C

LIST OF DISSERTATION SECTIONS AND PUBLICATIONS

In this dissertation, sections 2.1, 3.2, 3.2.1, 3.2.2, 3.3, 3.4, 3.5, 3.6, 3.9, 4.2, 4.2.1, 4.2.2, and 4.3 are reproduced either solely or in part from:

U. Sawant and R. Akl, *Subcarrier Allocation in LTE Network Deployment with Mobility*, IEEE UEMCON 2017 The 8th IEEE Annual Ubiquitous Computing, Electronics & Mobile Communication Conference, New York, USA, October 2017, 8 pgs.

Sections 3.2.1, 5.1, 5.3, 5.4, 5.5, and 5.6.1 are reproduced solely or in part from:

U. Sawant and R. Akl, *Evaluation of Adaptive and Non Adaptive LTE Fractional Frequency Reuse Mechanisms*, IEEE WOCC 2017 The 26th Annual Wireless and Optical Communications Conference, New Jersey, USA, April 2017, 6 pgs.

Sections 3.2.1, 5.1, 5.2, 5.3, 5.4, 5.5, 5.6, 5.6.1, 5.6.2, 5.6.3, 5.6.4, 5.6.5, and 5.7 are reproduced solely or in part from:

U. Sawant and R. Akl, *A Novel Metric to Study the Performance of Sectorized Fractional Frequency Reuse Techniques in LTE*, IEEE WTS 2017 The 16th Annual Wireless Telecommunications Symposium, Chicago, USA, April 2017, 7 pgs.

Sections 3.2, 3.2.1, 3.2.2, 3.3, 3.4, 3.5, 3.6, 3.9, 4.2, 4.2.1, 4.2.2, 4.3, and 4.4 are reproduced solely or in part from:

U. Sawant and R. Akl, *Performance Evaluation of Network Productivity for LTE Heterogeneous Networks with Reward-Penalty Weights Assessment*, IEEE CCWC 2017 The 7th Annual Computing and Communication Workshop Conference, Las Vegas, USA, January 2017, 6 pgs.

REFERENCES

[1] A. Ahmed, M. Islam, M. Ismail, and M. Ghanbarisabagh, *Dynamic resource allocation in hybrid access femtocell network*, The Scientific World Journal (2014), 1–7.

[2] R. Akl, *Cell design to maximize capacity in cellular Code Division Multiple Access networks*, Ph.D Dissertation (2000), 1–169.

[3] R. Akl, M. Hegde, and P. Min, *Effects of call arrival rate and mobility on network throughput in multi-cell CDMA*, IEEE Int. Conf. Communications 3 (1999), 1763–1767.

[4] R. Akl, M. Hegde, and M. Naraghi-Pour, *Mobility-based CAC algorithm for arbitrary call-arrival rates in CDMA cellular systems*, IEEE Transactions on Vehicular Technology 54 (2005), no. 2, 639–651.

[5] M. Alouini and A. Goldsmith, *Area spectral efficiency of cellular mobile radio systems*, IEEE Trans. Vehic. Tech. 48 (1999), no. 4, 1047–66.

[6] A. Andreev, V. Drozdova, and A. Loshkarev, *Study of the traffic channel blocking probability in multiservice LTE networks*, International Conference on Biomedical Engineering and Computational Technologies (SIBIRCON) (2015), 236–238.

[7] A. Antonopoulos, E. Kartsakli, L. Alonso, and C. Verikoukis, *Dealing with VoIP calls during "busy hour" in LTE*, Recent Advances in Wireless Communications and Networks, InTech (2011), 1–5.

[8] G. Arvanitakis and F. Kaltenberger, *Stochastic analysis of two-tier HetNets employing LTE and WiFi*, EUCNC 2016, 25th European Conference on Networks and Communications (2016), 1–6.

[9] M. Assad, *Optimal fractional frequency reuse (FFR) in multicellular OFDMA system*, 2008 IEEE 68th Vehicular Technology Conference (2008), 1–5.

[10] D. Bilios, C. Bouras, V. Kokkinos, A. Papazois, and G. Tseliou, *Optimization of fractional frequency reuse in Long Term Evolution networks*, 2012 IEEE Wireless Communications and Networking Conference (WCNC) (2012), 1853–1857.

[11] ———, *A performance study of Fractional Frequency Reuse in OFDMA networks*, 2012 5th Joint IFIP Wireless and Mobile Networking Conference (WMNC) (2012), 38–43.

[12] D. Bilios, C. Bouras, V. Kokkinos, G. Tseliou, and A. Papazois, *Selecting the optimal fractional frequency reuse scheme in Long Term Evolution networks*, Wireless Personal Communications 71 (2013), no. 4, 2693–2712.

[13] B. Blaszczyszyn and M. Karray, *Dimensioning of the downlink in OFDMA cellular networks via an erlangs loss model*, European Wireless 2009 - 15th European Wireless Conference (2009), 1–5.

[14] C. Bouras, G. Kavourgias, V. Kokkinos, and A. Papazois, *Interference management in LTE femtocell systems using an adaptive frequency reuse scheme*, Wireless Telecommunications Symposium (2012), 1–7.

[15] C. Bouras, V. Kokkinos, A. Papazois, and G. Tseliou, *Fractional frequency reuse in integrated femtocell/macrocell environments*, Wired/Wireless Internet Communication: 11th International Conference, WWIC 2013 (2013), 229240.

[16] F. Capozzi, G. Piro, L. Grieco, G. Boggia, and P. Camarda, *Downlink packet scheduling in LTE cellular networks: Key design issues and a survey*, IEEE Communications Surveys & Tutorials 15 (2013), no. 2, 678–700.

[17] V. Chandrasekhar, J. Andrews, and A. Gatherer, *Femtocell networks: A survey*, IEEE Communications Magazine 46 (2008), no. 9, 59–67.

[18] H. Chang and I. Rubin, *Optimal downlink and uplink fractional frequency reuse in cellular wireless networks*, IEEE Transactions on Vehicular Technology 65 (2015), no. 4, 2295–2308.

[19] Y. Chang, Z. Tao, J. Zhang, and C. Kuo, *A graph approach to dynamic fractional frequency reuse (FFR) in multi-cell OFDMA networks*, 2009 IEEE International Conference on Communications (2009), 1–6.

[20] Wikimedia Commons, *File:Channel Capacity with Power- and Bandwidth-Limited Regimes.png — Wikimedia Commons, the free media repository*, 2016, [Online; accessed 29-October-2017].

[21] E. Dahlman, S. Parkvall, and J. Sköld, *4G LTE/LTE-Advanced for mobile broadband*, Elsevier Ltd., Oxford, 2011.

[22] M. El-Fenni, *Opportunistic spectrum usage and optimal control in heterogeneous wireless networks*, Ph.D Dissertation (2012), 1–161.

[23] H. Elfadil, M. Ali, and M. Abas, *Fractional frequency reuse in LTE networks*, 2015 2nd World Symposium on Web Applications and Networking (WSWAN) 3 (2015), 32–35.

[24] L. Fang and X. Zhang, *Optimal fractional frequency reuse in OFDMA based wireless networks*, 2008 4th International Conference on Wireless Communications, Networking and Mobile Computing (2008), 1–4.

[25] G. Fodor, C. Koutsimanis, A. Rácz, N. Reider, A. Simonsson, and W. Müller, *Intercell interference coordination in OFDMA networks and in the 3GPP Long Term Evolution system*, Journal of Communications (2009), 445–453.

[26] European Union Forum, *COST (European Cooperation in Science and Technology)*, `http://grow.tecnico.ulisboa.pt/~grow.daemon/cost231/`, 1999.

[27] P. Godlewski, M. Maqbool, M. Coupechoux, and J. Kelif, *Analytical evaluation of various frequency reuse schemes in cellular OFDMA networks*, In Proceedings of 3rd International Conference on performance evaluation methodologies and tools (Valuetools 2008) (2008), 1–10.

[28] N. Hassan and M. Assad, *Optimal fractional frequency reuse (FFR) and resource allocation in multiuser OFDMA system*, 2009 International Conference on Information and Communication Technologies (2009), 88–92.

[29] P. Hosein, *Resource allocation for the LTE physical downlink control channel*, GLOBECOM Workshops (2009), 1–5.

[30] J. Ikuno, M. Taranetz, and M. Rupp, *A fairness-based performance evaluation of fractional frequency reuse in LTE*, 2013 17th International ITG Workshop on Smart Antennas (WSA) 8 (2013), 502–505.

[31] J. Ikuno, M. Wrulich, and M. Rupp, *System level simulation of LTE networks*, Vehicular Technology Conference (VTC 2010-Spring), 2010 IEEE 71st (2010), 1–5.

[32] V. Istratescu, *Fixed point theory: An introduction*, D. Reidel (1981), 274–281.

[33] R. Jain, D. Chiu, and W. Hawe, *A quantitative measure of fairness and discrimination for resource allocation in shared computer system*, DEC Technical Report 301 (1984), 1–37.

[34] M. Karray, *Evaluation of the blocking probability and the throughput in the uplink of wireless cellular networks*, Proc. of ComNet (2010), 1–8.

[35] N. Katti, M. Vijayalakshmi, and L. Kulkarni, *Enhancing QoS parameters in 4G (LTE) technology using soft frequency reuse*, Journal of IET Engineering (2015), 1–6.

[36] R. Khdhir, K. Mnif, K. Ali, and L. Kammoun, *Allocation algorithm based on CAC scheme for LTE network*, IJCSNS International Journal of Computer Science and Network Security 16 (2016), no. 6, 140–150.

[37] P. Lee, T. Lee, J. Jeong, and J. Shin, *Interference management in LTE femtocell systems using fractional frequency reuse*, The 12th International Conference on Advanced Communication Technology (ICACT) 2010 2 (2010), 1047–1051.

[38] G. Li and H. Liu, *Downlink radio resource allocation for multi-cell OFDMA system*, IEEE Transactions on Wireless Communications 5 (2006), no. 12, 3451–3459.

[39] J. Lim, R. Badlishah, and M. Jusoh, *LTE-fractional frequency reuse (FFR) optimization with femtocell network*, 2nd International Conference on Electronic Design (ICED) (2014), 527–532.

[40] D. Liu, *User association optimisation in HetNets: Algorithms and performance*, Ph.D Dissertation (2015), 1–162.

[41] S. Mahato, T. Do, B. Allen, E. Liu, and J. Zhang, *A hybrid model for throughput evaluation of OFDMA networks*, Journal of IET Engineering (2013), 1–9.

[42] I. Mahmoud, O. Elgzzar, S. Hashima, and H. Konber, *An accurate model of worst case signal to interference ratio for frequency reuse cellular systems*, 2016 11th International Conference on Computer Engineering and Systems (ICCES) (2016), 393–400.

[43] M. Mehta, R. Jain, and A. Karandikar, *Analysis of blocking probability in a relay-based*

cellular OFDMA network, In Proceedings of 3rd International Conference on Performance Evaluation Methodologies and Tools (Valuetools 2014) (2014), 1–33.

[44] M. Meribout and A. Al Naamany, *A collision free data link layer protocol for wireless sensor networks and its application in intelligent transportation systems*, Wireless Telecommunications Symposium (WTS '09) (2009), 1–6.

[45] A. Mitra, *Handoffs in hierarachical macro/femto networks and an algorithm for efficient handoffs*, Master's Thesis (2014), 1–66.

[46] G. Sasibhushana Rao, C. Venkata Rao, and K. Satya Prasad, *Teletraffic and blocking probability estimation of OFDMA system*, International Conference on Computational Modeling and Security (CMS 2016) (2016), 696–704.

[47] A. Roy, P. Chaporkar, and A. Karandikar, *Performance evaluation of optimal radio access technology selection algorithms for LTE-WiFi network*, CoRR abs/1705.07286 (2017), 1–16.

[48] A. Roy and A. Karandikar, *Optimal radio access technology selection policy for LTE-WiFi network*, 2015 13th International Symposium on Modeling and Optimization in Mobile, Ad Hoc, and Wireless Networks (WiOpt) 1 (2015), 291–298.

[49] N. Saquib, E. Hossain, and D. I. Kim, *Fractional frequency reuse for interference management in LTE-Advanced HetNets*, IEEE Wireless Communications 20 (2013), no. 2, 113–122.

[50] U. Sawant and R. Akl, *A novel metric to study the performance of sectorized fractional frequency reuse techniques in LTE*, The 16th Wireless Telecommunication Symposium (2017), 1–6.

[51] ———, *Performance evaluation of network productivity for LTE heterogeneous networks with reward-penalty weights assessment*, The 7th Annual Computing and Communication Workshop and Conference (2017), 1–6.

[52] S. Shahsavari, N. Akar, and B. Khalaj, *Joint cell muting and user scheduling in multi-cell networks with temporal fairness*, CoRR abs/1609.08476 (2016), 1–12.

[53] D. Sivakumar, *Radio Interface Techniques*, https://3g4g5gprotocols.blogspot.com/2016/04/radio-interface-techniques-fdmatdmacdma.html, 2016.

[54] R. Sivaraj, I. Broustis, N. Shankaranarayanan, V. Aggarwal, R. Jana, and P. Mohapatra, *A QoS-enabled holistic optimization framework for LTE-Advanced heterogeneous networks*, IEEE INFOCOM 2016 - The 35th Annual IEEE International Conference on Computer Communications (2016), 1–9.

[55] M. Sternad, T. Ottosson, A. Ahlen, and A. Svensson, *Attaining both coverage and high spectral efficiency with adaptive OFDM downlinks*, In Proceedings of IEEE 58th Vehicular Technology Conference (VTC 2003-Fall) 4 (2003), 2486–2490.

[56] K. Suleiman, *Interactions study of self optimizing schemes in LTE femtocell networks*, Master's Thesis 2012 (2012), 1–255.

[57] M. Taranetz, J. Ikuno, and M. Rupp, *Capacity density optimization by fractional frequency partitioning*, 2011 Conference Record of the Forty Fifth Asilomar Conference on Signals, Systems and Computers (ASILOMAR) (2011), 1398–1402.

[58] Technical Specification Group RAN, *E-UTRA; LTE RF system scenarios*, 3GPP Tech. Rep. TS25.814, September 2006.

[59] _____, *E-UTRA; LTE RF system scenarios*, 3GPP Tech. Rep. TS 36.942, December 2008-2009.

[60] I. Tsompanidis, A. Zahran, and C. Sreenan, *A utility-based resource and network assignment framework for heterogeneous mobile networks*, Globecomm 2015 (2015), 1–6.

[61] M. Usman, S. Lee, and S. Shin, *Shared/restricted hybrid access in femtocells for next generation wireless networks*, IJCCE 2015 4 (2015), 274–281.

[62] C. Vargas, *Communication network design and evaluation using shadow prices*, Ph.D Dissertation (1996), 1–241.

[63] C. Vargas, M. Hegde, and M. Naraghi-Pour, *Implied costs for multi-rate wireless networks*, J. Wireless Networks 10 (2004), no. 3, 323–337.

[64] A. Wajid, *Lecture 10 frequency reuse concepts*, faculty.kfupm.edu.sa/EE/wajih/files/EE499Lecture10.pdf, 2007.

[65] H. Wang, L. Ding, P. Wu, Z. Pan, N. Liu, and X. You, *Dynamic load balancing and throughput optimization in 3GPP LTE networks*, ACM IWCMC (2010), 939–943.

[66] Wikipedia, *Eb/N0 — Wikipedia, The Free Encyclopedia*, 2017, [Online; accessed 29-October-2017].

[67] ———, *Shannon—Hartley theorem — Wikipedia, The Free Encyclopedia*, 2017, [Online; accessed 29-October-2017].

[68] P. Xia, V. Chandrasekhar, and J. G. Andrews, *Open versus closed access femtocells in the uplink*, IEEE Transactions on Wireless Communications 9 (2010), 3798–3809.

[69] Y. Xiang and J. Luo, *Inter-cell interference mitigation through flexible resource reuse in OFDMA based communication networks*, In Proceedings of European Wireless (2007), 1–7.

[70] M. Yadav, M. Palle, and A. Hani, *Performance analysis of fractional frequency reuse factor for interference suppression in Long Term Evolution*, International Journal of Conceptions on Electronics and Communication Engineering 3 (2015), 32–35.

[71] P. Yen, Q. Zhan, and H. Minn, *New fractional frequency reuse patterns for multi-cell systems in time-varying channels*, IEEE Wireless Communications Letters 4 (2015), no. 3, 253–256.

[72] M. Zuair, *Development of an access mechanism for femtocell networks*, Journal of Theoretical and Applied Information Technology 51 (2013), 434–441.